Prevention of Incisional Hernias Using Mesenchymal Stromal Cells and Platelet-Rich Plasma treated Collagen Matrix Tape

by

Michael W. Diehl

Submitted in Partial Fulfillment of the Requirements

for the Degree of

Master of Science in Engineering

in the

Mechanical Engineering

Program

Youngstown State University

May, 2014

Prevention of Incisional Hernias Using Mesenchymal Stromal Cells and Platelet-Rich Plasma treated Collagen Matrix Tape

Michael Diehl

I hereby release this thesis to the public. I understand that this thesis will be made available from the OhioLINK ETD Center and the Maag Library Circulation Desk for public access. I also authorize the University or other individuals to make copies of this thesis as needed for scholarly research.

Signature:

Michael Diehl, Student Date

Approvals:

Dr. Hazel Marie, Thesis Advisor Date

Virgil Solomon, Committee Member Date

Dr. Diana Fagan, Committee Member Date

Dr. Johanna Krontiris-Litowitz, Committee Member Date

Dr. Salvatore A. Sanders, Associate Dean of Graduate Studies Date

ABSTRACT

Each year, there are over four million abdominal wall surgeries performed in the United States. These surgeries have a 10% - 20% chance of developing into an incisional hernia. Although new surgical techniques and technologies have been introduced to decrease the chance of a hernia occurring, there has been no method developed that can consistently decrease the likelihood of an incisional hernia. In a novel approach, this study investigated the healing effect that the combination of platelet-rich plasma (PRP) and mesenchymal stromal cells (MSCs) on collagen tape had on abdominal wall fascia repair. In the study, midline laparotomies were performed on Lewis rats and the incisions were treated with the addition of PRP, PRP + MSCs, and no treatment. At four and eight weeks, the fascia was extracted and uniaxial tensile tests were performed on the samples to obtained maximum stress, modulus of elasticity and modulus of toughness. Two other experiments were performed to investigate the effect that different cell concentrations of MSCs had on of the tensile test data. In the preliminary trial, the combination of PRP + MSCs showed a significant increase at four and eight weeks for maximum stress, modulus of elasticity, and modulus of toughness as compared to the non-treated and PRP treated groups. The dosage trials did not present any clear correlation between the cell concentrations of $2.5x10^4$, $5x10^4$, $1x10^5$, $2.5x10^5$, and 5x10 MSCs and the mechanical properties. More trials are needed to further investigate a correlation between MSC dosage and improvement in the healing of fascia. Results from the elastographic strain analysis showed excellent correlation between the elastography and tensile test strain. Computational modeling led to the development of a preliminary finite element model. In conclusion, the combination of PRP + MSCs demonstrated an enhancement of mechanical properties over the PRP treated and non-treated samples. Further work will focus on furthering the finite element and incorporating localized modulus of elasticity that will be obtained through elastography.

Youngstown
STATE UNIVERSITY

One University Plaza, Youngstown, Ohio 44555
School of Graduate Studies and Research
Office of the Dean
330.941.3091
Fax 330.941.1580
graduateschool@cc.ysu.edu

Monday, June 17, 2013

Dr. Diana Fagan
Department of Biological Sciences
UNIVERSITY

Re: **IACUC Protocol # 04-13**
Title: Determining dose of mesenchymal stromal cells needed to improve wound healing in a rat model.

Dear Dr. Fagan:

The Institutional Animal Care and Use Committee of Youngstown State University has reviewed the aforementioned protocol you submitted for consideration and determined it should be unconditionally approved for the period of June 17, 2013 through its expiration date of June 17, 2016.

This protocol is approved for a period of three years; however, it must be updated yearly via the submission of an Annual Review-Request to Use Animals form. These Annual Review forms must be submitted to the IACUC at least thirty days ***prior*** to the protocol's yearly anniversary dates of June 17, 2014 and June 17, 2015. If you do not submit the forms as requested, this protocol will be immediately suspended. You must adhere to the procedures described in your approved request; any modification of your project must first be authorized by the Institutional Animal Care and Use Committee.

Good luck with your research!

Sincerely,

Dr. Scott Martin
Interim Associate Dean for Research
Authorized Institutional Official

sm:dka

C: Dr. Walter Horne, Consulting Veterinarian, NEOUCOM
Dr. Robert Leipheimer, Chair IACUC, Chair Biological Sciences
Dawn Amolsch, Animal Tech., Biological Sciences

ACKOWLEDGEMENTS

I would like to express my sincerest appreciation to those who have made this project possible.

Thesis Advisor

Dr. Hazel Marie

Medical Advisor

Dr. Jeremy J. Heffner, MD*, Dr. Jonathan W. Holmes, MD*, Dr. Johnathan P. Ferrari MD*

Thesis Committee

Dr. Diana Fagan, Dr. Johanna Krontiris-Litowitz, Dr. Virgil Solomon

Corporate Partners

Humility of Mary Health Partners

Faculty

Dr. Yong Zhang, Anthony Viviano

Students

Zach Abraham

Table of Contents

List of Figures

List of Tables

Nomenclature

Symbol	Description
BMI	Body Mass Index
MSCs	Mesenchymal stem/stromal cells
PRP	Platelet-Rich plasma
EOA	External oblique aponeurosis
TAPP	Transabdominal preperitoneal
TEP	Totally extraperitoneal
PTFE	Polytetrafluoroethylene
ESC	Embryonic stem cell
AMSCs	Adipose derived Mesenchymal stem/stromal cells
BMSCs	Bone marrow derived Mesenchymal stem/stromal cells
ACL	Anterior cruciate ligament
BUN	Blood urea nitrogen
VEGF	Vascular Endothelial Growth Factor
ALT	Alanine aminotransferase
AST	Aspartate aminotransferase
SDFT	Superficial digital flexor tendon
ECM	Extracellular matrix
PLGA	Poly(laric-co-glycolic acid)
hMSCs	Human mesenchymal stem cells
bFGF	Basic fibroblast growth factor
DMEM	Dulbecco’s modified Eagle’s medium
WBS	Wound busting strength
RNA	Ribonucleic acid
FHA	Fluorohydroxyapatite

ADSCs	Adipose-derived stem cells
FBS	Fetal bovine serum
TSCs	Tendon stem cells
IACUC	Institutional Animal Care and Use Committe
ACD	Anticoagulant citrate dextrose
DMSO	Dimethyl Sulfide
MEM	Minimum essential medium
PBS	Phosphate-buffered saline
EDTA	Ethylenediaminetetraacetic acid
VT	Virgin tissue
CoTa	CollaTape™
Fps	Frames per second
μm	Micrometer
I	Inferior
S	Superior
FEA	Finite element analysis

CHAPTER 1

INTRODUCTION

1.1 Background

When the body sustains injuries to the skin, fascia, or connective tissue, it automatically responds to heal the damaged tissue. If the body is unable to heal the wound fast enough, scarring begins to form and this creates a weak spot. Scarring is one of the major concerns surgeons face today because of the serious complications that can arise if there is poor fascial healing.

One of the biggest complications of poor healing is the recurrence of a hernia. A hernia is described as a protrusion made of fatty tissue and sometimes parts of an organ through the cavity that normally contains them. In severe cases, the protruding organ can become strangulated, meaning the blood supply is cut off. This can lead to additional swelling, infection, gangrene, and death.

Hernias can happen just about anywhere in the body, but typically occur around the lower torso of the abdominal wall where the muscles and tissues of the abdomen come together with the groin region in the leg causing a natural weak spot. This area is weaker in strength than most other places of the body because you have muscle, tendons, and fascia from several regions joining and it is being stretched every time you move.

Although the exact cause of a hernia is unknown, there are several factors that can increase the chances of developing one. One of those factors is a person's gender. A male is anywhere from 15 to 20 times more likely to get a hernia than a female. In studies done by Hay et al. (1995) and Rutkow (1992), they showed that 95.5% and 95% of their patients, respectively, were males. One reason is that males are likely to participate more in strenuous activities, such as heavy lifting and sports like football, hockey, soccer, and wrestling. Males also have an added natural weak spot in their lower abdominal area, the inguinal canal, from when their testicles dropped into the scrotum while still in the womb.

Another factor is the age of the person. People over the age of 55 and babies are at the highest risk of suffering a hernia. For older people, this is due to a lifetime of wear and tear on the abdominal region as well as the body's inability to keep up with the healing of damaged tissue. It is more common to have had a surgery on the abdominal wall area, which could lead to an incisional hernia. Babies, especially premature babies, have a high risk of developing a hernia because there are several weak spots or holes in the abdomen when born. One of these is from the umbilical cord and the other, as mentioned previously, is in the inguinal canal. These areas usually heal over time but are very vulnerable until then. The inguinal canal, however, does not always heal properly and can continue to be a risk for the rest of a male's life. Studies done by Burcharth et al.(2013) and Davies et al. (1985) have shown that babies have the highest rate of suffering an inguinal hernia with rates of 8 per 1,000 and 6 per 1,000. The same studies also showed that age groups from 5-35 had no higher than a rate of 1 per 1,000 chance.

Obesity is another risk factor and is becoming one of the leading causes of hernia cases. A study down by Sauerland et al. (2013) showed that as a person's body mass index (BMI)

increases, so does their risk of getting a hernia. In his study, 62.3% of the patients that were treated for hernias had a BMI > 25 kg/m^2. Another study by Rosemar et al. (2010) had similar findings in that they found only 3.5% of the 49,094 patients suffering from a hernia, had a BMI < 20 kg/m^2. The main reason why an obese person is at a higher risk of getting a hernia is that as BMI increases, the pressure on the abdominal wall increases. This increase in pressure stretches and weakens the abdominal wall.

Determining a more effective procedure for repairing a hernia has been a priority for surgeons. (Kingsnorth et al.,2003) Each year over 800,000 hernia surgeries are performed but, contain a 20-40% chance of having the hernia reoccur. This doesn't account for the other 4 to 5 million other abdominal wall surgeries that take place and each have a 10-20% chance of developing into a hernia. These high recurrence rates have led to extensive research in improving the techniques that doctors use in order to improve the healing time and the effectiveness of the surgery. This has led to numerous options when it comes to suture material, incision location and orientation, and method of closure. Researchers are now looking into the benefits of meshes and growth additives to improve the healing process. One such method is the application of mesenchymal stem cells (MSCs) and platelet rich plasma (PRP) to the wound site.

1.2 Naturally Occurring Hernias

Hernias can happen one of two ways in the abdominal wall. The first way is a natural hernia, which can develop in one of four ways: inguinal, femoral, umbilical, and epigastric.

1.2.1 Inguinal Hernia

(1) Introduction An inguinal hernia occurs when the bowel pushes through a weakness in the inguinal canal, an opening between layers of the abdominal muscle near the groin. There are two types of inguinal hernias: direct and indirect. Direct hernias are when the protrusion enters through the wall of the canal. These are most likely caused by the body not being able to keep up with the repair of worn out tissue. Increase in pressure or straining can also weaken the tissue. (Kingsnorth et al. 2013) Direct hernias make up 25-30% of inguinal hernias and are usually in men over forty years of age. Indirect hernias enter through the internal ring at the top of the inguinal canal. These are mostly seen in men because when they are born; as previously mentioned, men have a natural opening in the groin for the testicles and the spermatic cord to pass out of the abdomen and into the scrotum. This opening does not always close properly and weakens the abdominal wall.

(2) Incidence (Bendavid, 2001). Several risks factors that can lead to an inguinal hernia are premature birth, obesity, constipation, chronic cough, heavy lifting, or a family history of inguinal hernias. The inguinal hernia is the most common type of hernia in the groin area and result in 75 to 80% of all hernia surgeries. In the United States alone, there were 800,000 inguinal surgeries, making it the most common surgery in America. In a lifetime, men have a 27% chance of getting an inguinal hernia, where as women only have a 3% chance. They are also seen mostly in males under the age of one or over fifty-five years

old. Figure 3.4 in Williams et al. (1992) shows an age and gender distribution of inguinal hernias. In this Figure, it is seen that from the age of zero to one there is an 8 in 1000 chance in getting an inguinal hernia. The bar chart then follows an inverted bell curve where the minimum chance for getting an inguinal hernia is between the ages of fifteen and twenty-four, where there is an 1 in 2000 chance in getting an inguinal hernia. From the age of twenty-four, the chance of developing an inguinal hernia increases by a rate of 1 out of 1000 every nine years

(3) <u>Anatomy</u> (Catlin et al., 2009) The inguinal region is located in the anterolateral abdominal wall. This section is made up of nine layers, as follows, from superficial to deep: skin, superficial fascia fatty layer/Camper fascia, superficial fascia membranous layer/Scarpa fascia, obliquus externus, obliquus internus, transversus abdominis, deep fascia transversalis, extra-peritoneal fat, and parietal peritoneum. Figure 1.1 shows these layers.

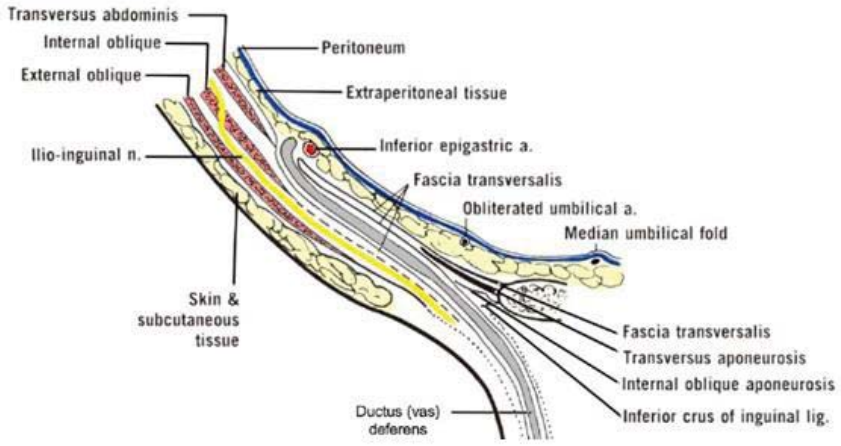

Figure1.1: Layers of the Inguinal Region (Catlin et al., 2009)

The Camper fascia and the Scarpa fascia contain the superficial circumflex, the epigastric, and the external pudendal arteries. These three things make up the superficial branches of the femoral vessels. After this layer is removed, the inguinal canal can be observed.

The inguinal canal serves as a passageway in the anterior of the abdominal wall which is used to carry the spermatic cord and the ilioinguinal nerve in men and the round ligament and the ilioinguinal nerve in women. The canal is larger in men, and each person has two of them, one on the left side and one on the right side. The external oblique serves as the roof of the inguinal canal. It opens up adjacent to and above the pubic tubercle and is where the superficial inguinal ring exit of the canal appears. Figure 1.2 shows the inguinal ring.

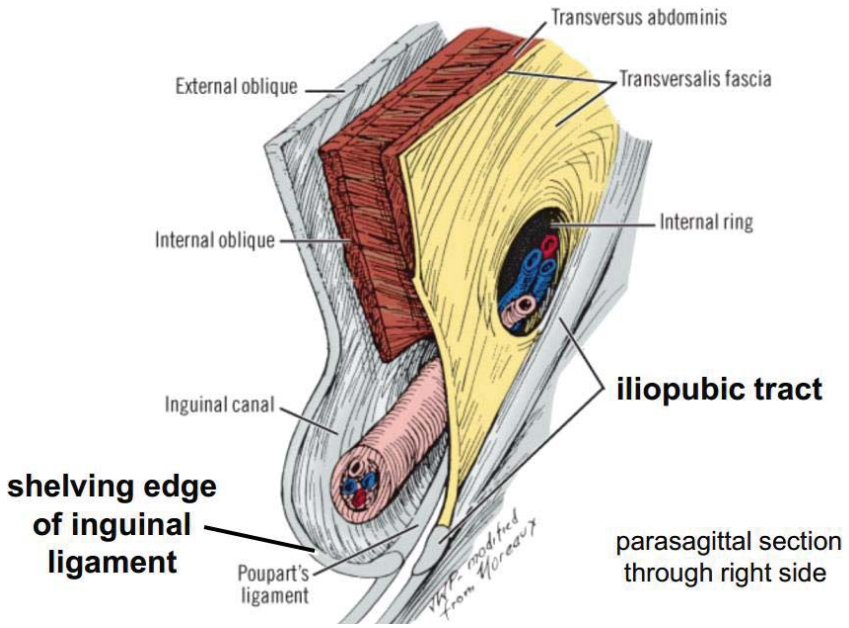

Figure 1.2: The Inguinal Canal and Ring (Menon and Brown, 2003)

The floor of the canal is formed from the transversus abdominis and transversalis fascia. The inferior wall is the inguinal ligament and is formed by the lower edge of the external oblique aponeurosis. The ligament folds over itself to form a shelving edge and it is this section that forms the lower wall of the inguinal canal. The superior wall consists of a combination of the internal oblique and the transversus muscles aponeurosis.

(4) <u>Treatment</u> The Egyptians, in 2500 B.C., were the first civilization to show some sort of hernia treatment. Their methods, however, only consisted of surface treatment and bandaging. It wasn't until the Romans in the first century AD that surgery was involved as a treatment. They treated an inguinal hernia by tying up the protrusion and suturing the external ring closed. This approach lead to a frequent recurrence, but showed an understanding of the problem and a way of treatment that would last until the late 19th century (Brewer, 1980). In the second half of the 19th century, Von Czenry (1877) described a treatment in which the hernia sac was tied up without opening the hernia canal. The external ring was then closed and patients were advised to wear a truss around the hernia site to keep pressure on the site. This technique, however, seemed very similar to the technique the romans used and had a very high recurrence rate with one study showing 132 recurrences out of 136 surgeries. Around the same time, William Wood (1863) developed a technique to treat an inguinal hernia. Wood's method attempted to reinforce the inguinal canal by folding the hernia sac back onto itself and use it as a blockage for the internal ring. The aponeurosis of the outer oblique was then repaired and the external ring was closed. Like Czerny's method, Wood's technique also had a high recurrence rate.

It wasn't until Bassini (1887) that a valid procedure was developed. According to Bassini, the main reason behind the failure of previous techniques was the dependence on a single layer of scar tissue to enclose the hernia. He created a method referred to as a triple layer repair of the inguinal floor. He did this by suturing parts of the internal oblique, abdominis muscle, and transversalis fascia to the inguinal ligament and then sutured the skin closed. By doing this, he was able to reconstruct the posterior wall of the inguinal canal. The recurrence rate significantly improved to between 5% and 10%.

Bassini's technique was the preferred hernia treatment until the late 1940's when Edward Shouldice (1953) developed a technique that is still used today and is considered the gold standard when comparing newer techniques. His method stressed the importance of the transversalis fascia. The main difference between the two techniques is the final layering to reinforce the inguinal ligament. Where Bassini is a three layer, Shouldice used the cremasteric fascia, internal spermatic fascia, the external oblique, and the transversalis fascia to create a four layer reinforcement. Because of the difficulty of this technique, the procedure is becoming less common in developed countries since newer method like Desarda, Laparoscopic, and Lichtenstein are faster and require less skill to perform; however when done properly, Shouldice's technique still has the smallest recurrence rate of 2%.

There is still no clear consensus to how an inguinal hernia should be repaired; because of this, there are several repair techniques that can be grouped into three categories: tension repair, tension-free repair, and laparoscopic repair. Bassini, McVay, and Shouldice are the three kinds of tension techniques used and can be modified using meshes that were mentioned before in the incisional hernia section. Bassini and Shouldice are still done as described earlier and McVay will be explained in Section 1.2.2 in the femoral treatment as it is usually only used to treat an inguinal hernia if a femoral hernia exists as well.

Desarda (2003) and Lichtenstein(1986) are the two most commonly used tension free techniques. Desarda procedure follows the same sets to excision the hernia sac as other techniques. Once the sac has been removed, a strip of the external oblique aponeurosis (EOA) needs to be separated from the medial leaf, but still has to be connected to either end. The strip is then sutured to the inguinal ligament and the arch of the muscle above. By doing this, additional strength is given to the internal oblique and transverse abdominis and works

as a shield to prevent recurrence. Desarda (2001) technique has a 2% - 5% chance of recurrence.

The Lichtenstein (1986) procedure starts with a 5-6cm incision from the pubic tubercle and extends laterally along the Langer's line. The EOA is then opened and separated from the spermatic cord. Separation of the upper leaf of the external oblique from the internal oblique muscle is made to allow a mesh to overlap the internal oblique. The cremasteric sheath is cut longitudinally at the deep ring to look for hernia sacs. The groin area is also examined in case of a coexisting femoral hernia. Once the hernia has been treated, a 7 x16 cm sheet mesh made of polypropylene is used to support the site. The lower corner of the mesh is placed over the pubic tubercle, overlapping it by 1.5 -2.0cm and stretched medially. It is then sutured to the rectus sheath above the pubic bone and the suturing continued to the inguinal ligament up to the internal ring.

On the loose end of the mesh, a slit is made dividing the mesh into a wide section (2/3 the width) and a narrow section (1/3 the width). The wide end of the patch is sutured to the rectus sheath and internal oblique aponeurosis, making sure not to harm the internal oblique muscle. The lower edge is attached to the inguinal ligament and any excess mesh is then trimmed off. The skin incision is then closed. Lichtenstein's tension-free procedure has produced recurrence rates of 1% - 3%.

Laparoscopic repair is a minimal invasive repair that doesn't require a large incision. The advantage to this sort of treatment is less pain, less analgesic, better cosmesis, sooner return to normal activity, and the absence of wound related problems. The procedure, however, is more costly than open repair and has a longer operating time. Transabdominal preperitoneal

(TAPP) and totally extraperitoneal (TEP) are the two standardized laparoscopic repair techniques for inguinal hernia repair (McCormack et al., 2005). The TAPP repair is easy to learn but requires the surgeon to cut through the peritoneal cavity and has the possibility of bowel adhesions to the mesh. The TEP is a difficult procedure to learn and the surgeon needs to have a great understanding of the unfamiliar anatomy of the abdominal wall. It has the advantage of not cutting the peritoneal cavity and having direct access to posterior defects (Krishna et al. 2012).

For TAPP repair, the intra-abdominal cavity's pressure is set to around 14mmHg with CO_2 usually by a Veress needle. Three trocars, portals used to insert other instruments, are then placed into the abdomen: one 10-12mm trocar is placed 1cm below the umbilicus for the insertion of the laparoscope (telescope) and the other two are placed 5-6 cm on either side of the umbilicus and are 5mm trocars. Using the trocars, the inguinal hernia is reduced and repair on the area starts. The membrane lining the abdomen cavity is cut laterally to the inferior epigastric vessels to the umbilical ligament in order to create a peritoneal flat. Space is then created to insert the 15 x 10 cm polypropylene mesh. The mesh is rolled up and put into the body by using the trocar below the umbilical. It is then unrolled and used to cover the opening. The mesh is not fixed in place but is held by suturing the peritoneal flap back into place. The intra-abdominal pressure on the wall is released and ports are stapled shut. The recurrence rate for the TAPP procedure is 0 %– 3% (Kapiris et al., 2001).

The TEP procedure requires three ports along the midline. A 10-12mm port for the telescope is made just below the umbilicus. The other two ports, 5mm, are made above pubic symphysis and half way between the pubic symphysis and the umbilicus. From the pubic symphysis, dissection proceeds laterally up to the anterior superior iliac spine. The

peritoneal flap is then raised and the hernia sac should be visible. Once the sac has been treated, the mesh is inserted into the body through the umbilical port. It is then unrolled in the preperitoneal space and covers the deep inguinal ring, Hasselbach's triangle, and femoral hernia sites. The meshed is not fixed and the fascia of the umbilical port is closed using 1-0 Vicryl. The ports are then stapled shut. The TEP technique has a 1% - 2% recurrence rate (Tamme et al, 2003).

1.2.2 Femoral Hernia

(1) Introduction It is believed that elevated pressure in the abdominal area is the main reason behind femoral hernias because they are most common in women who have had more than one baby. Besides Pregnancy, constipation and bronchitis can add pressure on the abdominal wall (Colville et al., 2000). A study done by Keith (1923-1924), the intra-abdominal pressure dilates the femoral vein and stretches the femoral ring. This allows fat tissue into the ring and leads to the hernia sac.

There are several types and classifications of femoral hernias. They differ by their location within the femoral triangle, the upper inner thigh. The most common type is when the protrusion comes from femoral canal and passes through the femoral triangle medially to the femoral vessels. This is called a femoral hernia. A Hasselbach's hernia is when a protrusion comes through the cribriform fascia and presents a lobular outline (Papanikitas et al., 2008). Hernias that are found to be anterior to the femoral vessels are called velpeau hernias (prevascular) and posterior are referred to as serafini hernias (retrovascular). The last types are Cloquet and Laugier hernias and occur medially to the femoral vessels and pass through an opening in the lacunar ligament, Lugier, or through the aponeurois of the pectineus

muscle, Cloquet (Paquet et al., 2008). Figure 1.3 shows the locations where each type of femoral hernia could occur.

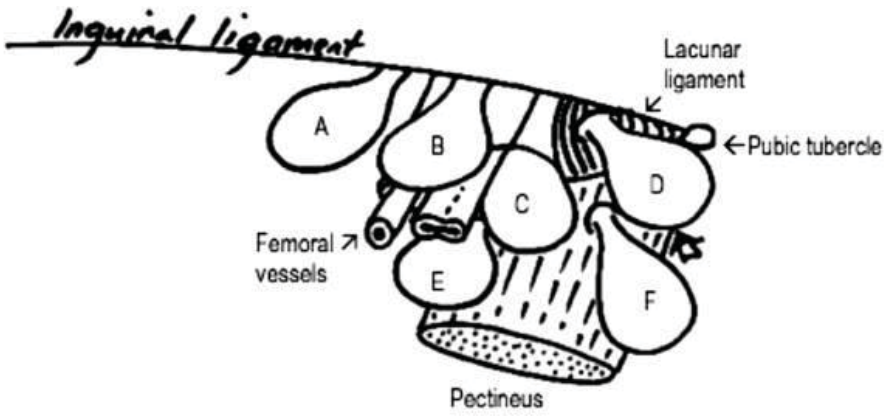

Schematic view of right femoral region

A. Hesselbach's hernia
B. Velpeau's hernia (prevascular)
C. Femoral hernia
D. Laugier's hernia
E. Serafini's hernia (retrovascular)
F. Cloquet's hernia

Figure 1.3: Femoral Hernia Sites (Papanikitas et al. 2008)

There are four femoral hernia classifications: incarcerated, irreducible, reducible, and strangulated. An incarcerated femoral hernia is when a piece of intestine gets stuck in the hernia but is not strangulated. Irreducible femoral hernia occurs when a hernia gets stuck in the femoral canal and requires surgery to fix. This causes an obstruction to the intestine. When the femoral hernia can be pushed back into the abdominal cavity and it heals on its own is called a reducible femoral hernia. A strangulated femoral hernia is a condition in which the intestine becomes intertwined around the hernia preventing blood flow and intestinal functions (Rutkow and Robbins, 1998).

(2) <u>Incidence</u> A femoral hernia is the second most common type of hernia, but has the highest rate of developing into a strangulated hernia. It accounts for 3% to 10% of all hernias with most occurring between the ages of 40 to 70 (Dahlstrand et al., 2009). When

they do appear in children, it is due to one of three main situations: (1) a connective tissue disorder that weakens the tissue in the femoral sheath and femoral canal, (2) the incomplete closing of the area during development, or (3) from a condition that increases the pressure on the intra-abdominal wall. Femoral hernia is four to five time more likely to occur in females than males; this is attributed to the wider bone structure in women. (Kingsnorth and LeBlanc, 2003) The wider bone structure causes there to be more abdominal pressure that expands the femoral vein and stretches the femoral ring. There are, however, studies that dispute this and say the distribution is equal between the genders, but these studies are based on a certain ethnicity.

(3) <u>Anatomy</u> A femoral hernia occurs just below the inguinal ligament, in a natural weak spot called the femoral canal. The canal is one of three compartments in the femoral sheath; the femoral artery and femoral vein are the other 2 compartments. The femoral canal lies in the medial compartment and is the smallest of the three. It houses the lymphatic vessels and a lymph node, called Cloquet's node that are embedded in areolar tissue. The femoral canal allows room for the femoral vein to expand and allow more blood to return from the leg during periods of activity. The canal is cone shaped and about 1.25 cm in length. The base, called the femoral ring, is directed upward and is oval in shape. This is the location of femoral hernias. The long diameter of the oval measures 1.25cm. Figure 1.4 shows the anatomy of this region.

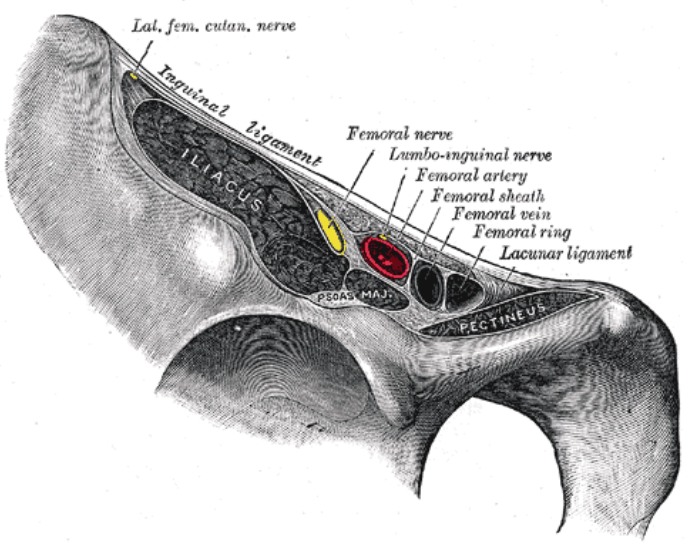

Figure 1.4: Anatomy of Femoral Region (McEwen, 2012)

(4) <u>Treatment</u> Guey de Chauliac (Read, 2004) was the first to write about the differences with inguinal and femoral hernias when he wrote Chirugia Magna in 1363. It wasn't until Socin(1879), however, that a specific approach to femoral hernia repair was developed. His repair was performed by cutting the hernia sac and returning the peritoneal stump to the abdomen. This procedure had a very high recurrence rate. This method would be modified over a twenty year span by the surgeons Bassini, Marcy, and Cushing. Each of their methods involved different ways of closing the femoral ring using sutures and surrounding tissues and ligaments. Even with this modification, the recurrence rate was still over 5% and the femoral approach was abandon, in favor of the inguinal approach, for almost seventy-five years.

Lichtenstein and Shore (1974) re-popularized the femoral hernia method by creating a tension-free surgery. His approach introduced a cylindrical shape plug that had been rolled from a polypropylene mesh. This plug was inserted into the femoral canal from the femoral side.

Arthur Gilbert (1989) modified the plug's shape into a cone or umbrella in the late 1980's. Around the same time, Rutkow and Robbins (1993) were designing a pre-shaped mesh plug called PerFix that could be used to repair either inguinal or femoral hernias. In a study by Shulman et al. (1992), the efficiency of this technique was shown by having a less than 2% recurrence rate.

Besides Lichtenstein's plug technique, there are four common approaches used today; Lockwood's low inguinal approach, Lotheissen's high inguinal approach, Cheatle and Henry midline operation, and McEvedy's high approach. Each method has their own advantages and disadvantages and largely depends on the circumstances of the hernia and the surgeon.

Lockwood's (1893) approach was introduced in 1893. For this procedure, the incision was to be made below the inguinal ligament in the thigh. This would uncover the femoral sac. The hernia sac would then be removed and the femoral ring would be closed at its lower end. This approach is favored for children and simple cases that don't show a strangulated hernia. However, this method is beginning to fall out of favor with surgeons due to its high recurrence rate, poor visualization of the hernia sac, and high operation risk due to the difficulty if strangulation exists.

In 1875, Annandale (1876), while operating on a direct inguinal hernia, used the inguinal technique to treat a femoral hernia that had been located on the same side during surgery. He noted that through the inguinal incision, it was easy to locate and reduce the femoral hernia. After that, he began treating femoral hernias using the high inguinal approach. The technique didn't become popular until Lotheissen published his review of the technique in 1898 and at the congrès de la Société Internationale de Chirurgie at Brussels in 1908. Since

then, his name has been attached to the high inguinal operation. An overview of the surgery can be described by opening the inguinal canal, and then making an incision on the posterior wall. Next the hernia sac is identified and treated accordingly. The femoral ring is closed by suturing cooper's ligament to the poupart's ligament. The advantages to this technique are a good view of the protrusion, the intestines can be easily examined, the operation is only in the inguinal region, and an inguinal hernia can be treated at the same time. The high operation approach has been criticized by surgeons because it is common to develop a direct inguinal hernia at the site of incision (Sheehan, 1955).

The extraperitoneal midline operation was developed by Lenthal Cheatle (1920) and A. K. Henry (1936). Both doctors noted how easy it was for the femoral ring to be seen. The procedure required an incision from the umbilicus to the pubis. The right rectus muscle and the parietal spectrum are separated from the abdominal wall. The hernia sac is then located and treated. The femoral canal is closed by turning up a triangular flap of fascia and suturing it to the poupart's ligament or by suturing the poupart's ligament to the Cooper's ligament. This procedure is useful for thin patients, combined inguinal and femoral hernias, and when the intestine must be cut out. The disadvantages to this procedure are the difficulty in removing large (over 8 cm) hernias, the approach to the femoral ring in large patients, and the risk of damaging the bladder.

The lateral rectus procedure was created by Peter G. McEvedy (1950). For his method, a vertical incision was made over the femoral canal to three inches above the Poupart's ligament. Then a cut needs to be made in the muscle near the external ring. The hernia should then be able to be recognized. The protrusion is treated and tied off above the femoral canal. The femoral ring is then closed by suturing the Cooper's ligament to the conjoined

tendon. Through this procedure, there is better exposure for inspection, resection, anastomosis, and repair then other procedures offer. There is also no chance of a direct inguinal hernia developing since the inguinal canal is not touched. The method can cause a hernia through the Spigelian line at the lateral part of the abdominal wall and can cause damage to the nerves in the area of the incision.

1.2.3 Epigastric Hernia

(1) Introduction Epigastric hernias are found in the linea alba, linea semilunaris, or one of the transversus of the rectus sheath of the anterior abdominal wall between the xiphoid and umbilicus. They usually start as small protrusions of preperitoneal lipomas. An increase in the internal pressure on the abdominal wall can have them enter the fascial openings of the perforating neurovascular bundles. The sac typically starts at 2mm but as the internal pressure on the abdominal wall increases, the size of the sac can exceed 20cm (Robin, 1989).

(2) Incidence Epigastric hernias account for 1-5% of abdominal wall hernia surgeries, but are found in about 5-10% of autopsies. They are typically found in patients between the ages of twenty to fifty years and have a male to female ratio of 3:1. Most of them occur in athletes or soldiers because of the large amount of stress they put on their abdominal area with 80% of them appearing just off of the midline (Klinge et al., 2003).

(3) Anatomy The linea alba of the abdominal wall is formed by the midline junction of the rectus abdominis sheaths. When the sheaths join, they form a triple layer of interlocked collagenous fibers, uniting the anterior and posterior sheaths. This conjoining makes the strong fascial complex that allows the abdominal wall to resists the powerful lateral pulling of the external and internal oblique and transversus abdominis muscles. It is

strongest and narrowest at the umbilicus and can be as wide as 2.5cm at the xyphoid (Lang et al. 2002).

Askar (1984) showed that epigastric hernias occur more often in people whose collagen fibers intersected only once than in individuals who had their fibers intersect multiple times. He also showed that there were structural attachments between the diaphragm and the linea alba. These attachments, he believed, could lead to disproportionate tension during coughing, strenuous activities, or vomiting. Ten paired neurovascular penetrate this fascia and create small openings and this could explain why 20% of patients with multiple epigastric hernias.

(4) <u>Treatment</u> In 1285, Arnauls de Villeneuve (Kingsnorth and LeBlane, 2003) first described an epigastric hernia, but didn't go in great detail and mainly just clarified that it was different than other known hernias. De Grengeot (1748) defined the hernia and said it was due to pathology from the abdominal organs. Early procedures had little success rate and often lead to peritonitis, injury of the intra-abdominal viscera, or a recurrence.

The method in which Epigastric hernias are dealt with today vary depending on size and if there are multiple of them. If the hernia is under 7 cm diameter, considered a small or medium hernia, a vertical incision is made at the site of the hernia to easily see if there are multiple hernias. From here, the bulge is removed and the neck opening is closed with sutures. For larger hernias, the dome of the sac should first be found. This is usually found in the subcutaneous tissue close to the skin. A vertical incision is made and the sac separated from the fat surrounding, at least 3 cm on each side. The hernia can then be fixed and sutured closed. Closing for all types of Epigastric hernias can be done by tension suturing

using meshes and plugs or tension free suturing using Kugel patch procedure or Desarda technique as mentioned in Section 1.2.1 (Muschaweck, 2003).

1.2.4 Umbilical Hernias

(1) Introduction An umbilical hernia occurs around the belly button and is caused by a weakness in the connective tissue and abdominal muscles. The weakness allows fat and intestine to protrude and develop a bulge under the skin. There are three types of umbilical hernias and are classified based on when they develop in life. The first type of umbilical hernia is an omphalocele and can be divided into two groups: fetal and embryonic. A fetal omphalocele develops eight weeks into pregnancy when the gut returns to the abdominal cavity. If this doesn't happen naturally, a defect occurs in the abdominal wall. Through this defect, a hernia sac of amnion appears that has the umbilical vessels (Blumberg, 1980). Embryonic omphalocle is due to the abdominal wall failing to close before eight weeks. It has a wide abdominal defect and the umbilical cord joins the abdominal wall perimeter instead of the apex. The liver and bowel are herniated and patients have a 50% chance of exhibiting other anomalies like congenital heart defects, trisomy 21, and renal abnormalities (Runyon anfd Jular, 1985). Infantile umbilical hernia is the second type. This kind of umbilical hernia only presents a fascial defect and is frequently present in newborns. They are highest in African Americans and premature babies and typically close on their own in five years. For the first two types, surgery should only be considered if the hernia is incarcerated, fascial defect is larger than 1 cm, and in girls over two years, or boys over five years (Lemmer et al., 1983).

The last type of umbilical hernia is called an adult umbilical hernia. This is an acquired hernia that is an indirect hernia through the umbilical canal. Herniation is due to an increase in intra-abdominal pressure and causes a gradual yielding of the tissue that encloses the umbilical ring. The risk of an adult umbilical hernia can be increased due to obesity, multiple pregnancies, ascites, and diabetics. They have a ratio of 3:1 in women and are particular in females over forty years old. There is also no relationship to having an umbilical hernia as a child and developing one as an adult as only 10% exhibited hernias during their childhood. This type of hernia has a high mortality rate due to the high tendency of incarceration and strangulation and surgery is usually done right after diagnosis (Muschaweck, 2003).

(2) <u>Treatment</u> Umbilical hernias were first mentioned in 100 AD by Celsus and called them "an indecent prominence of the naval." They were first treated by the tying and transfixion of the sac. This led to the tissue cells dying and further complications. It wasn't until 1898 that an adequate procedure was created by William Mayo. His technique began with an incision of the skin around the hernia site and the clearing of any fascia on the abdominal wall. The sac was then examined, treated and the wound was closed by overlaying the surrounding layers of fascia. At the time, this was a revolutionary technique but now has been shown to have a recurrence rate of 20% to 30% (Deveney, 1994).

Besides the Mayo technique, mentioned earlier, several other methods involving meshes are used today to treat an umbilical hernia. One technique is the Rives-Stoppa, which was developed to treat incisional hernias. For this method, a prosthetic material is placed between the rectus abdominis muscle and the posterior sheath. The recurrence rate is between 5% and 10% and has an unusually long surgery time of almost three hours. In

general though, mesh techniques have a recurrence rate of fewer than 3% and suture techniques are around 10% (Arroyo et al., 2001).

1.3 Incisional Hernia

1.3.1 Introduction

The second way a hernia can occur on the abdominal wall is by an incisional hernia. They occur when a bulge or protrusion develops through a prior incision on the abdominal wall. They usually develop within the first thirty to sixty days after the surgery took place, usually when the patient begins to resume normal activity. This is most often do to the tissue not being completely healed yet and having poor tensile strength. This can be attributed to the tension that the sutures place on the tissue or due to inadequate healing caused by infection, poor nutrition, obesity or disease. The hernia, because of size, may not be noticed for months or years. These hernias can be small and easy to treat or large and very complex. They can develop from small laparotomies, like an appendectomy or a laparoscopy, to large procedures like intestinal and vascular surgery.

1.3.2 Anatomy

The anatomy of the abdominal wall is made up of several layers of muscles and muscle fibers. It is a hexagonal configuration and is bordered by the pelvic wall, pubic symphysis, costal margin, xiphoid, and midaxillary line. The rectus abdominis muscles start at the costal margins and run vertically into the pubic symphysis. Each rectus muscle is attached to the thorax by three digitations to the outer part of the fifth and sixth rib and the seventh costal cartilage. It starts out wide, 10-12 cm, at the costal margin and narrows to 2-3 cm at the pubis symphysis (Caix, 1999).

The side abdominal wall is made up of three layers: external oblique, internal oblique, and the transversus abdominis. The fibers of each muscle run in different directions. The transversus abdominis runs horizontally, the external oblique runs downward and forward, and the internal oblique runs forward and upward. This formation makes it very rare for hernias to occur on the sides of the abdominal wall. They become aponeurotic medially and form the anterior and posterior rectus sheath and insert into the midline of the linea alba (Arslan, 2005)

The linea alba is formed by intersecting fibers of the rectus sheath. It is a medium raphe that runs vertically down the abdominal wall. It is the most common site for incisional hernias because open surgeries typically involve a midline insertion through the linea alba in order to obtain access to the abdominal cavity. At the umbilicus, the linea alba is about 2.24 cm and is about 1.72 cm above and 0.66 cm below. Figure 1.5 shows the orientation and location of the major muscles of the abdominal wall.

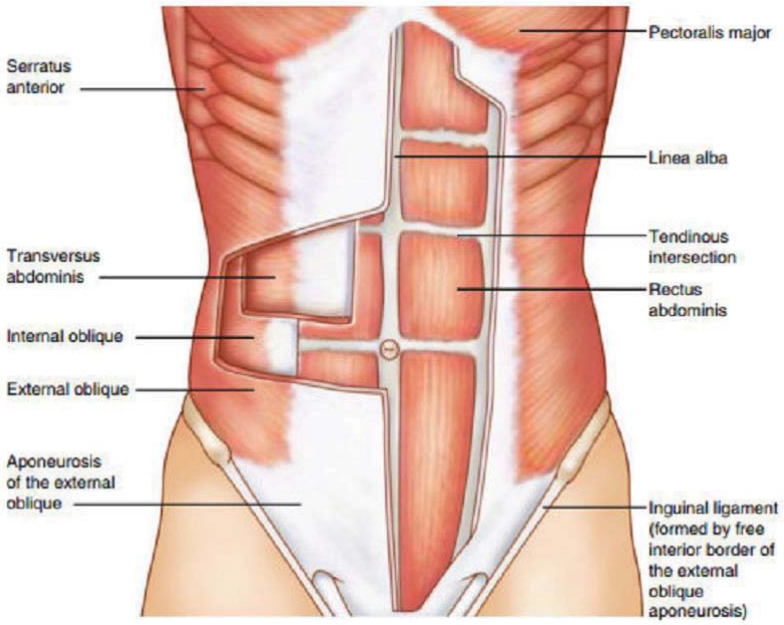

Figure 1.5: Abdominal Wall Muscle Locations (Garcia et al., 2014)

1.3.3 Incidence

Each year, there are anywhere from 3 to 5 million laparotomies. One of the major complications to laparotomy surgery is an incisional hernia, which have a 10% to 20% chance of occurring. This percentage increases to 30% percent if a wound infection develops and can be as high as 60% if it is the repair of a previous incisional hernia or a large hernia, greater than 12cm in diameter. Other factors that put the patient at risk are age, being of male sex, type of surgery, and obesity. Nearly 50% of incisional hernias happen within the first two years after surgery and 74% develop by three years. There are around 600,000 to 800,000 incisional hernia surgeries performed each year (Höer et al. 2002).

1.3.4 Treatment

Before the 1850s, little surgical treatment on incisional hernias was known and most treatments were designed to prevent the growth of the hernia and involved wearing a guarder around the waist. Surgical treatment became popular in the 1880s and 1890s with the use of aponeurotic suturing techniques. One such technique was introduced by Quena (1896). His method required the suturing of several layers of muscle that were adjacent to the incision. This technique was recommended for cases when the rectus abdominis muscle had separated from the rest of the abdomen. Surgical treatments would evolve over the years by using the adjacent muscles to form a "U" shaped muscle over the hernia and aponeurosis suture stitches. The goal of this was to reconstruct and reinforce the incisional area in order to stop the pathology of the hernia.

Up until the 1960s, recurrence rates ranged from 24% to 54% for incisional hernias. This changed when Usher (1962) introduced polypropylene mesh repair in 1958. By using his tension free technique, recurrence rates dropped to 10% to 20%. This drop lead to the production of numerous types of meshes made of various material like: dacron, ivalon, mersilene, nylon, polytetrafluoroethylene, teflon, and velourlined silicone. For incisional hernias, mersilene, polytetrafluoroethylene (PTFE), and velourlined silicone are ideal to use as reported by Arnaud et al. (1977) because the mesh material used in surgery needs to be non-toxic, have longevity, be flexible, resistant, strong, and have minimal tissue reaction. It was soon realized though that the placement and fixation of the mesh was much more important than the mesh material when it came to the quality of the repair. By placing the mesh in a preperitoneal, retormuscular position with a 5cm overlap over the hernia incision in all directions, the recurrence rate was found to be 3% to 5%. The low recurrence rate led to the American Hernia Society to declare the use of mesh as a standard care for incisional hernia repair. The use of mesh has led to an increase in wound infection and other related complications due to the requirement of a wide dissection of soft tissue. In an effort to reduce these complications, recent research has focused on the development of a combine mesh composed of nonabsorbable and absorbable materials.

Laparoscopic, minimal invasive, technique with the addition of using a mesh was made popular in the 1990s by Leblanc and Booth (1993), Franklin et al. (1998), and Kavic (1998). The main advantages to using laparoscopic surgery over open surgery are the lower risk of infections and other post-surgical complications.

When an incisional hernia is discovered, it needs to be repaired quickly, as it will only increase in size and physiologic imbalances. The actual size of the hernia is usually larger

than the visible portion because the tissue surrounding the hernia has also been weaken and needs repaired.

Today both laparoscopic and open surgeries, with the addition of a mesh, are used in the repair of incisional hernia. The type of surgery depends on the country and experience of the surgeon. For open surgery, there are now four techniques used to apply the mesh: inlay, onlay, sublay and component's separation techniques.

Chevrel (1998) first popularized the onlay technique. For this method, the mesh is placed over the abdominal wall closure in the subcutaneous prefascial space. The technique is flexible and allows surgeons to use it for other defects that aren't along the midline of the abdominal wall. For this reason and the fact that it avoids direct contact with the bowel and has less tension on the repair site, it has become the most common techniques for hernia repair accounting for 55% to 65% of all open repairs. The disadvantages of the onlay technique is that it requires a wide tissue undermining that increases the risk of wound complications, and the pressure needed to disrupt the mesh is less than other techniques. Recurrence rates are 15% to 20% if a mesh isn't used, 4% to 7% if a polypropylene mesh is used, and 1% if a fibrin glue is added to keep the mesh in place.

The inlay technique was made popular by Rives and Stoppa (1984). For this approach, the hernia sac is kept and used as a buffer between the mesh and underlying viscera. The mesh is then placed above the posterior rectus sheath and below the rectus muscle. The inlay technique avoids the wide undermining that the onlay techniques requires, but has a much higher recurrence rate of 10% to 20%. This technique has recently be recognized as an inferior operation for its lack of restoring the anatomy and physiology of the abdominal wall as well as the expensive double layer mesh that is required to perform this technique.

Rives et al. (1977) also introduced the sublay technique. For this, the mesh is placed over the closed posterior rectus sheath and peritoneum. Next, the rectus muscles are put into their natural position over the mesh and the sheath is closed. Recurrence rates for the sublay technique are 3% - 5% and it is described to be the best technique for applying a mesh for hernia repair, but there are no randomized case studies to back this statement. The disadvantages for this approach are that it is a more difficult surgery than the other techniques and can only be used on midline hernias.

The components separation technique has been described by Ramirez et al.(1990). It allows for the repair of hernias with gaps of up to 20cm by using flaps from the rectus muscle, anterior rectus sheath, and internal oblique transversus. The external oblique is released from the rectus muscle and a plane is made between the external and internal oblique. The last step is the release of the rectus abdominus muscle from the anterior and posterior sheaths. This method allows for larger incisional hernias to be repaired without meshes, a lower recurrence rate, restoration of dynamic abdominal wall function, and an improvement in the back and postural abnormalities. The components separation technique has been shown to have high wound complications due to the large undermining needed for the surgery.

Laparoscopic has made great advancements since its Introduction. The technique used is similar to those described in Section 1.2.1 in the laparoscopic repair for an inguinal hernia. Studies have shown advantages such as low recurrence rates from 2% to 5%, shorter hospital stays, and a lower risk of infection and complications. Disadvantages are seroma formation at the hernia site, severe pain right after surgery, longer surgical time, and more expensive surgery.

1.4 Background and usage of Mesencymal Stem Cells

Stem cells are usually one of two types: embryonic stem cells (ESC) and adults stem cells. ESCs are gathered from the inner cell mass of the blastocyst and are linked with the formation of tumors. Legal and ethical issues are involved with the use of ESCs whereas these issues are far smaller with the use of adult stem cells (Ding et al., 2011). Multipotent is one of several types of adult stem cells and have the ability to develop into different cell types. A certain type of multipotent stem cells is mesenchymal stem cells (MSCs), also known as mesenchymal stromal cells. MSCs can be gathered from tissues like adipose tissue, bone marrow, endometrial polyps, lung, menses blood, skeletal muscle, synovial membrane, trabecular bone, and umbilical cord. These sites are the most practical because of the ease of harvest and quantity that can be obtained at each site (Rosenbaum et al., 2008). Adipose tissue and bone marrow are the two most common sources to derive MSCs from. Both have the ability to develop into different cells and tissues of mesodermal origins. Adipose derive MSCs (AMSCs) have the advantage of being easier to collect over bone marrow derived MSCs (BMSCs); however, BMSCs have a greater potential for osteogenesis and chondrogenesis. They also possess a greater likelihood of experiencing partial growth arrest and ability to differentiate into osteocytes and chondrocytes than AMSCs. In bone marrow, MSCs only make up 0.01% of the total cell population that can be found in the marrow, but can easily be expanded in cell cultures (Tae et al., 2006).

Studies have used MSCs as possible treatments for many injuries and defects. These studies range from repairing kidney or liver damage to torn anterior cruciate ligaments (ACLs) and Achilles Tendons.

Morgi et al. (2004) looked into the potential of mesenchymal and hematopoietic stem cells to cure acute renal failure. He did this by subcutaneous injections cis-diaminedichloroplatinum dissolved in sterile 0.9% saline into female mice. The mice were then divided into two groups: group 1 was given saline and group 2 was given BMSCs at a concentration of 2×10^5 cells. The mice were then killed at four, seven, eleven, and twenty-nine days. There was also a group 3 which received hematopoietuc stem cells at a concentration of 2×10^5 and were euthanized at four, seven, eleven, and twenty-nine days. By looking at the blood urea nitrogen (BUN), it was shown that the mice that had been treated with MSCs were more protected against renal failure when given cisplatin than the saline group.

The effects of BMSCs had on acute liver failure has been looked at by Yuan et al. (2013). Sixty rats underwent a D-galactosamine model/ lipopolysaccharide induced liver failure. They were then split into two groups: a control group that was given a saline injection and the MSCs group that received an injection 1.4×10^7 cells/kg of MSCs in the vein of the tail. Samples were then taken at twenty, twenty-four, one hundred twenty, and one hundred sixty-eight hours.

It was found that serum levels of alanine aminotransferase (ALT) and aspartate aminotransferase (AST) were much lower in the BMSCs group than the control group. HEstaining showed a significant reduction in inflammatory cell infiltration in the BMSCs group compared to the control group and the liver lobular was in recovery. TUNEL method was used to examine the apoptosis levels. The BMSCs group had lower levels of apoptosis than the control group. From this study, it was found that after BMSCs were implanted, liver function gradually improved, liver cell necrosis gradually reduced, promoted hepatocyte

proliferation and liver angiogenesis, and regulated the immunity and inflammatory responses of liver in hepatic failure rats.

Pacini et al. (2007) investigated the effects BMSCs had on superficial digital flexor tendon (SDFT) in horses. Eleven horses showing lameness underwent ultrasound examinations and showed lesions on their SDFT. MSCs at a 1.6 x 10^6 cell concentration were then injected inside the core lesion. A control group of fifteen horses were treated in a veterinary department using standard therapy for SDFT lesion. Of the eleven horses, nine were able to return to racing form. The ultrasound images showed initial healing at one month and appeared to be completely healed at six months and were able to return to the same level of competition before injury within nine to twelve months. After two years, all horses were still active and have shown no signs of reinjuring the tendon. For the two horses that didn't recover, one died during the study and the other received less than 1 x 10^6 cell dosage and the tendon was re-injured during recovery. The control group's ultrasound images showed fibrosis during healing and all tendons were re-injured around seven months. The Pacini study shows that MSCs can make a significant contribution in the healing of SDFT in horses.

Merritt et al. (2010) studied how BMSCs could be used to help repair traumatic skeletal muscle injuries. Mice were placed into two groups: group 1 extracellular matrix (ECM) only and group 2 ECM-CELL which received the stem cells seven days after surgery. The surgery involved creating a defect in the lateral gastrocnemius by the removal of a Section of muscle. This Section was then weighed and dimensioned so that an equal weight and dimensioned portion of ECM could be implanted in its place. The mice were then euthanized at seven, fourteen, twenty-eight, and forty-two days.

Histological and maximal isometric tetanic force values were higher in the ECM-CELL than the ECM-ONLY group at forty-two days. The number of desmin-positive fibers per square millimeter was also significantly greater in the ECM-CELL group and there were more myogenin-positive nuclei. From this data, it was shown that MSC seeded ECM can help repair injured muscle that cannot functionally regenerate without treatment. The ECM-CELL group also exhibited muscle that was similar to noninjured muscle after forty two days. The muscle tissue also presented near-normal function per unit of cross-sectional area.

Ouyang et al. (2002) investigated the healing effects bMSCs had an Achilles tendon repair in rabbits. For this study, sixteen rabbits were divided into three groups: group 1 had six rabbits and were treated with a knitted PLGA graft and seeded with $1x10^7$ bMSC, group 2 had six rabbits and were treated with just the knitted PLGA scaffold, and group 3 had four rabbits and were repaired by sutures only. At two, four, eight, and twelve weeks; rabbits were euthanized and the tendons were harvested so that macroscopic and histological examinations could be performed.

From the macroscopic report, it was observed that group 1 had more regenerated tissue than groups 2 and 3. The histological exam showed that group 1 had more eosinophilic tissue formation and could be seen after two weeks. This pattern continued with each of the harvest times as the collagen seemed more organized and the tissue more mature. The Ouyang study proved that the healing process of a rupture Achilles tendon could be improved with the addition of BMSCs to the PLGA scaffold.

Young et al.(1998) performed a similar study to Ouyang and focused on repairing the Achilles tendon by using mesenchymal stem cells in a collagen matrix. For this

investigation, fifty-three female New Zealand White rabbits had a 1 cm long defect created in their Achilles tendon and were treated by either suturing the tendons together, control group, or by suturing and adding $4x10^6$cell/ml MSCs, treated group. The rabbits were euthanized at four, eight, and twelve weeks and the tendons were extracted for testing.

The cross sectional areas of the treated tendon was 15.1±6.8, 10.4 ±3.7, and 7.4 ±2.8 mm^2 for four, eight, and twelve respectively weeks compared to 8.4 ±1.9, 6.3 ±1.9, and 5.4 ±2.6 mm^2 for the control. A normal Achilles tendon is 4.3 ±1.3mm^2 in area. The treated tendon is considered to be healing better because a significantly faster decline in area over the course of twelve weeks ($p < 0.05$). For the structural properties, the stiffness, force, and energy (max and failure) in the treated samples were found to be twice that of the controls, Table 1.1. All treated means in Table 11.1 were significantly greater than controls ($p < 0.05$) The treated samples also had higher material properties than the control and increased significantly more over the twelve weeks, Table 1.2.

Table 1.1: Structural properties for Treated (T) and Controlled (C) Repairs (Young et al.)

Structural properties	Normal (n=5)	Repair	4 wk (n=13)	8 wk (n=13)	12 wk (n=13)
Stiffness (N/mm)	36.5 ± 10.6	T	19.8 ± 1.9	22.9 ± 3.3	23.0 ± 2.5
		C	9.7 ± 1.9	11.4 ± 1.5	11.5 ± 2.2
$Force_{max}$ (N)	189.0 ± 26.8	T	124.0 ± 13.0	114.3 ± 18.3	130.3 ± 16.0
		C	58.0 ± 11.3	60.3 ± 10.4	57.3 ± 11.7
$Energy_{max\ force}$ (n*mm)	555.5 ± 79.7	T	525.1 ± 90.5	365.8 ± 84.3	485.6 ± 91.6
		C	199.9 ± 44.6	196.1 ± 39.4	168.7 ± 36.0
$Energy_{failure}$ (n*mm)	901.1 ± 317.2	T	710.5 ± 88.8	539.1 ± 101.0	737.0 ± 182.1
		C	311.7 ± 47.5	353.4 ± 47.5	290.5 ± 52.1

Table 1.2: Material properties for Treated (T) and Controlled (C) Repairs (Young et al.)

Material properties	Normal (n=5)	Repair	4 wk (n=13)	8 wk (n=13)	12 wk (n=13)
Modulus (MPa)	337.5 ± 205.8	T	53.4 ± 4.9	90.3 ± 10.4	114.4 ± 7.6
		C	33.5 ± 7.0	62.2 ± 9.2	67.9 ± 9.8
$Stress_{max}$ (MPa)	41.6 ± 18.9	T	8.6 ± 0.8	10.5 ± 1.4	15.5 ± 1.1
		C	4.7 ± 1.1	7.2 ± 1.3	8.0 ± 1.2
Strain Energy $Density_{max\ stress}$ (N*mm/mm^3)	3.9 ± 0.4	T	1.0 ± 0.1	0.8 ± 0.2	1.4 ± 0.2
		C	0.4 ± 0.1	0.5 ± 0.1	0.6 ± 0.1
Strain Energy $Density_{failure}$ (N*mm/mm^3)	6.7 ± 3.6	T	1.3 ± 0.1	1.2 ± 0.2	2.1 ± 0.4
		C	0.7 ± 0.1	0.9 ± 0.1	1.0 ± 0.1
Toe limit stress (MPa)	6.8 ± 0.6	T	2.2 ± 0.3	2.8 ± 0.4	3.9 ± 0.4
		C	1.4 ± 0.3	1.6 ± 0.2	2.7 ± 0.4
Toe limit strain (%)	9.0 ± 2.3	T	11.2 ± 1.0	8.9 ± 1.3	10.0 ± 0.7
		C	11.8 ± 1.3	12.5 ± 5.3	13.8 ± 5.2

All treated means were significantly greater than controls ($p < 0.05$), except for toe limit stress, toe limit strain, and eight week strain energy density values. Figure 5 in Young's study showed a stress-strain curve comparing the MSC treated samples and the control samples at twelve weeks recovery. The stress between the two groups remains relatively the same until a strain of 0.10 mm/mm where the MSC treated group begins to see a drastic rise in stress as the strain increases. The maximum stress for the treated group was 12 MPa at a strain of 0.18 mm/mm compared to the 6 MPa at a strain of 0.15 mm/mm for the control.

This study showed how MSCs in a collagen matrix can be used for Achilles tendon repair. Through mechanical testing, it was shown that not only did the treated samples have significantly higher structural and material properties, but it was also shown that these properties increased at a faster rate over time than in the control.

Ge et al. (2005) looked at repairing the anterior cruciate ligament, ACL, by using bone marrow derived mesenchymal stem cells and a fascia wrap. Forty-eight male New Zealand

White rabbits were used and divided into four groups: group 1 was repaired only using 2 scaffolds, group 2's repair was performed with 2 scaffolds and a concentration of 3 million MSCs, group 3 consisted of 2 scaffolds, MSCs and the fascia wrap, and group 4 had 2 scaffolds and the fascia wrap. After twenty weeks, the rabbits were euthanized and histology, mechanical testing, and western plot analysis were performed.

The MSCs and fascia wrap were able to improve collagen type 1 and type 3 regeneration and excretion, however, they were not able to improve the maximal tensile load: 14.0 ± 7.8N, 14.9 ± 6.6N, 20.9 ± 4.5N, and 15.8 ± 6.8N for groups 1, 2, 3, and 4. The same was seen for the stiffness: 8.6 ± 2.3N/mm, 7.8 ± 3.2N/mm, 8.4 ± 2.2N/mm, and 7.4 ± 3.4N/mm. The normal value for tensile load is 151.8 ± 20.8N and for stiffness is 50.4 ± 5.3 N/mm.

In a study done by Ju et al. (2008), MSCs were investigated to see how they enhanced the healing of tendon-bone in ACL repair. For the study, eighteen rats were put into two groups, the control group and the MSC group, and were killed at one, two, and four weeks for histological examination. In the MSCs group, a concentration of $1x10^7$ was immobilized in 0.2ml atelocollagen gel and injected into the bone tunnel. The control group received same treatment without the MSCs.

At one week, the presence of grafted tendon was found in the proximal tibia tunnel. In the control group, the tendon-bone interface was made of cellular and vascular fibrous tissue; where as in the MSCs' group, there had been an increase in collagen fibers. The results at two weeks showed that the tendon-bone interface still existed in both groups. Quantification analysis showed a much higher amount of oblique collagen fiber area to the interface for the MSC group compared to the control group. At four weeks, the implanted tendon seemed to

be attached to the bone in both groups and interface tissue could not be observed. Based on the results, MSCs could be used as a potential way to accelerate tendon-bone healing. Similar studies done by Ouyang et al. (2004) and Dong et al. (2012) on the use of MSCs for bone to tendon healing have come to the same conclusion.

Nakagawa et al. (2005) performed a study to see if human mesenchymal stem cells (hMSCs) and varying amount of basic fibroblast growth factor, bFGF, could improve skin-substitute wound healing. For this, seventy-five male rats were used in the experiment. The rats were broken down into five groups with four groups having $5x10^6$ cells/ml of hMSCs, 5 µL of Dulbecco's modified Eagle's medium, DMEM, and a varying amount of bFGF: 0, 1, 10, or 100 µg. The other group was a control group and it only received 5 µL of DMEM. During surgery, 1.5 x 1.5 cm, an area of 2.25 cm^2, of skin tissue was taken off the rats and hMSCs and the varying bFGF were applied to the area. Five animals in each group were then killed three, seven, and forty-two days post-surgery.

After three days, there wasn't much of a difference in wound size in any of the groups as they were still around the original area of 2.25 cm^2. At seven days, there was a significant difference between the hMSCs groups and the control group. There was also a significant difference between the hMSCs alone and any of the bFGF groups. The wound sizes were 1.21 ±0.171 cm^2, 0.76 ± 0.139 cm^2, 0.35 ± 0.129 cm^2, 0.15 ± 0.069 cm^2 and 0.15 ± 0.160 cm^2 for the control group, hMSCs, hMSCs + 1µL bGF, hMSCs + 10µL bFGF, and hMSCs + 100µL bFGF. By day forty-two, the wounds in all groups were healed. When looking at the histology reports, the hMSCs groups contained a higher cell density than the control at seven days. Also, the group that contained 10 and 100µg of bFGF were almost covered with

epithelium; this wasn't seen in the other three groups. The control group did exhibit more defects on the edges than any of the hMSCs treated group.

The study showed that hMSCs alone can aid the healing process of wounds and can be aided further with the addition of bFGF. It was shown that the hMSCs + 10μg bFGF produced the best results both in healing rate and in histology reports.

Liu et al. (2006) investigated how BMSCs affected the mechanical mechanism during wound healing. In his study, adult male rats had a 5 cm incision made on the midline abdominal fascial using a scalpel. The incision was then sutured closed and a MSC concentration of $2x10^6$ was injected into the tail vein once daily for four days starting twenty-four hours after surgery. The rats were euthanized at seven and fourteen days and their wound busting strength was tested.

The rats that received a daily dosage of BMSCs had a significantly higher bursting strength than the controlled rats that were only repaired with sutures. The untreated rats had strength of 6.49 ± 2.1N at seven days and 8.20 ± 0.39N at fourteen days. The treated rats bursting strength was 11.43 ± 2.3N and 11.43 ± 4.9N for seven and fourteen days respectively. These results show that by adding bone marrow stromal cells to midline abdominal fascial incisions can increase the wound bursting strength. Similar studies done by Kwon et al. (2008) and Stoff et al. (2009) have showed similar results in terms of increased wound bursting strength.

Wu et al. (2007) performed a study in which mice were treated one of three ways: BMSCs, allogeneic neonatal dermal fibroblasts, or vehicle control medium. The treatments were for chronic wounds in diabetic and nondiabetic mice. The mice were divided into three groups and two 6mm excisional skin wounds were created on each side of the midline. Each group

was then treated one of the three ways mentioned earlier, the amount of BMSCs applied was 1 million cells/ml. At days zero, three, seven, ten, fourteen, twenty-one, and twenty-eight; pictures of the wound were taken and used to measure the percent closure. Mice were also sacrificed at seven, fourteen, and twenty-eight days for histologic data.

Both diabetic and nondiabetic mice healed faster when treated with BMSCs than those that were treated with fibroblast or vehicle medium. The BMSCs exhibited wound healing as early as three days and was noticeable at seven days. At twenty-eight days, 4 of the 12 wounds in the diabetic BMSCs treated group were completely healed; whereas none of the wounds were healed in the other groups. Due to complications, the nondiabetic group stopped measuring at fourteen days.

The histology report was only done on the nondiabetic mice. At seven days, there was complete covering of epithelium on all 10 wounds examined that had been treated with BMSCs whereas the fibroblast had only 6 out of 10 sample covered and 4 out of 10 samples were covered with epithelium for the vehicle medium treated. The BMSCs group also exhibited a higher cellularity, an increase in vasculature, and granulation tissue seemed to be thicker and larger at seven and fourteen days. This group also showed a higher amount of skin appendages, 10.2 ± 0.79 per wound section compared to fibroblast 4.7 ± 0.53 and vehicle medium 4.5 ± 0.42, which suggests enhanced cutaneous regeneration.

This study establishes the benefits of BMSCs in cutaneous regeneration and wound healing in nondiabetic and diabetic mice. Administration of allogeneic BMSCs may represent a novel therapeutic approaches in the treatment of chronic wounds and other conditions.

In McFarlin et al. (2006) study, BMSCs were used to heal fascial and cutaneous incisional wounds in Sprague-Dawley rats. A 5 cm long cut was made on the midline abdominal fascial and sutured closed. The BMSCs were applied four ways: group 1 got daily injections in the tail vein of $2x10^6$ cells for four days starting twenty-four hours after surgery, group 2 got a single treatment of $5x10^6$ cells twenty-four hours after treatment spread along 10 locations of the wound, group 3 had 6×10^6 BMSCs applied right after closure, and group 4 was a dosage of $5x10^6$ cell/ml injected into the tail one time twenty-four hours after surgery. The control group was not treated with any material. After seven and fourteen days, the rats were euthanized and their mechanical strength was tested. The study also wanted to see if syngeneic BMSCs, groups 1, 2, & 3, would have the same effect as allogeneic BMSCs, group 4, and to see if BMSCs migrate to the wound.

The wound busting strength (WBS) was found to be 2-3 times greater in group 1 treated rats than the controlled rats. Group 1 had strength of 11.6 ± 3.3N at day 7 and 14.8 ± 2.9N for day fourteen, where the controlled had strength of 4.1 ± 1.0N and 8.0 ± 0.4N. The healing of cutaneous skin was found to be of greater strength in group1, 8.28 ± 3.9N, than in the control, 3.4 ± 0.9N after seven days. For group 2, it was found to have a WBS of 9.48 ± 3.3N vs. the 3.47 ± 0.9N of the control group. Group 3 showed a 10.03 ± 3.8 N vs. 4.71 ± 2.1N for the control group. For the allogeneic BMSCs, the WBS of group 4 was found to be 11.44 ± 3.1N compared to the 3.69 ± 1.2N of the control group. In order to determine if the BMSCs go to the site of the wound, $1x10^6$ iron and DiI-labeled BMSCs were injected into the tail vein twenty-four hours after surgery and tissue from the wound was harvested six days later. The wound tissue and surrounding muscles showed iron positive cells and through fluorescent microscopy, it was shown to have fluorescent positive cells at the same

locations. Group 1 was also tested for collagen levels at seven & fourteen days and was found to be much higher, 1,054.6 ± 47ug/g and 1,373.4 ± 59.7ug/g, than the control group, 855.6 ± 43.9ug/g and 1,213.1 ± 29.3ug/g. The histology of the treated tissue had obvious difference from the control group in the form of tissue organization, cellular infiltration, neovascularization, and collagen matrix.

In conclusion, this study showed that BMSCs could be used to treat fascia wounds and that they can be delivered two different ways. It was shown that BMSCs migrate to wounded areas, increase collagen levels, and improve the histology of the tissue. The study also showed that allogeneic BMSCs had the same effect on wound healing as syngeneic BMSCs.

1.5 Background and Usage of Platelet-Rich Plasma to Enhance MSCs

Platelet-rich plasma (PRP) is an autologous product that has been an evolving resource for orthopedic surgery and regenerative medicine. (Smith and Webbon, 2007) It concentrates a large number of platelets in a small volume of plasma and functions as a fibrin tissue adhesive. It differs from fibrin glue as it promotes wound healing and improves osteogenesis. PRP helps accelerate endothelial, epithelial, and epidermal regeneration, stimulates angiogenesis, boosts collagen synthesis, helps soft tissue healing, decreases dermal scarring, improves the hemostatic response to injury, and reverses the inhibition of wound healing caused by glucocorticoids. The high leukocyte concentration of PRP has an added antimicrobial effect. Since PRP is an autologous blood product, it carries no risk of transmitting infectious disease.

Lucarelli et al. (2003) found that PRP has the ability to enhance the proliferation of stem cells. This was verified in a study done by Mishra et al. (2009) who investigated PRP to see

if it could be used to help the healing process of cartilage regeneration. To do this, a cell culture experiment was created where MSCs were grown in a controlled media and a media enhanced with inactivated buffered PRP. The proliferation and messenger RNA level of the osteogenic, chondrogenic, and aggrecan were checked after seven days. For each of these readings, the media that had been enhanced with PRP showed significantly higher results than the control media. The control media had a proliferation of 0.199 compared to 1.041 of the PRP buffered media. For the messenger RNA level of the osteogenic, chondrogenic, and aggrecan; the PRP media had readings of 52.84, 29.74, and 21.04 where the control readings were 26.88, 1.93, and 2.29. From these results, it was confirmed that PRP can enhance the proliferation of MSCs and that PRP causes chondrogenic differentiation of MSC in vitro.

Pieri et al. (2009) used eight minipigs to see the effect that PRP and BMSCs at a concentration of $4x10^7$ cells had on the defects on the alveolar ridge. For this experiment, the second and fourth premolar teeth were removed on both sides and left to heal naturally for two months. Next, a standardized cylindrical bone defect was made in each root that measured 3.5mm in diameter 8mm in depth. They were then filled one of four ways: fluorohydroxyapatite (FHA) granules alone (negative control), autogenous mandibular bone (positive control), FHA granules mixed with PRP, and FHA granules mixed with MSCs and PRP. The minipigs were left to heal for three months.

Histologic examination revealed that there was more new bone with fewer marrow spaces in the MSCs + PRP + FHA group than the other groups. The bone morphology was more mature and organized than the FHA and PRP + FHA groups. The histomorphometric evaluation looked at the vital bone, residual graft particles, and newly formed bone in direct contact with the FHA particle surroundings. These results can be seen in Table 1.3.

Table 1.3: Root Healing after 12-Week Period (Pieri)

Group	Vital Bone	Residual Graft Particles	New bone in contact with FHA
FHA	33.80%±1.40%	33.80%±1.40%	46.43%±5.20%
PRP + FHA	37.95%±2.23%	32.83%±1.39%	48.37%±4.11%
MSCs + PRP + FHA	45.28% ± 2.01%	30.73%±1.61%	59.23%±3.53%

The study showed that the addition of MSCs to PRP + FHA enhanced the amount of new bone seen in the minipigs when compared to FHA and FHA + PRP. The MSCs grouped also produced similar results to those seen when autogenous bone grafts are used.

In a study done by Kawaguchi et al.(2004), MSCs were used to regenerate periodontal tissue, also known as gum tissue, which had been weakened by disease. The studied was done on 12 female beagle dogs. The MSCs were taken from the iliac crest of each animal and the cell culture was expanded in vitro by the technique laid out by Tsutsumi (2001). After two weeks, the MSCs were harvested, mixed with atelocollagen (2% type 1 collagen), and surgery was performed on each dog. The dogs were broken down into five groups; four cell concentrations and a control group. The four concentrations were $2x10^6$ cells/ml, $5x10^6$ cells/ml, $1x10^7$ cells/ml, and $2x10^7$ cells/ml and the control group consisted of just the atelocollagen.

After one month, tissue healing was evaluated by histological and morphometric analyses. The defects that were shown due to the gum disease were regenerated with new amounts of bone, periodontal ligament, and cementum in the MSCs group while in the control group, no cementum was regenerated in the bone loss area. The study showed that for the percentage of new cementum there wasn't much of a difference between each of the concentration groups, but there was a difference when compared to the control group. The MSCs groups of

$2x10^6$, $5x10^6$, $1x10^7$, and $2x10^7$ cells/ml were 93.9% ± 14.3%, 96.7% ± 5.23%, 91.3% ±12.3%, and 94.4% ± 8.27% of new cementum, whereas the control group only had 70.5% ± 12.0%, Figure 1.13a. For new bone area, there was a noticeable difference between each of the concentrations and the control group. The MSCs groups of $2x10^6$, $5x10^6$, $1x10^7$, and $2x10^7$ cells/ml were 62.6% ± 14.6%, 62.5% ± 13.6%, 65.8% ± 9.62%, and 68.1% ±10.7% whereas the control group only had 54.8% ± 10.7%,.

This study showed that the addition of MSCs helped in healing of periodontal tissue by providing a significant amount of new cementum length and of new bone area when compared to the control group. It was also important to point out that the 68.1% of new bone area for the dosage of 2 $x10^7$ is very close to the 73% found in normal specimens.

Pham et al. (2013) investigated the effect PRP had on Adipose-derived stem cells (ADSCs) when used to regenerate articular cartilage. They theorized that by using PRP, the efficiency of the treatment would be an improvement over just using ADSCs alone. The experiment was done in vivo on mice with four groups: ADSCs and fetal bovine serum (FBS), 10% concentration of PRP and ADSCs, 15% concentration of PRP and ADSCs, and 20% concentration of PRP and ADSCs.

To see the effects that PRP had on ADSCs, a cell proliferation was performed. The difference between the three PRP groups and the FBS10 group could be seen three days after surgery. At day 7, the difference was even greater between the groups, with the 15% and 20% concentration of PRP being significantly higher than the 10% PRP concentration.

The PRP showed an increase on the amount of collagen type II, Sox9, and aggrecan. The FBS10 group had 20.7± 5.13 type II collagen were as the PRP concentrations of 10%, 15%,

and 20% had 60.33±11.68, 67.67±23.80, and 69.00±15.62. Sox9 was 41.33±7.09, 54.33±10.07, and 44.33±6.03 in PRP10, PRP15, and PRP20 compared to 4.67±2.08 for FBS10. Aggrecan was also significantly less in FBS 10, 3.00±1.00, compared to PRP10, 27.67±6.51, PRP15, 45.00±6.24, and PRP20, 41.33±5.86. There was also less VEFG-A found in the PRP concentration than in the FBS10: 536.67±40.41ng/ml, 336.67±51.32ng/ml, 380.00±50.00ng/ml, and 1,493.33±143.64ng/ml for PRP10, PRP15, PRP20, and FBS10. The last thing looked at was the cartilage regeneration. When compared to a negative control group, PBS injection, the PRP15 had a recovery time for hind leg movement of 15±4 less days, whereas the FBS10 group was the same as the negative control group. The histological analysis should the PRP15 group showed a mean area of damaged joint cartilage of 70% with 45% regenerated cartilage after forty-five days. The FBS10 had the same percentage of damaged cartilage but only had 30% regenerated cartilage and the negative control group had 80% damaged cartilage with only 20% regenerated cartilage.

By measuring the amount of type II collagen, Sox9, aggrecan, and VEFG-A and histological analysis, the study was able to show the advantages PRP can have on ADSCs when compared to FBS for regenerating joint cartilage.

The effects that AMSCs and BMSCs had on cartilage regeneration were investigated by Xie et al. (2012). In thirty-six rabbits, bilateral patellar groove osteochondral defects were created on both knees giving seventy-two total defects. The defects were then randomly treated one of four ways: left unfilled, filled with PRP, PRP with AMSCs, or PRP with BMSCs. The rabbits were euthanized at six, nine, and twelve weeks.

The BMSCs responded to the PRP more efficiently than the AMSCs with a significant statistical difference. In chondrogenic, collagen I, collagen II, and Aggrecan protein; BMSCs yielded better results than the AMSCs. At twelve weeks, the tissue treated with BMSCs appeared well integrated with the adjacent regions and the surface resembled smooth, opawue hyaline cartilage. The adipose treated tissue seemed fibrillated and less mature. The histological evaluation was 773.9 ± 82.4 and 928.6 ± 130.6 for the adipose group and 841.6 ± 98.9 and 1048.1 ± 164.3 for the bone marrow group at six and twelve weeks.

In conclusion, even though AMSCs did improve the healing of patellar defects, they had a lower response to PRP stimulation and were inferior in chondrogenic differentiation in vitro and in vivo when compared to the BMSCs.

Kitoch et al. (2004) investigated BMSCs and PRP as a possible enhancement during distraction osteogenesis, the reconstruction of skeletal deformities and lengthen of the long bones in the body. Ten limbs from seven different patients were to be treated; but since four patients were still under treatment at the time, only three could be fully evaluated. At the time of surgery, bone marrow stem cells were taken out of each patient and expanded to a concentration in the 10^7 range. The patients received BMSCs injections at twenty-one days post-surgery and at the end of distraction.

For distraction osteogenesis, the results are usually measured in terms of the amount of length gained, complications or additional procedures, and numerical parameters such as healing index. The three patients had no major complications and no further surgeries were needed. The average healing index was 23.0 days/cm which is substantially less than the average of 38.7 days/cm for the 30 limb extensions that were used as a control value. Even

though the study only offered a small sample size, it provided promising results towards the advancement of distraction osteogenesis.

Chen et al. (2011) investigated the effects that tendon stem cells (TSCs) seeded with PRP had on Achilles tendon repair. For the study, ninety-six rats were divided into four groups: tendon stem cell treatment, PRP treatment, PRP and TSCs treatment, and phosphate-buffered saline. The TSCs were at a concentration of $3x10^6$cells/ml. At three and fourteen days after surgery, 6 rats per group were euthanized and the morphology and histology of the Achilles tendon was checked. Through the histology and morphology examinations, the PRP with tendon stem cells treatment showed more collagen type 1, collagen type 3, and tenascin C than any of the other groups. From the results, it can be seen that the addition of PRP to tendon stem cells can enhance performance of cells in the healing of an Achilles tendon repair.

Lee et al. (2013) investigated the effectiveness of MSCs with PRP gel in the repair of damaged articular cartilage in rabbits. In his experiment, eighty-one male New Zealand rabbits had an osteochondral defect created in their trochlear groove of the femur and were divided into three groups: the control group in which the defect was left untreated, the PRP which group had the defect filled with PRP, and the PRP and MSCs group which had the defect filled with an autologous of SMSCs ($2x10^7$ cells/mL) embedded in PRP.

After twenty-four weeks, the defects were examined. In both groups containing PRP, the defect was repaired with hyaline cartilage whereas the control group had fibrous tissue. The PRP groups also showed higher levels of safranin O staining, type 2 collagen immunostaining, glycosaminoglycan content, cumulative histologic scores, and number of

proliferation cells than the control group. The PRP group exhibited incomplete bone regeneration and irregular cartilage surface whereas the PRP and MSCs group did not. This study has shown that MSCs with PRP could be used to help resurface the defect with cartilage and restore the subchondral bone.

1.6 Histology Analysis

For the study that will be described in Section 2.3.2, a histological analysis was performed by Heffner et al. (2012). Four observers scored the samples on a scale from 0 – 3 for collagen organization, collagen abundance, and myocyte degeneration. The mean and standard deviations for each group can be seen in Table 1.4.

Table 1.4: Histological Analysis Data Summary for Groups 1A - 3B (Heffner et al., 2012)

Groups	Organization	Abundance	Degeneration	Neovascularization
Control at 4 wks	1.21 ± 0.96	1.11 ± 0.69	1.32 ± 1.06	2.0 ± 1.3
Control at 8 wks	1.46 ± 1.04	1.32 ± 0.86	0.93 ± 0.66	1.5 ± 0.8
PRP at 4 wks	1.11 ± 0.69	1.57 ± 0.74	1.93 ± 0.94*	1.4 ± 1.1
PRP at 8 wks	1.07 ± 0.86	1.25 ± 0.80	1.18 ± 0.94	1.5 ± 0.7
PRP + MSCs at 4 wks	1.57 ± 0.63	2.36 ± 0.73*	1.32 ± 0.77	4.2 ± 2.3*
PRP + MSCs at 8 wks	1.42 ± 0.88	1.83 ± 0.82*	0.96 ± 0.75	5.9 ± 2.8*

*$P < 0.05$ on the basis of Mann-Whitney paired analysis and Kruskal-Wallis group analysis. Data is given as mean and standard deviations for all groups.

The histology analysis performed by Heffner showed that the combination of PRP + MSCs produced significantly higher collagen abundance and neovascularization for both four and eight weeks over the control and PRP alone groups at four and eight weeks. The PRP alone group at four weeks also had a significant difference in degeneration compared to the other five groups. This study showed that the combination of PRP + MSCs produced better histology scores at four and eight weeks than the control and PRP alone groups at four and eight weeks.

For the study that will be described in Section 2.3.3, a histological analysis was performed by Bown (2013). Three observers scored the samples on a scale from 0 – 3 for collagen organization, collagen abundance, and myocyte Regeneration. The mean and standard deviations for each group can be seen in Table 1.5.

Table 1.5: Histological Analysis Data Summary for Groups 9A – 13A (Bown, 2013)

Concentration	Organization	Abundance	Regeneration
2.5 x 10^4 cells/ml	1.28 ± 0.17	1.43 ± 0.14	1.52 ± 0.19
5 x 10^4 cells/ml	1.76 ± 0.17	1.95 ± 0.13	1.09 ± 0.22
1 x 10^5 cells/ml	2.14 ± 0.14	2.24 ± 0.14	1.00 ± 0.18
2.5 x 10^5 cells/ml	1.71 ± 0.18	1.95 ± 0.13	1.19 ± 0.20
5 x 10^5 cells/ml	1.66 ± 0.22	1.75 ± 0.18	1.24 ± 0.22

The cell concentration of 1x10^5cells/ml had the most collagen abundance and organization. It had significantly higher collagen organization than the concentration 2.5 x 10^4 cells/ml ($p < 0.002$). The concentration of 2.5 x 10^5 cells/ml also had significantly higher abundance that concentrations 2.5 x 10^4 cells/ml ($p < 0.001$) and 5 x 10^5cells/ml ($p < 0.001$). The concentration of 5 x 10^4 cells/ml ($p = 0.013$) and 2.5 x 10^5 cells/ml ($p=0.013$) were significantly higher than the concentration of 2.5 x 10^4cells/ml. There was no significant difference between the myocyte regeneration. From this data, Bown concluded that the concentration of 1 x 10^5cells/ml had the best histology scores and was the optimal dosage.

1.7 Finite Element Analysis

A validated finite element model can provide researchers with the opportunity to investigate biomechanics of the abdominal fascia and serve as a intermediate for testing surgical techniques and implant designs. It can also provide a way of obtaining results without having to do clinical studies. A selection of finite element models are presented here to give

an indication of just how finite element models have been used for medical applications. A selection of articles in which metal samples underwent a tensile test and finite element models were made to simulate these test were also selected to get an idea of how close our finite element models should be.

Jounet et al. (2007), Paulino et al. (1999), Niebur et al.(2000), and Davis et al. (2013) each performed studies to simulate tensile tests and compared their results to the experimental tensile test data. The studies performed by Joun and Paulino were done on metal samples and show that if a material has the same material properties throughout, a finite element model can be made to perfectly simulate a tensile test. Niebur and Davis simulated tensile tests on soft tissue.

Joun's study emphasized on predicting the necking of a low-carbon steel using a finite element model and comparing it to the necking that occurs during a tensile test. The stress-strain curves from the finite element models match the stress-strain curves from the tensile test data. The correlation between the two stress-strain curves allowed the necking to be perfectly predicted in the finite element models. Paulino performed fracture testing and finite element modeling of pure titanium in-order to develop a J-R testing protocol and numerical procedures that could be used to functionally grade titanium/titanium boride layer material. Similar to Joun's study, Paulino was able to perfectly replicate the experimental stress-strain curve using the finite element model data.

Niebur investigated the ability to predict trabecular bone, bone tissue or supportive connective tissue, failure using computational models. To simulate failure of seven bovine tibial specimens, a bilinear constitutive model with asymmetric tissue yield strains was made.

Yield stress for tension, compression, and shear tests were found experimentally and by finite element models. For each test, the yield stress was found to be slightly higher in the experimental models than the simulated models. The difference in tension was 3.6%, compression 0.1%, and shear 2.0%. These low percent differences establish that finite element models can be considered an effective replacement for a real specimen.

Davis's study focused on comparing tensile test data of liver samples obtained from a study done by Kemper et al. (2011) to a computational model using a material law, which took strain rates into account, proposed by Samur et al. (2007). The average percent difference of the peak tensile stress was 13%, 12%, 24%, and 50% at strain rates of 10 mm/s, 1 mm/s, 0.1 mm/s, and 0.01mm/s respectively. It was also discovered that hexahedral mesh types more accurately predict the stress-strain curves than the tetrahedral mesh. Davis's study showed that soft tissue tensile test could be modeled with accurate results at high strain, but had poor results at lower strain rates.

1.8 Scope of Work

In consideration of the literature review covering hernia biomechanics, repair techniques, treatments, and finite element analysis, several objectives were created in order to create an experimental protocol and computer model that would help analyze the healing of the hernia tissue. The end goal is a model that can accurately simulate a tensile test of the repaired hernia tissue.

1.8.1 Create an Experimental Design

This study focused on the repair and prevention of hernias on the abdominal wall. As a preliminary study, a simple model that can be easily repeated needed to be designed for

testing the healing effects of MSCs and PRP. References for such a design were indicated in Sections 1.4 and 1.5. For these investigations, a rat model was used to test the healing effects of certain treatments on fascia wounds. To keep the experimental samples as consistent as possible, a stamp was used to harvest abdominal wall tissue to keep the length and width similar for each sample. To investigate the healing of the tissue, a tensile test was performed on the samples.

1.8.2 Develop a Finite Element Model

In order to develop a finite element model, a 3-dimensional model of the tissue sample was created in SolidWorks using the dimensions taken from the actual sample before the tensile test. The SolidWorks model was imported into Autodesk Simulation Multiphysics 2012 and appropriate boundary conditions and mesh conditions were applied. To validate the model, a displacement from the tensile test data was used and the force from the finite element model was compared to the tensile test force at that same displacement.

1.8.3 Provide Future Insight on Work

Once the experimental and computational results were complete, trends that needed further investigation or abnormalities in the data were addressed through changes in protocol or the development of a new protocol. Further refinement of the finite element model was then incorporated to get more accurate results to match the experimental data.

CHAPTER 2

METHODS AND EXPERIMENTAL TECHNIQUE

2.1 Test Specimen and Protocol

For the studies performed in Section 2.3, 7th generation inbred rats weighing 250g – 300g were used to investigate the healing effects of the combination of PRP + MSCs on collagen tape. The Institutional Animal Care and Use Committee at Youngstown State University approved the experimental protocol for the following procedures, IACUC protocol #02-09. Rats for each study were obtained from Charles River Laboratories International, Inc., in Wilmington, Massachusetts. They were housed for one week prior to the experimental procedure at the animal care facilities of Youngstown State University.

2.2 Treatment Methods

The studies in Section 2.3 were performed in several different ways. Section 2.2 describes the process in which each treatment additive was obtained, grown, and stored prior to surgical use.

2.2.1 Collagen Matrix

The CollaTape™ type I bovine collagen was purchased from Zimmer Dental in Mississauga, Ontario, Canada. The collagen scaffold was made using collagen from bovine deep flexor (Achilles) tendons. It is a porous, pyrogen-free, sterile, biodegradable material which came in 2.5cm x 7.6cm strips that were cut into 1cm x 6cm strips for surgical repair.

2.2.2 Platelet-Rich Plasma

Maekawa et al. (2003) method was the basis for the collection of PRP. Rats from previous surgeries had blood taken from a heart puncture using a 21 gauge needle and a 10 mL syringe that had 1/10th volume of anticoagulant citrate dextrose (ACD). The blood was then centrifuged at room temperature for twenty minutes at 200 x g. This separated the plasma layer from everything else. The plasma layer was removed and centrifuged again for ten minutes at 700 x g. All but 1ml of the platelet poor layer of plasma was removed and frozen at -20°C. The remaining plasma containing platelets was resuspended in 5 µl of DMSO (5%) and placed in a cryovial to be slowly frozen to -80°C. Once at -80°C, the vials were placed in liquid nitrogen for storage.

To prepare the plasma for use, the platelet-poor plasma was brought to to 37°C and1 ml was placed in a separate tube. The platelets that were kept in liquid nitrogen were thawed until it was possible to free from the cryovial and them then rapidly thawed by mixing with the warm plasma. The mixture was then centrifuged at 700 x g for ten minutes at 4°C. The plasma portion was removed and discarded and the platelet pellet was resuspended in the remaining plasma. The PRP was then ready to be used.

2.2.3 Bone Marrow-derived Stromal Cells

Bone marrow-derived stromal cells were obtained following the procedure described by Heffner et al. (2012). A 21-gauge needle was used to flush bone marrow from the tibias and femurs of Lewis rats. 30mL of minimum essential medium (MEM) alpha media containing 10 U/mL of heparin was used to flush the bone marrow. The clumps were allowed to settle for five minutes and then the supernatant was removed, leaving the bottom 0.5mL that contained the clumps. The MSCs, which are contained in the supernatant, were centrifuged at room temperature and 400 x g for ten minutes. The resulting pellet was then removed and resuspended in 10 mL of complete media (MEM alpha media containing 20% fetal calf serum (FCS), 2mM of L-glutamine, 100 U/mL of penicillin, 100 µg/mL of streptomycin and 25 ng/mL of amphotericin). A cytometer using 4% acetic acid was use to count the nucleated cells. These were then diluted in complete media to the appropriate cell concentration in cells/ml. 10mL of the solution was placed in a T75 culture flask and incubated for four days. The non-adherent cells were removed in media and discarded. The media was replaced every three days until the cells reached 80% confluence. The cells were passaged by treating 0.25% trypsin and 1mM of EDTA. The cells were then resuspended in complete media and split into two flasks and the expansion was continued till the third passage. Next, the cells were collected, centrifuged at 600 x g for five minutes, resuspended, and counted. The MSCs were frozen by slowly decreasing the temperature to -80°C in a media containing 10% DMSO and stored in liquid nitrogen. Prior to use, the MSCS were thawed rapidly in 5 mL of complete media, resuspended in complete media, and incubated in a T25 flask at 37°C for twenty-four hours. Trypinization was used to remove the cells from

the flask and centrifuged at 400 x g for ten minutes at room temperature. It was re-suspended in 0.5mL of PRP and were then ready to be used in the experiments.

2.3 Study Design

The following studies were performed to see if the combination of PRP + MSCs on collagen tape can aid in the healing of hernia repair. Further studies were performed to look at how the dosage of MSCs affected the healing of the fascia. Each study followed the surgical procedure outlined in Section 2.4 and was repaired according to the group the rats were in.

2.3.1 Master Control Group

The master control group consisted of 5 rats that yielded 10 samples. These samples were used to obtain mechanical properties of the abdominal wall fascia that had not yet undergone any type of surgery. These samples were also known as virgin tissue, VT.

2.3.2 Study Design 1

This preliminary trial focused on seeing if the combination PRP + MSCs on collagen tape aided the healing of the repaired tissue. The study consisted of 42 rats that were separated into three groups each containing fourteen rats. Each group was then separated into two subdivisions: subgroup "A" was analyzed following four weeks of recovery and subgroup "B" was analyzed eight weeks after the surgery. The control, group 1, had only a suture repair done on the midline fascial incision, discussed in Section 2.4. Group 2 underwent the same suture repair as group 1 but with the additions of CollaTape^{TM}(CoTa) onlay implant and PRP. Group 3 was repaired the same way as group 2 with the addition of $1x10^6$ MSCs.

2.3.3 Study Design 2

The focus of this study was to find the minimum concentration of MSCs required to improve wound healing. This study had 35 rats that were placed into five groups each consisting of seven rats. All groups underwent the same surgical procedure described in Section 2.4 and were treated with CollaTape^{TM}, PRP, and MSCs. This time, the concentration of MSCs were varied for each group: groups 9A, 10A, 11A, 12A, and 13A had cell concentrations of $5x10^4$ cells/ml, $1x10^5$ cells/ml, $2.5x10^5$ cells/ml, $5x10^5$ cells/ml, and $2.5x10^4$ cells/ml respectively. The samples were extracted four weeks post operation.

2.3.4 Study Design 3

There were questions concerning the accuracy of the results in study design 2. Thus, this study was done to repeat several groups from that study in order to verify the results that were obtained. Groups 11A, 12A and 13A were repeated and were named 11R, 12R, and 13R.

2.4 Fascial Incision and Repair

The surgical procedure and hernia repair followed the method outlined by Heffner et al. (2012). An EZ-AF9000 Auto Flow System anesthesia device with isoflurane (3-5%) for induction and isoflurane (1-3%) for maintenance was used to put the rats under an inhalational anesthesia. The rats were under anesthesia for twenty to thirty minutes while their respiration, tissue color, and toe pinch reflex were monitored. Buprenorphine 0.025mg/kg was administered prior to incision and then twelve and twenty-four hours after surgery.

The Aseptic technique was followed for surgeries and the surgical equipment was kept sterile by autoclave or with a dry sterilization unit. The instruments were also cleaned in-between surgeries with 70% ethanol solution, dried, and placed in a Germinator 500 dry bead sterilizer from Cellpoint Scientific, Inc. From the pubis to the xiphoid, a midline abdominal skin incision is made. Once the skin had been made into bilateral skin flaps, a 6 cm midline incision was made on the fascia, Figure 2.1.

Figure 2.1: Rat after 6 cm Fascia Incision

The fascia was then repaired using fifteen interrupted 5-0 Vicryl sutures. The rats were then treated according to the group they were in, as shown in Table 2.1. The skin of the rat was then sutured closed using interrupted 5-0 Vicryl subcuticular sutures.

Table 2.1: Closure Technique According to Group

Experimental Group	Technique for Closure	Number of Rats
1A	Primary suture repair	7
1B	Primary suture repair	7
2A	Same as group 1 + PRP + CoTa	7
2B	Same as group 1 + PRP + CoTa	7
3A	Same as group 2 + MSCs at $1x10^6$ cells/ml	7
3B	Same as group 2 + MSCs at $1x10^6$ cells/ml	7
9A	Same as group 2 + MSCs at $5x10^4$ cells/ml	7
10A	Same as group 2 + MSCs at $1x10^5$ cells/ml	7
11A	Same as group 2 + MSCs at $2.5x10^5$ cells/ml	7
12A	Same as group 2 + MSCs at $5x10^5$ cells/ml	7
13A	Same as group 2 + MSCs at $2.5x10^4$ cells/ml	7
11R	Same as group 2 + MSCs at $2.5x10^5$ cells/ml	7
12R	Same as group 2 + MSCs at $5x10^5$ cells/ml	7
13R	Same as group 2 + MSCs at $2.5x10^4$ cells/ml	7

2.5 Post Procedure Monitoring

Following surgery, the rats were placed in clean bedding and monitored once daily for the first week of recovery for signs of infection and autophagia; none of the rats had these signs. After one week, the rats were observed two or three times weekly.

2.6 Recovery of Fascia

Depending on the recovery time for the group, the abdominal fascia was removed at either four or eight weeks. To do this, the rats were placed under inhalational anesthesia as described previously. The previous midline skin incision was reopened and the skin was pulled aside to expose the abdominal wall muscle. The abdominal aponeurosis, including the incision site, was removed and cut into five pieces using a hand press that was designed for this protocol, Figure 2.2.

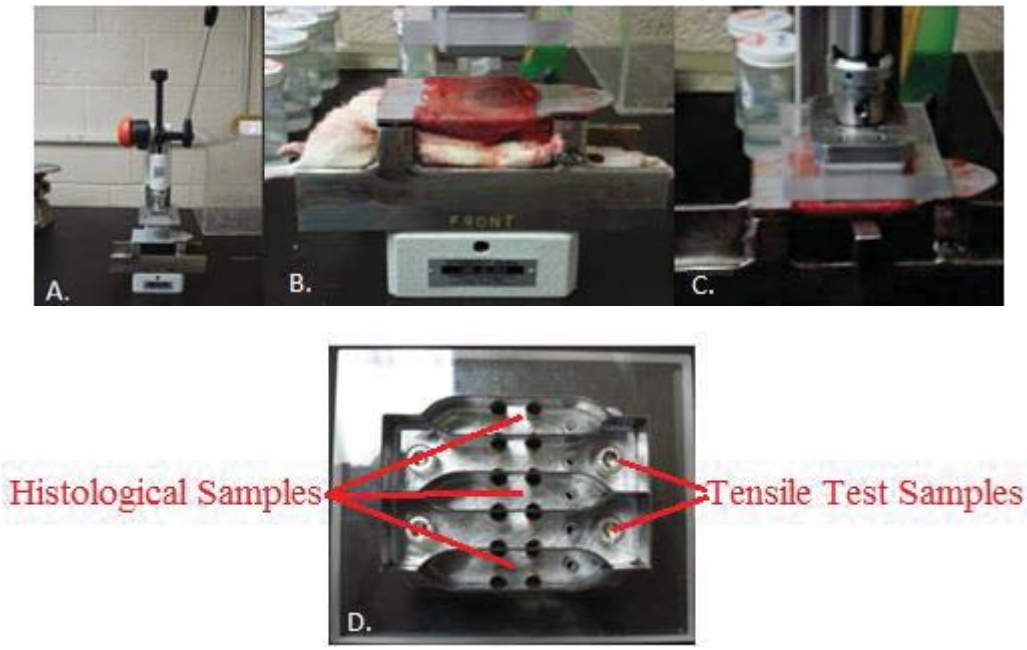

Figure 2.2: Extraction Equipment and Process a) Entire View of Press b) Plate Seperating Abdominal Muscle from body of rat c) Abdominal Muscle being cut d) View of Press that Cuts Abdominal Muscle

The two dumbbell-shaped segments, I for inferior and S for superior,were used for stress and strength analysis and the remianing three pieces were used for histologic analysis two collagen analysis.

2.7 Mechanical Testing

Standard tensionmetric analysis was used to determine mechanical properties of the fascia defects. Each group of rats produced 14 specimens, which were preserved in a phosphate-buffed saline solution at 4°C until the tensile strength test. Testing was performed using an Instron Tensiometer Model 5697, Figure 2.3a, equipped with a 100N load cell capable of 0.25% accuracy over the entire range. Machined grips, Figure 2.3b, were made in order to reduce the amount of slippage and breakage at the attachment sites. Aluminum foil was

placed around each end of the sample before it was placed in the grips to help prevent shearing at the grips, Figure 2.3c. Failures at the attachment site were not included in the final analysis.

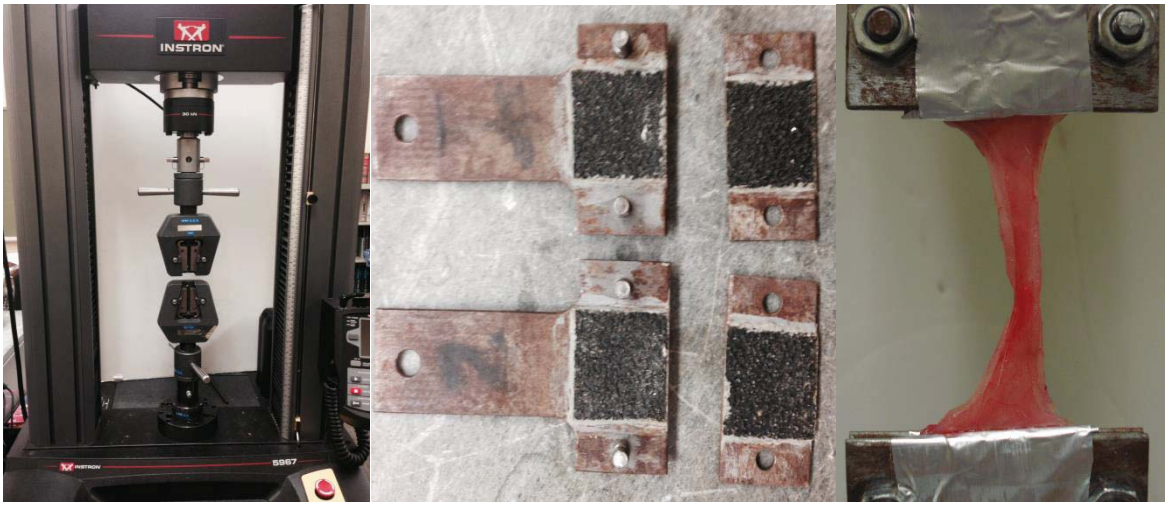

Figure 2.3: Tensile Test Equipment a) Instron Tensiometer Model 5697 equipped with 100N Load Cell b) Mechanical Grips c) Tissue Placed in Grips before Instron Test

Before testing began, a digital caliper was used to measure the length between each grip, the width of the tendon at three spots (top, middle, and bottom), and the thickness at three spots (top, middle, and bottom). Pictures were also taken of all four sides of the sample and used for a more precise dimensioning in the finite element modeling.

Each specimen had a constant extension rate of 10mm/min applied by the crosshead until a tissue disruption occurred. Force and tissue deformation data was simultaneously recorded, and data analysis was performed with the use of the Bluehill 3 software package (Instron Corp).

This data was used to determine the following mechanical properties: tensile strength (maximum stress tolerated by the tissue), strain (measure of deformation representing the

displacement between particles in the body in relation to a reference length), modulus of elasticity (stress required to strain the material 1 mm/mm in the linear region of the stress-strain curve), and modulus of toughness (energy needed to completely rupture the tissue). The tensile strength was found by taking the load recorded at each time step and dividing it by the original average cross sectional area of the tissue. The strain of the tissue was calculated by taking the extension of the tissue and dividing it by the original length of sample. The stress and strain were then plotted to obtain a stress-strain curve. From this curve, the modulus of elasticity and modulus of toughness could be found. The modulus of elasticity can be found by taking the slope of the linear portion of the curve. The modulus of toughness is the area under the whole curve until failure occurs. This area was found by taking the integral of a curve-fit equation up until failure and evaluating it from zero to strain at failure. For the studies performed, a linear line was used to find the modulus of elasticity and a fourth order polynomial was used to find the modulus of toughness.

2.8 Finite Element Analysis

An image of the tissue, taken before the tensile test took place, was enlarged and printed out. The tissue was then outlined making sure that only the front surface was included in the outline, Figure 2.4a. The length from grip to grip in the picture was measured as well as widths of the tissue at seventeen locations. The measured length of the actual tissue, taken from grip to grip with a caliper before the tensile test, was used to scale the picture. The scale was then used so that the actual widths of the tissue could be determined from the picture. The thickness was measured, before the tensile test, at the top, middle, and bottom using a caliper. It was assumed that the thickness gradually decreased until the middle.

SolidWorks 2013 was then used to model the tissue with the scaled dimensions from the picture, Figure 2.4b.

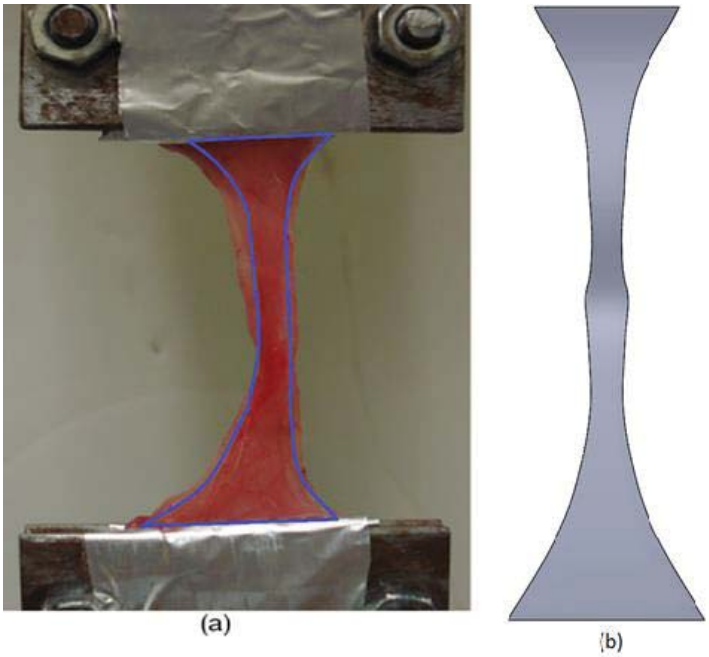

Figure 2.4: Images of a Virgin Tissue Sample:
(a) Tissue before Tensile Test, (b) SolidWorks Model

The model was imported into Autodesk Simulation Multiphysics. The models were meshed using 8 nodded brick and tetrahedral elements and an absolute mesh size of 0.35mm so that there would be a minimum of five elements across any surface. The bottom of the tissue was constrained from moving in the x, y, and z -directions as well as from rotating in the x, y, and z-direction. A nodal displacement boundary condition was used for the top of the tissue. A displacement that had been recorded by the Instron was entered in the y-direction and a stiffness of one billion was entered to make the model stable. Figure 2.5 shows the placement of the boundary conditions.

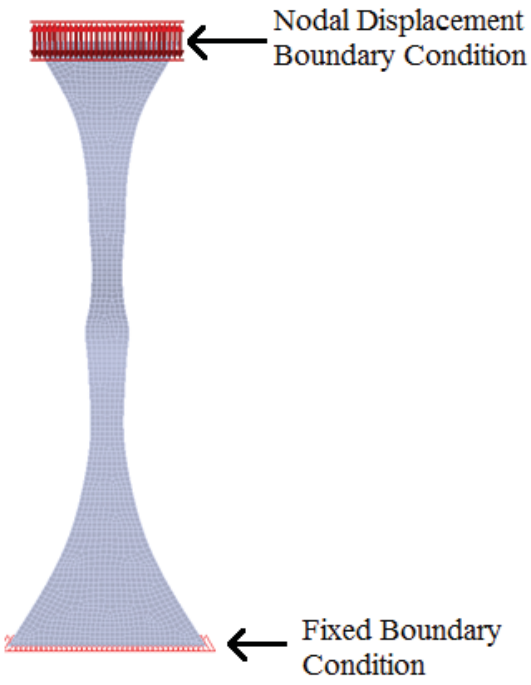

Figure 2.5: Mesh Finite Element Model of Tissue

The model was displaced to two-thirds of the linear slope of the stress strain curve. The modulus of elasticity used in the finite element models was obtained from the experimental stress-strain curves using the Instron tensile test, as previously noted.

2.9 Non-Invasive Elastography

Elastography is an emerging method used in the medical field to map the elastic properties of soft tissue. It can be performed in several ways including magnetic resonance elasticity, tactile imaging, and ultrasound elasticity imaging. From Marie et al. (2010), Optical elastography is non-invasive technique meaning that there is no direct contact being made with the samples. In theory, this will allow linear, plastic, and post-rupture strains to be seen. Four steps are needed to obtain elastograms of the tissue samples. They are as follows:

1. Capturing the tissue deformations using a video camera
2. Breaking down the video sequence into individual frames
3. Tracking the motion of the pixels across multiple frames
4. Obtaining a strain elastogram from the tracked pixels

Under normal indoor lighting, a SONY high-definition camcorder was used to capture each tissue sample's tensile test at a capture speed of 30 frames per second, fps.

A brightness conservation equation is the optical flow algorithm that was used to estimate the mixel's motion, Equation 2.1.

$$\frac{\partial I}{\partial x}\frac{dx}{dt}+\frac{\partial I}{\partial y}\frac{dy}{dt}+\frac{\partial I}{\partial t}=0, \tag{2.1}$$

In Equation 2.1, $I(x, y, t)$ is the image brightness function, with x and y as rows and columns of an image and t as the frame interval (time). The resulting motion vector of a point is given by Equation 2.2

$$\boldsymbol{u} = (u, v)^T,\ u=dx/dt,\ v=dy/dt \tag{2.2}$$

Since a unique solution does not exist, various constraints, often in the form of a regularization term, need to be imposed:

$$obj\,(u,v)=(I_x u+I_y v+I_t)^2+\lambda(u_x^2+u_y^2+v_x^2+v_y^2), \tag{2.3}$$

where I_x, I_y, u_x, u_y, v_x and v_y denote the partial derivatives of the corresponding variables, and λ is the Lagrange multiplier (or the regularization coefficient). As a result, an optical flow solution (u, v) obtained by minimizing the above objective function is a compromise between the observed motion and the smoothness constraint. More detailed descriptions of the

algorithm can be found in (Black and Anandan, 1996, Marie et al., 2010, and Horn and Schunck, 1981).

2.10 Statistical Analysis

For the statistical analysis (Moore and McCabe, 1989), Chauvenet's criterion was used to find any outlying values. The Chauvenet's criterion states that, "reject any observation if the probability of obtaining it is less than 1/2N," where N is the number of observations.

This analysis was used on the maximum stress, maximum strain, modulus of elasticity, and modulus of toughness data for each of the groups. To start with, the mean of each group for the four mechanical properties were found by taking the sum values and dividing it by the amount of samples, Equation 2.4. Next, the mechanical property for each sample was subtracted by the mean to find the deviations, Equation 2.5. The standard deviation, Equation 2.6; degrees of freedom, Equation 2.7; and the probability, Equation 2.8, for the readings were found following Chauvenet's criterion.

$$\text{Mean}(\bar{x}) = \sum_{i=1}^{n} \frac{x_i}{n} \tag{2.4}$$

$$\text{Deviation} = (x_i - \bar{x}) \tag{2.5}$$

$$\text{STDV of ind. values (S)} = \sqrt{\frac{\sum_{i=1}^{n}(x_i - \bar{x})^2}{n-1}} \tag{2.6}$$

$$\text{Degrees Freedom (v)} = n - 1 \tag{2.7}$$

$$\text{Probability (Pr)} = \frac{1}{2N} \tag{2.8}$$

The value of "t", which is based on the probability, could be found using the student's t-distribution curve shown below in Figure 2.6.

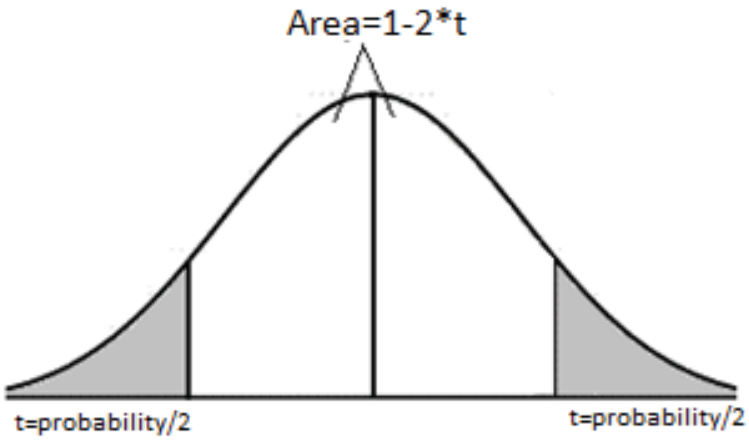

Figure 2.6: Student's t-Distribution (Moore and McCabe, 1989)

In Figure 2.6, the shaded regions represent the area for the outlying values, while the "A" value represents the area for acceptable values and is white. Knowing the degrees of freedom, the value of $t_{probability/2}$ was found by using Table D on page T-11 of *Introduction to the Practice of Statistics*. The maximum and minimum range for the data was then found with Equation 2.12. The maximum and minimum ranges were then used to find any outlying values that should be disregarded. The mean, median, and standard deviation were found again using Equation 1, 2, and 3. The standard deviation of mean values was then used when calculating t_{max} and t_{min} the second time, Equation 2.13, because it is a tighter deviation than the standard deviation of individual values. Table 3.5 was used again to find the value for t with respect to the degrees of freedom the area for the shaded regions were 0.025 since the

mean population value was to be found for a 95% confidence limit, shown in Figure 2.7. The values for t_{max} and t_{min} were then found by Equation 2.14.

$$t = \frac{x_{max} + \bar{x}}{S} \qquad t = \frac{x_{min} - \bar{x}}{S} \tag{2.12}$$

$$STDV\ of\ ind.Mean\ (S\bar{x}) = \frac{S}{\sqrt{n}} \tag{2.13}$$

$$t = \frac{x_{max} + u}{S\bar{x}} \qquad t = \frac{x_{min} - u}{S\bar{x}} \tag{2.14}$$

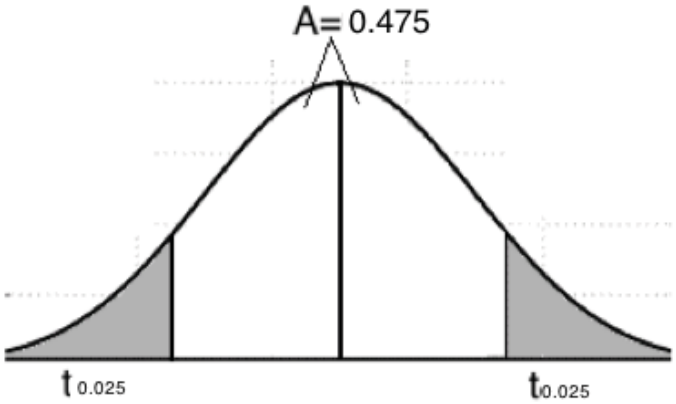

Figure 2.7: Student's t-Distribution for 95% Population Mean (Moore and McCabe, 1989)

After a 95% population mean was found, significant differences among the data for each group were found using the TTest function in Excel.

CHAPTER 3

EXPERIMENTAL RESULTS AND DISCSSION

At the conclusion of each tensile test, the failure site for each tissue sample was noted. As mentioned earlier, any sample that failed at the grips or failed due to slipping out of the grips was disregarded. The load and displacement at failure was recorded for each specimen in the group. Using the load and deflection data, stress-strain curves were then made for each of the samples in the treated groups in order to find the modulus of elasticity and modulus of toughness. A mean for each of these were taken and compared to the control group and virgin tissue group values. The deflection and modulus of elasticity were also used in the finite element models so that the force obtained through simulation could be compared to the experimental force for that sample. Finally, each test was filmed with a high definition video camera in order to evaluate the usefulness of optical elastography for calculating displacement and strain. This information was then used to aid in the validation of the finite element models and to see if it is a viable technique to use for human hernia repairs, as a means to evaluate the strength of the repaired hernia tissue.

3.1 Virgin Tissue Trial

The purpose of the virgin tissue study was to obtain measurements and mechanical properties for hernia tissue that had not undergone surgery. The surgically repaired tissue results would then be compared to the virgin tissue results to evaluate the repaired tissue.

3.1.1 Experimental Results

For the virgin tissue trial, there were a total of ten samples. One of the samples was discarded because it slipped at the grips. Table 3.1 shows the number of samples in each group, the average thickness, the average width, and the average area of the tissue. Individual sample measurements are in Table A.1. in Appendix A.

Table3.1: Average Dimensions of Virgin Tissue

Group	Number of Samples	Width(mm)	Thickness(mm)	Area(mm^2)
VT	10	6.11 ± 0.64	2.29 ± 0.30	14.04 ± 2.85

From the statistical analysis described in the Section 2.11, there were no outlying values for any of the maximum stress, maximum strain, modulus of elasticity, or modulus of toughness values and a mean population of 95% were found. Table 3.2 shows the mean values and the mean population range for maximum stress, maximum strain, modulus of elasticity and modulus of toughness. Mechanical properties for each sample can be seen in Table B.1 in Appendix B.

Table 3.2: Mechanical Properties for Virgin Tissue Group

Group	95% Mean Population of Max Stress (kPa)	95% Mean Population of Max Strain (mm/mm)	95% Mean Population of Elasticity (kPa)	95% Mean Population of Toughness (kPa)
VT	638 ± 118	0.247 ± 0.038	4978 ± 838	99 ± 18

Four samples had a modulus of elasticity, modulus of toughness, maximum stress, and maximum strain which were within the 95% mean population values. These samples were 10I, 10S, 13I, and 14I and thus were the best representatives for the virgin tissue group. Figure 3.1 shows the stress-strain curves for these samples. Stress-strain curves for every virgin tissue sample can be seen in Figure C.1 in the Appendix C.

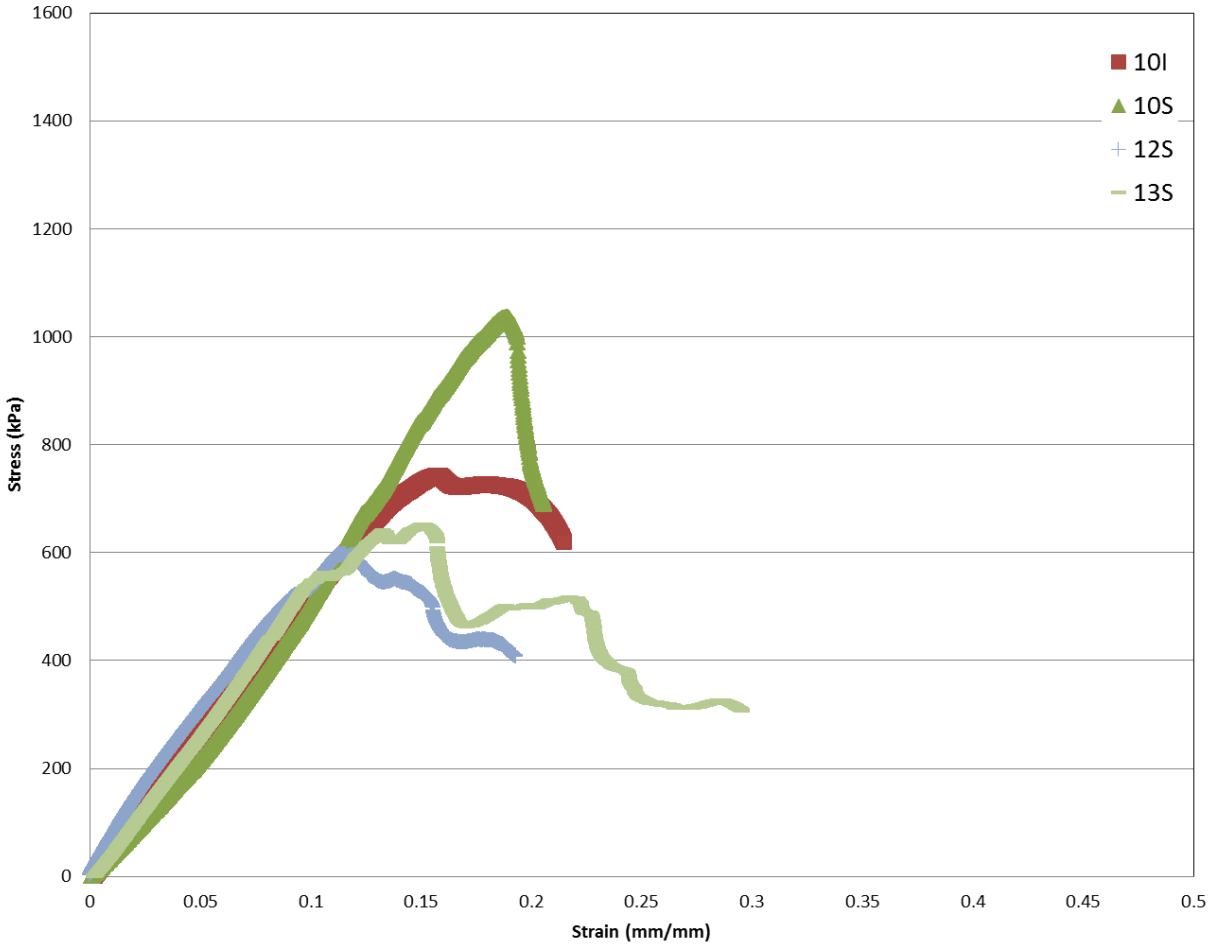

Figure 3.1: Stress-Strain Curves for Virgin Tissue Sample

3.1.2 Finite Element Analysis

The representative samples of the virgin tissue group were chosen to be modeled. Section 2.8 outlines how the models were created, the software used, and the boundary conditions

that were applied. The force needed to displace the sample in the finite element model was compared to the experimental force needed at the same displacement. The finite element and experimental forces can be seen in Table 3.3. Figure 3.2 shows the finite element model of the sample and where the force was taken.

Table 3.3: Comparison of FEA Forces and Tensile Test Forces

Sample Number	Displacement (mm)	Tensile Force (N)	FEA Force (N)	% Difference
VT-10I	4.50	5.99	6.18	3%
VT-10S	4.50	4.23	4.15	2%
VT-13I	4.50	5.77	6.31	9%
VT-14I	4.50	3.47	4.45	22%

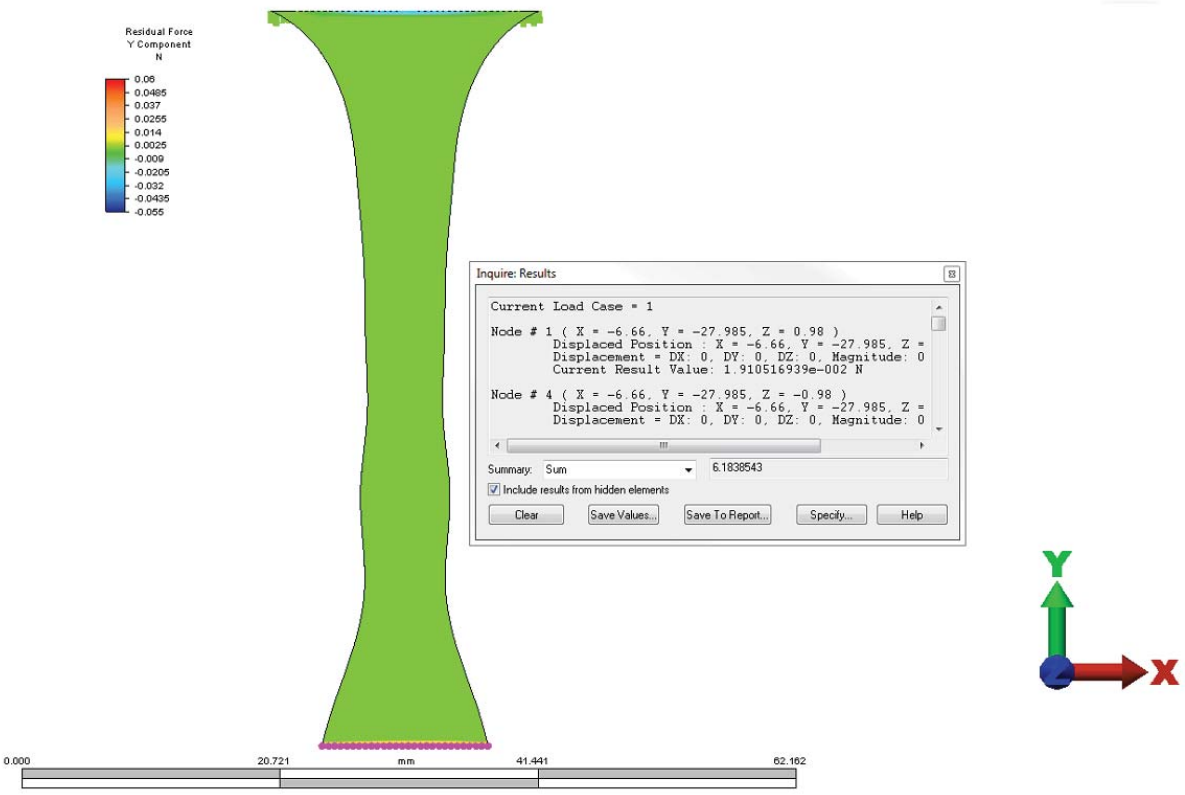

Figure 3.2: FEA Model of Tissue Sample 10I

3.1.3 Discussion of Finite Element Models

FEA models of samples 10I, 10S, 13I, and 14I were made and the reaction force in the Y-direction were compared to the load force recorded by the Instron in order to verify the models. The percent difference of the forces were 3%, 2%, 9%, and 22%. The difference in the forces could be due to inaccurate dimensioning of the tissue. However, since the percent differences are low, the finite element models can still be considered accurate as all but one had a percent difference lower than 10%.

3.2 Preliminary Trial

The preliminary trial followed the design study mentioned in Section 2.3.2 and was performed to see if the combination of PRP + MSCs on Collagen Tape aided in the healing of hernia repair. This trial consisted of the groups in Table 3.4.

Table 3.4: Preliminary Trial Groups

Experimental Group	Technique for Closure	Number of Rats
1A	Primary suture repair	7
1B	Primary suture repair	7
2A	Same as group 1 + PRP + CoTa	7
2B	Same as group 1 + PRP + CoTa	7
3A	Same as group 2 + MSCs at $1x10^6$ cells/ml	7
3B	Same as group 2 + MSCs at $1x10^6$ cells/ml	7

There were a total of eighty-four samples, ten of which were discarded because they either tore or slipped out of the grips.

3.2.1 Experimental Results

Table 3.5 shows the number of samples in each group, the average thickness, the average width, and the average area of the tissue. Individual sample measurements are in Table A.2 – A.7 in Appendix A.

Table 3.5: Average Dimensions for Groups 1A – 3B

Group	Number of Samples	Width(mm)	Thickness(mm)	Area(mm^2)
1A	13	8.02 ± 1.40	4.44 ± 0.70	33.57 ± 7.01
1B	12	6.43 ± 1.31	3.91 ± 0.46	25.06 ± 5.50
2A	13	6.79 ± 0.90	4.02 ± 0.53	27.36 ± 5.61
2B	11	6.09 ± 0.75	3.15 ± 0.32	19.25 ± 3.70
3A	13	5.41 ±0.91	2.76 ± 0.51	14.86 ± 3.36
3B	12	6.12 ± 0.80	2.65 ± 0.30	16.14 ± 2.40

Significant differences can be seen in Figure 3.3.

Figure 3.3 shows the thickness for each group and the virgin tissue group. Using the TTest function in Excel, significant differences were found when comparing the results for each treated group.

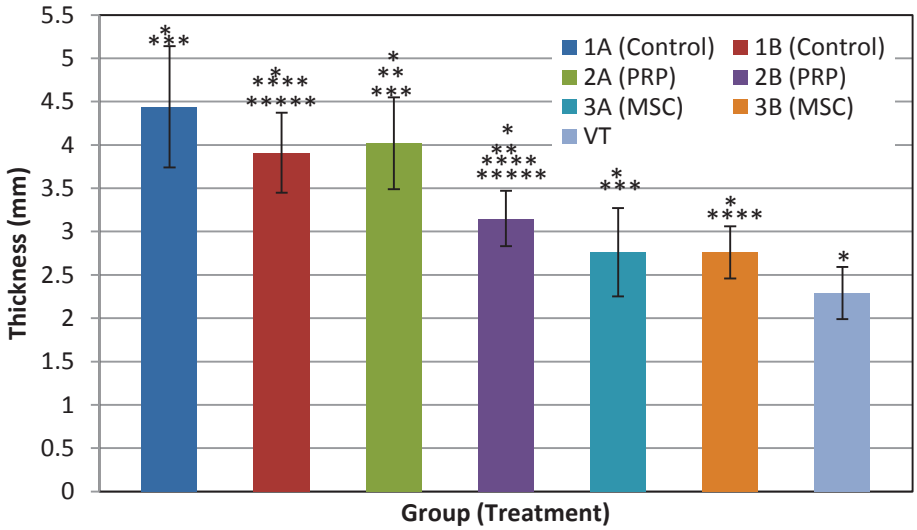

Figure 3.3: Average Thickness for Groups 1A, 1B, 2A, 2B, 3A, 3B, and VT. Error bars represent a 95% mean population range. Statistical significance was found in the thickness of all groups when compared to the virgin tissue group (*:$p < 0.002$). There was also a significant difference in thickness when comparing the PRP group at four weeks to the PRP group at eight weeks (**:$p < 0.001$). At four weeks, both the control and PRP group had a statistical significance when compared to the MSC + PRP group (***:$p < 0.001$). Similarly, statistical significance is seen at eight weeks for the control and PRP group when compared to the MSC + PRP group (****:$p < 0.001$). There was also statistical significance when comparing the control group at eight weeks to the PRP group at eight weeks (*****:$p < 0.001$). No statistical significance was found between the control at four and eight weeks or when comparing the MSC + PRP group at four and eight weeks. There was also no statistical significance between the control group at four weeks and the PRP group at four weeks.

The statistical analysis described in the Section 2.11 was used to find any outlying mechanical properties. For this section, none of the mechanical values were found to be outliers. Table 3.6 shows the mean values and the mean population range for maximum

stress, maximum strain, modulus of elasticity and modulus of toughness. Mechanical properties for each sample can be seen in Table B.2 – B.7 in Appendix B.

Table 3.6: Mechanical Properties of Preliminary Trial Groups

Group	95% Mean Population of Max Stress (kPa)	95% Mean Population of Max Strain (mm/mm)	95% Mean Population of Elasticity (kPa)	95% Mean Population of Toughness (kPa)
1A	204 ± 40	0.223 ± 0.049	1334 ± 287	28 ± 7
1B	422 ± 128	0.227 ± 0.072	2865 ± 980	60 ± 23
2A	410 ± 82	0.272 ± 0.055	2179 ± 459	63 ± 17
2B	582 ± 229	0.275 ± 0.114	3760 ± 1493	111 ± 53
3A	817 ± 179	0.249 ± 0.059	5086 ± 1370	119 ± 31
3B	917 ± 262	0.289 ± 0.085	5076 ± 1551	145 ± 43

Significant differences can be seen in Figure 3.5 to 3.8. Table 3.7 shows the samples that had a modulus of elasticity, modulus of toughness, maximum stress, and maximum strain that were within the 95% mean population range. These samples were perceived to be the best representatives for their respective group.

Table 3.7: Quality Samples for Groups 1A – 3B

Group	Sample
1A	4S, 5I, & 7S
1B	2I & 7I
2A	1S, 2I, 3I, 3S, 4I, 4S, 5S, & 6S
2B	2I, 2S, 3I, 3S, 4S, 5S, & 7I
3A	5S
3B	1S, 2S, 3I, 3S, 4I, 4S, 5I, 5S, 6I, & 6S

Figure 3.4 shows the stress-strain curves for these samples. Stress-strain curves for every sample can be seen in Figure C.2 – C.7 in Appendix C.

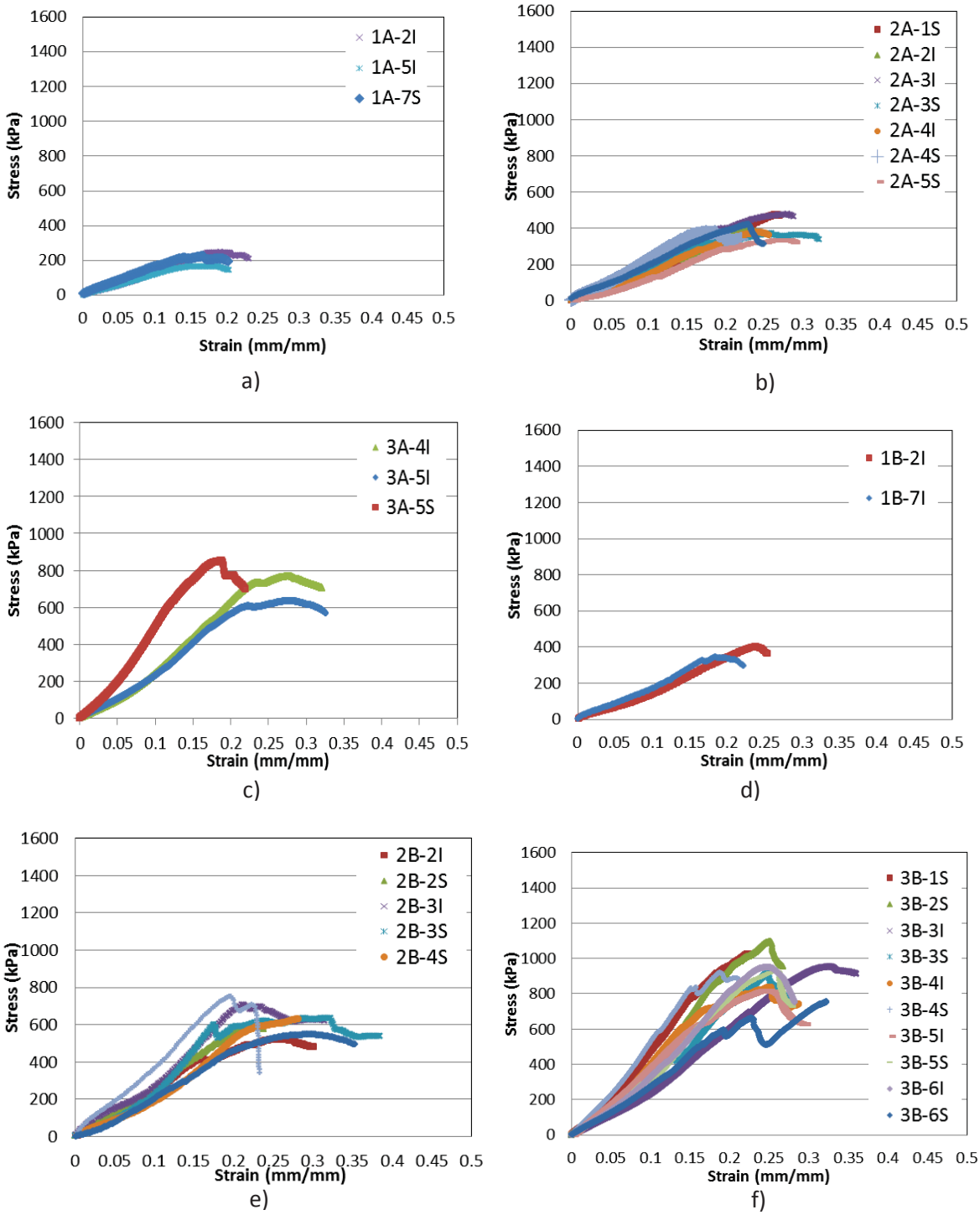

Figure 3.4: Stress-Strain Curves for Groups a) 1A, b) 1B, c) 2A, d) 2B, e) 3A, and f) 3B

Figure 3.5 shows the variation in the maximum stress, Figure 3.6 the maximum strain, Figure 3.7 the modulus of elasticity, and Figure 3.8 modulus of toughness for each group.

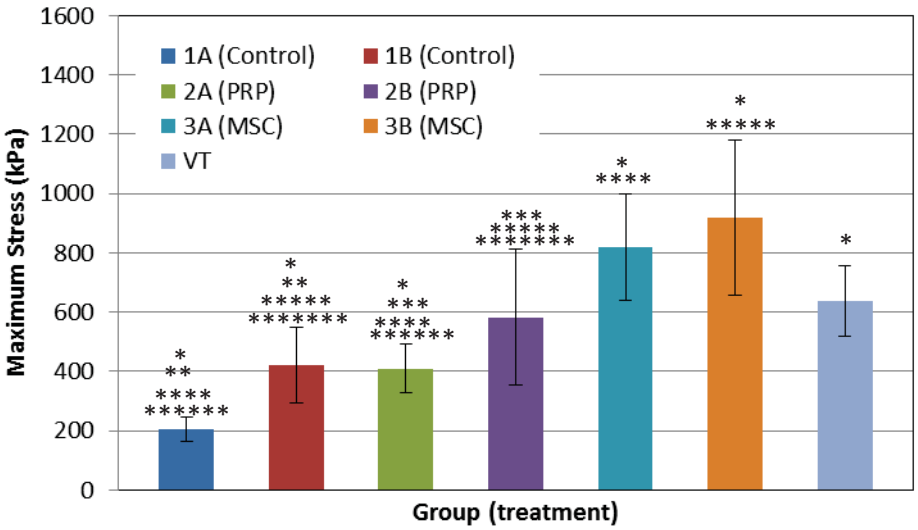

Figure 3.5: Maximum Stress for Preliminary Trial Groups. Error bars represent a 95% mean population range. Statistical significance was found in the maximum stress of all groups except the PRP group at eight weeks when compared to the virgin tissue group (*:$p < 0.01$). There was also a significant difference in the maximum stress when comparing the control group at four weeks to the control group at eight weeks (**:$p < 0.001$). There was a significant difference when comparing the PRP group at four weeks to the PRP group at eight weeks (***:$p < 0.001$). At four weeks, both the control and PRP group had a statistical difference when compared to the MSC + PRP group (****:$p < 0.001$). Similarly, statistical significance is seen at eight weeks for the control and PRP group when compared to the MSC + PRP group (*****:$p < 0.001$). There was also statistical significance when comparing the control group at four weeks to the PRP group at four weeks (*******:$p < 0.001$). There was also statistical significance when comparing the control group at eight weeks to the PRP group at eight week (*******:$p < 0.001$). No statistical significance was found between the MSC + PRP group at four and eight weeks.

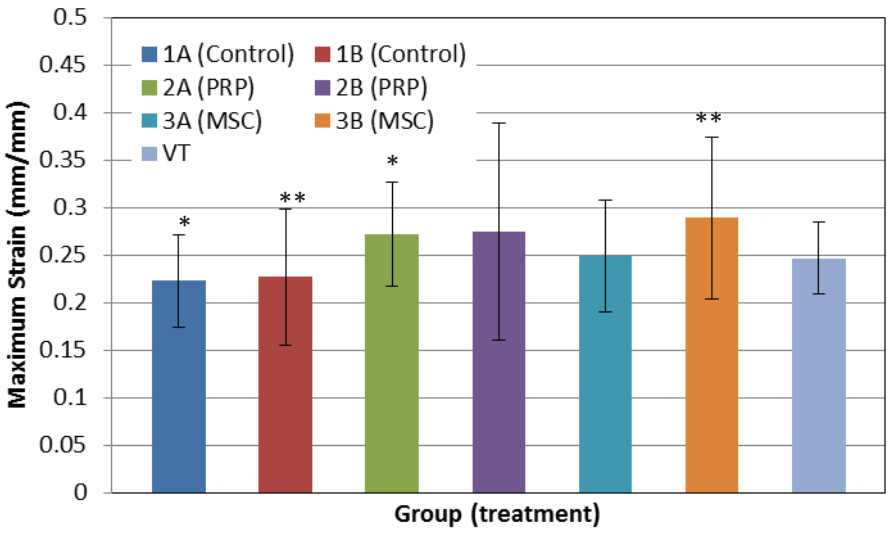

Figure 3.6: Maximum Strain for Preliminary Trial Groups. Error bars represent a 95% mean population range. Statistical significance was found in the maximum strain of the control at four and the PRP group at four weeks (*:$p < 0.01$). There was also a significant difference in maximum strain when comparing the control group at eight weeks to the PRP + MSCs group at eight weeks (**:$p < 0.001$). No statistical significance was found between the MSC + PRP group at four and eight weeks. There was also no significant difference between the virgin tissue and any of the treated groups. When comparing the same treatment at four and eight weeks, there was no statistical significance in the maximum strain.

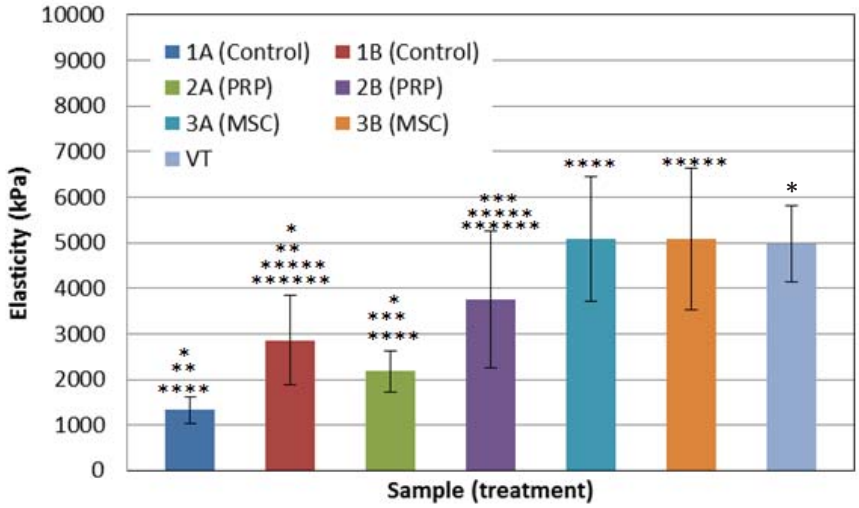

Figure 3.7: Modulus of Elasticity for Preliminary Trial Groups. Error bars represent a 95% mean population range. Statistical significance was found in the modulus of elasticity of the control at four and eight weeks and the PRP group at four weeks when compared to the virgin tissue group (*:$p < 0.001$). There was also a significant difference in modulus of elasticity when comparing the control group at four weeks to the control group at eight weeks (**:$p < 0.001$). There was a significant difference in the elasticity when comparing the PRP group at four weeks to the PRP group at eight weeks (***:$p < 0.001$). At four weeks, both the control and PRP group had a statistical difference when compared to the MSC + PRP group at four weeks (****:$p < 0.001$). Similarly, statistical significance is seen at eight weeks for the control and PRP group when compared to the MSC + PRP group at eight weeks (*****:$p < 0.001$). There was also statistical significance when comparing the control group at eight weeks to the PRP group at eight weeks (*******:$p < 0.001$). No statistical significance was found between the MSC + PRP group at four and eight weeks or for the virgin tissue group when compared to the PRP group at eight weeks and the MSC + PRP group at four and eight weeks.

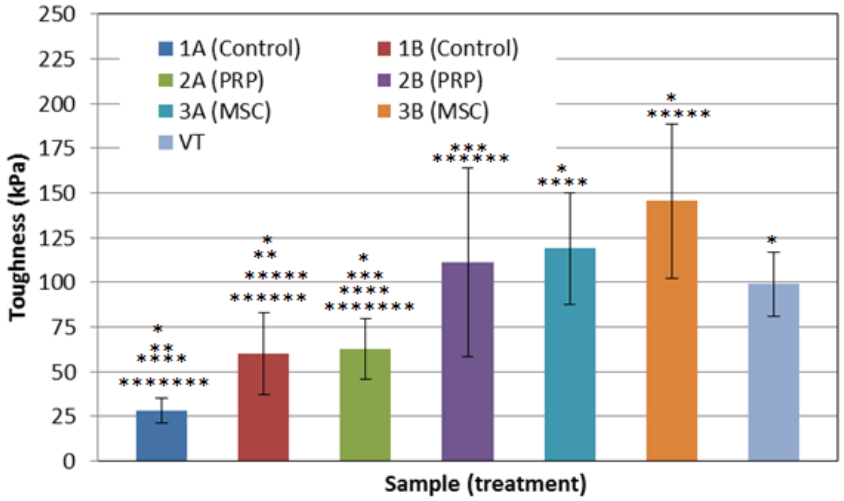

Figure 3.8: Modulus of Toughness for Preliminary Trial Groups. Error bars represent a 95% mean population range. Statistical significance was found in the modulus of toughness of the control at four and eight weeks, the PRP group at four weeks, and the MSC + PRP group at four and eight weeks when compared to the virgin tissue group (*:$p < 0.001$). There was also a significant difference in modulus of toughness when comparing the control group at four weeks to the control group at eight weeks (**:$p < 0.001$). There was also a significant difference in the toughness when comparing the PRP group at four weeks to the PRP group at eight weeks (***:$p < 0.001$). At four weeks, both the control and PRP group had a statistical difference when compared to the MSC + PRP group at four weeks (****:$p < 0.001$). Similarly, statistical significance is seen at eight weeks for the control when compared to the MSC + PRP group at eight weeks (*****:$p < 0.001$). There was also statistical significance when comparing the control group at eight week to the PRP group at eight week (*******:$p < 0.001$). There was also statistical significance when comparing the control group at four weeks to the PRP group at four weeks (*******:$p < 0.001$). No statistical significance was found between the MSC + PRP group at four or the PRP group at eight weeks and the MSC + PRP group at eight weeks.

3.2.3 Discussion

(1)Mechanical Properties Since the tissue samples were cut to a certain width, only the thickness of the tissue can be used for comparison. As can be seen in Table Figure 3.3, the average thickness of the tissue at four weeks recovery significantly decreased with the applied treatment of PRP + MSC, group 3A, when compared to the PRP treated samples, group 2A, and the control sample, group 1A. The PRP + MSCs group at four weeks was also

closer to the thickness of the virgin tissue than groups 1A and 2A, as it was only 20% larger compared to 97% and 75%. This shows that the combination of PRP + MSCs aided in decreasing the swelling of the repaired fascia.

The trend in the thickness stayed the same at eight weeks, as the control had the largest thickness and the combination of MSCs + PRP had the smallest thickness. However, the PRP + MSCs treated group had no significant decrease in thickness from four to eight weeks. This data shows that even after eight weeks, none of the treatments were able to get back to the virgin tissue thickness. It also shows that after four weeks, the combination of PRP+ MSCs decreased to a steady thickness more rapidly than the PRP group and control.

At four weeks recovery, the control and PRP only groups, 1A and 2A, were found to have a maximum stress, modulus of elasticity, and modulus of toughness all significantly lower than the virgin tissue group and the PRP + MSCs group. The PRP + MSC group, 3A, however, had significantly higher values for tensile strength and modulus of toughness and no significant difference in modulus of elasticity to those found in the virgin tissue group at four weeks recovery. The PRP alone group also had significantly higher mechanical properties at four weeks than the control. These differences in mechanical properties show that the combination of PRP and MSCs has a significant contribution in the healing of the hernia tissue.

At eight weeks recovery, the control, group 1B, still had a maximum strength, modulus of elasticity, and modulus of toughness significantly less than the virgin tissue. The PRP treated samples at eight weeks, group 2B, had no significant difference in its mechanical properties when compared to the virgin tissue. Like with the thickness measurements, the PRP + MSCs

group, 3B, saw no significant change in maximum strength, modulus of elasticity, and modulus of toughness when compared to the PRP + MSCs group at four weeks recovery. This further provides evidence the PRP + MSCs treated samples are close to be healed at four weeks.

When looking at the samples that had all four mechanical properties fall within the 95% mean population range, Table 3.7, the PRP group had the most with eight samples. The control group had three samples and MSC treated group had one sample. This shows that the results obtained for the PRP + MSCs group, 3A, have a wider range and are not as consistent as the PRP only group, 2A.

At eight weeks, the control group and PRP group followed the same trend as they had; two and seven samples respectively fell within the 95% mean population. The PRP + MSCs group at eight weeks, 3B, however, saw a significant increase with ten samples that fell within the 95% mean population. This could be due to the MSCs + PRP group being completely healed between at some point between four and eight weeks.

From these results, it is evident that the MSC + PRP treated hernia groups, 3A and 3B, showed significantly accelerated healing when compared to the other four groups. The maximum stress, thickness, modules of elasticity, and modulus of toughness were all very similar or greater than the virgin tissue samples. When looking at these groups 3A and 3B, it is evident that the effects MSCs have on healing reach their full capability at or before four weeks; as the thickness, maximum stress, modulus of elasticity, and modulus of toughness all showed no significant difference from four to eight weeks. This conclusion led to future studies being done at only four weeks recovery time.

3.3 Dosage Trial

The purpose of the Dosage study was to investigate the minimum number of MSCs required to improve wound healing. Table 3.8 shows the groups and MSC concentrations for this trial.

Table 3.8: Dosage Trial Groups

Experimental Group	Technique for Closure	Number of Rats
13A	Same as group 2 + MSCs at $2.5x10^4$ cells/ml	7
9A	Same as group 2 + MSCs at $5x10^4$ cells/ml	7
10A	Same as group 2 + MSCs at $1x10^5$ cells/ml	7
11A	Same as group 2 + MSCs at $2.5x10^5$ cells/ml	7
12A	Same as group 2 + MSCs at $5x10^5$ cells/ml	7

3.3.1 Experimental Results

For this trial, there were a total of 84 samples. Table 3.9 shows the number of samples in each group, the average thickness, the average width, and the average area of the tissue. Individual sample measurements are in Table A.8 – A.12 in Appendix A.

Table 3.9: Average Dimensions for Groups 9A – 13A

Group	Number of Samples	Width(mm)	Thickness(mm)	Area(mm^2)
13A	14	4.45 ± 0.55	2.11 ± 0.29	9.35 ± 1.42
9A	14	4.49 ± 0.58	2.47 ± 0.36	11.19 ± 2.53
10A	14	4.37 ± 0.74	2.29 ± 0.37	10.05 ± 2.76
11A	14	3.87 ± 0.48	2.51 ± 0.42	9.75 ± 2.26
12A	14	4.33 ± 0.81	2.31 ± 0.42	9.91 ± 2.38

Significant differences for the thicknesses can be seen Figure 3.9. Figure 3.9 shows the thickness for each group and the virgin tissue group. Using the TTest function in Excel, significant differences were found when comparing the results for each dosage group.

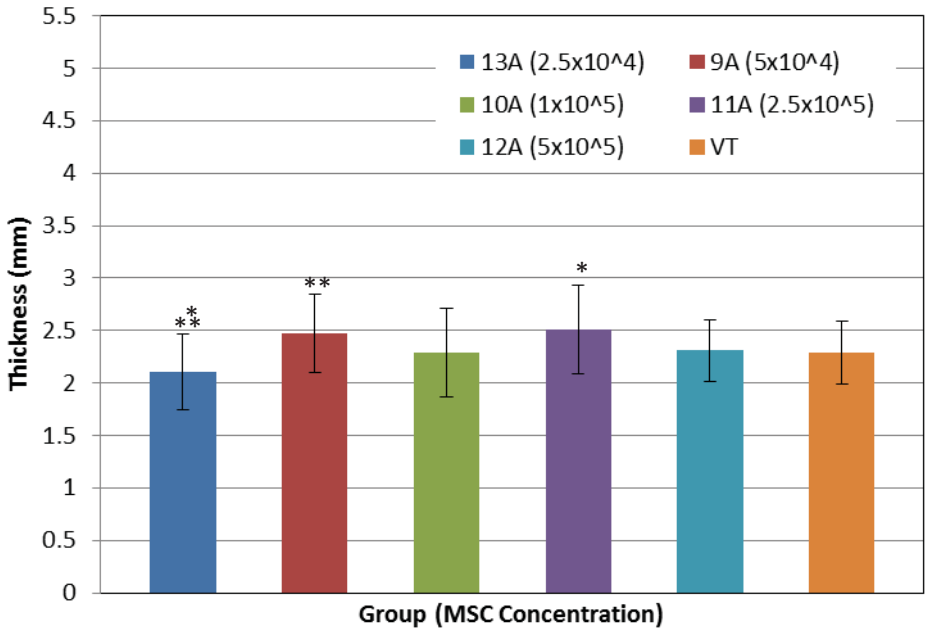

Figure 3.9: Average Thickness for Groups 9A, 10A, 11A, 12A, 13A, and VT. Error bars represent a 95% mean population range. Statistical significance was found in the thickness of the cell concentration of 2.5 x 10^4cell/ml and the cell concentration of 2.5 x 10^5cell/ml, (*: $p < 0.05$). There was also a significant difference in the thickness when comparing the concentration of 2.5 x 10^4 cells/ml and 5 x 10^4cells/ml (**: $p < 0.001$). There was no significant difference when comparing any of the concentrations to the virgin tissue.

Similar to the previous two studies, the statistical analysis described in the Section 2.11 was used to find any outlying mechanical properties. Table 3.10 shows the mean values and the mean population range for maximum stress, maximum strain, modulus of elasticity and modulus of toughness. Mechanical properties for each sample can be seen in Table B.8 – B.12 in Appendix B.

Table 3.10: Mechanical Properties of Dosage Trial Groups

Group	95% Mean Population of Max Stress (kPa)	95% Mean Population of Max Strain (mm/mm)	95% Mean Population of Elasticity (kPa)	95% Mean Population of Toughness (kPa)
13A	999 ± 125	0.325 ± 0.061	4670 ± 906	178 ± 46
9A	865 ± 131	0.305 ± 0.033	4274 ± 836	139 ± 24
10A	1050 ± 136	0.239 ± 0.021	6705 ± 1081	140 ± 24
11A	936 ± 95	0.338 ± 0.027	4223 ± 434	160 ± 34
12A	1135 ± 245	0.265 ± 0.028	7061 ± 1267	164 ± 26

Significant differences for the mechanical properties can be seen in Figures 3.11 to 3.14. Table 3.11 shows the samples that had a modulus of elasticity, modulus of toughness, maximum stress, and maximum strain which were within the mean population range. These samples were perceived to be the best representatives for their respective group.

Table 3.11: Quality Samples for Groups 9A – 13A

Group	Sample
13A	5S
9A	4S, 5I, & 7S
10A	2I & 7I
11A	1S, 2I, 3I, 3S, 4I, 4S, 5S, & 6S
12A	2I, 2S, 3I, 3S, 4S, 5S, & 7I

Figure 3.10 shows the stress-strain curves for these samples. Stress-strain curves for every virgin tissue sample can be seen in Figure C.8 – C.12 in Appendix C.

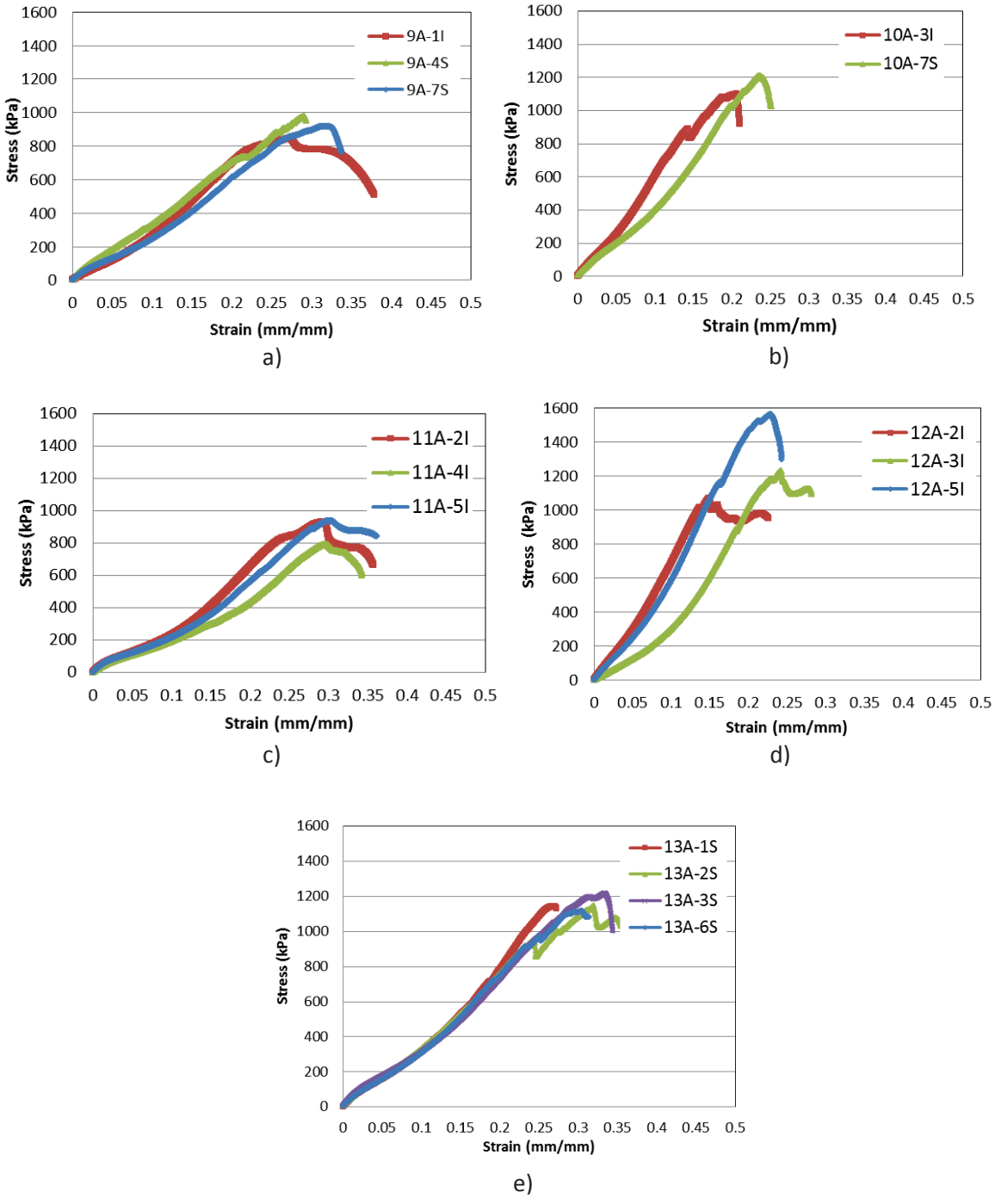

Figure 3.10: Stress-Strain Curves for Groups a) 9A, b) 10A, c) 11A, d) 12A, and e) 13A

Figure 3.11 shows the variation in the maximum stress, Figure 3.12 the maximum strain, Figure 3.13 the modulus of elasticity, and Figure 3.14 modulus of toughness for each group.

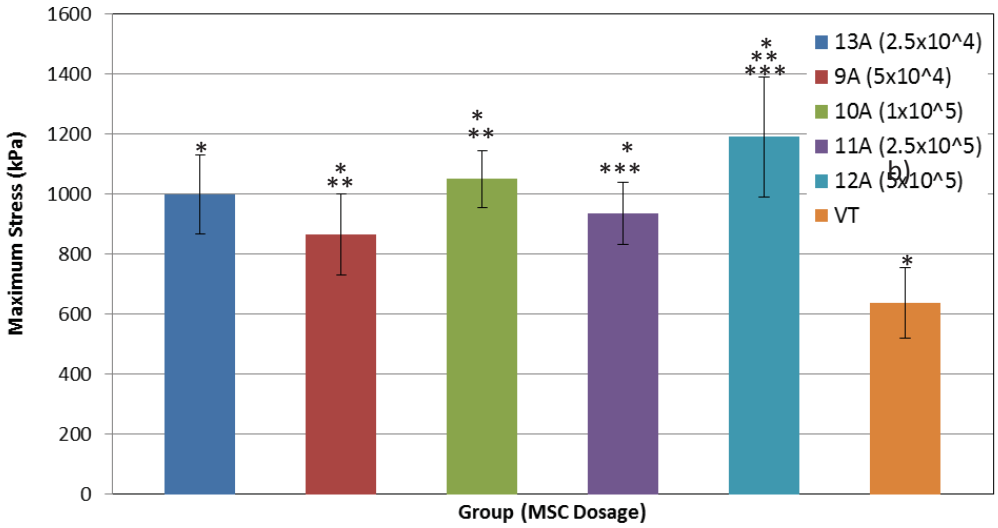

Figure 3.11: Maximum Stress for Cell Concentration Groups. Error bars represent a 95% mean population. Statistical significance was found in the maximum stress of all the cell concentrations compared to the virgin tissue, (*:$p < 0.001$). There was also a significant difference in the maximum stress when comparing the concentrations of 5 x 10^5cell/ml and 1 x 10^5cell/ml to the concentration of 5 x 10^4cell/ml (**:$p < 0.05$). When comparing the maximum stress of concentrations 2.5 x 10^5cell/ml and 5 x 10^5cell/ml, there was a statistical significance (***: $p < 0.05$).

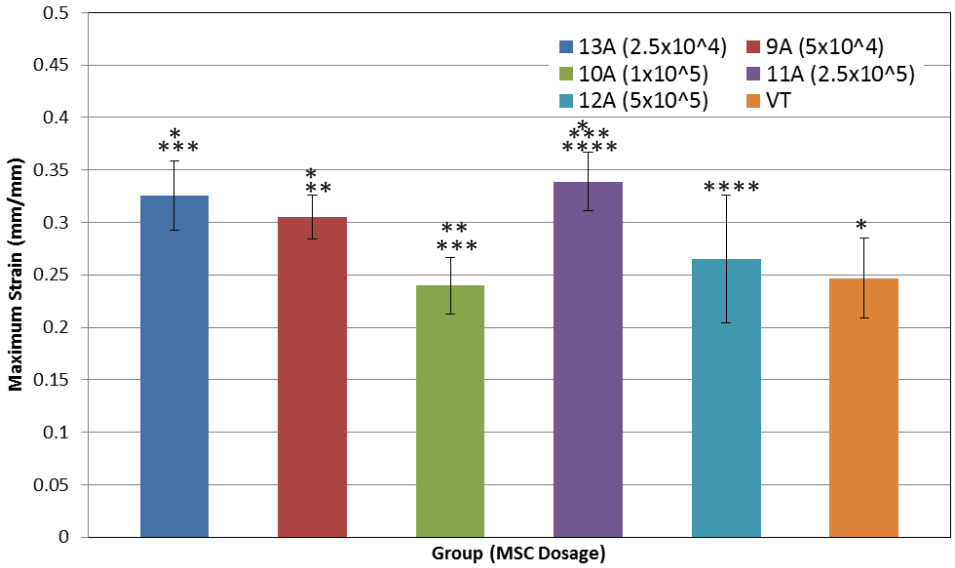

Figure 3.12: Maximum Strain for Cell Concentration Groups. Error bars represent a 95% mean population. Statistical significance was found in the maximum strain of the cell concentration of 2.5 x 10^4cell/ml , 5 x 10^4cell/ml, and 2.5 x 10^5cell/ml when compared to the virgin tissue (*:$p < 0.05$). There was also a significant difference in the maximum strain when comparing the concentration of 5 x 10^4cells/ml when compared to 1 x 10^5cell/ml (**: $p < 0.01$). Statistical significance was also found in the concentrations 2.5 x 10^4cell/ml and 1 x 10^5cell/ml (***: $p = 0.006$) Concentrations 2.5 x 10^5cell/ml and 5 x 10^5cell/ml were significantly different (****: $p < 0.001$).

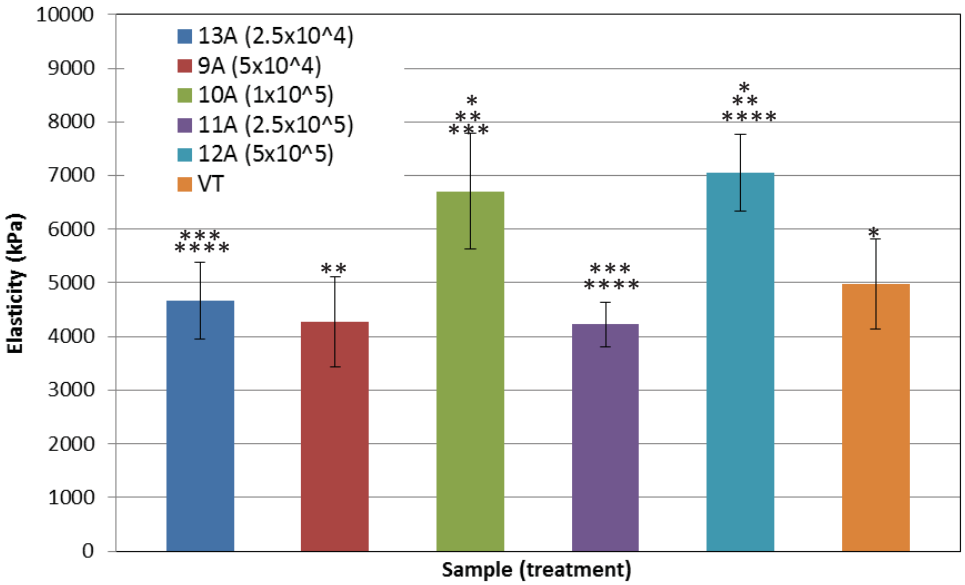

Figure 3.13: Modulus of Elasticity for Cell Concentration Groups. Error bars represent a 95% mean population. Statistical significance was found in the modulus of elasticity of the cell concentration of 1 x 10^5cell/ml and the cell concentration of 5 x 10^5cell/ml when compared to the virgin tissue (*:$p < 0.05$). There was also a significant difference in the elasticity when comparing the concentration of 5 x 10^4cells/ml when compared to either 1 x 10^5cell/ml and 5 x 10^5cell/ml (**: $p < 0.001$). Concentrations 2.5 x 10^5cell/ml and 5 x 10^5cell/ml were significantly different from 1 x 10^5cell/ml (***: $p < 0.006$) and 5 x 10^5cell/ml (****: $p < 0.003$).

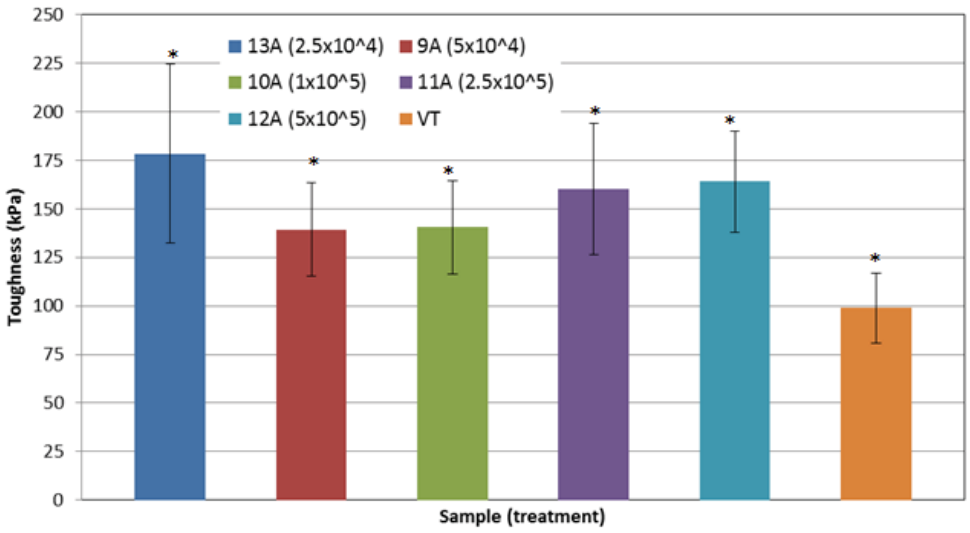

Figure 3.14: Modulus of Toughness for Cell Concentration Groups. Error bars represent a 95% mean population. Statistical significance was found in the modulus of toughness of the all cell concentrations when compared to the virgin tissue (*:$p < 0.001$). There was no statistical significance between the cell concentrations for the modulus of toughness.

3.3.2 Finite Element Analysis

The representative samples of the Dosage study, Figure3.12, were chosen to be modeled. Section 2.8 outlines how the models were created, the software used, and the boundary conditions that were applied. The force needed to displace the sample in the finite element model was compared to the experimental force needed at the same displacement. The finite element and experimental forces can be seen in Table 3.2. Figure 3.15 shows the finite element model of the sample and where the force was taken.

Table 3.12: Comparison of FEA Forces and Tensile Test Forces

Sample	Displacement (mm)	Tensile Force (N)	FEA Force (N)	% Difference
9A-1I	10.05	7.3	7.33	0%
9A-4S	10.05	6.4	6.43	0%
9A-5I	10.05	6.1	8.19	26%
9A-7S	10.05	6.5	6.71	3%
10A-3I	6.63	5.5	7.49	27%
10A-7S	6.63	4.0	6.82	41%
11A-2I	11.90	7.0	7.65	9%
11A-4I	11.90	5.7	6.18	9%
11A-5I	11.90	5.7	6.1	6%
12A-2S	6.00	8.4	7.07	19%
12A-3I	6.00	3.0	5.4	45%
12A-5I	6.00	6.3	6.68	6%
13A-1S	7.58	5.0	6.31	21%
13A-2S	7.58	7.2	6.98	2%
13A-3S	7.58	3.8	4.74	20%
13A-6S	7.58	3.4	4.23	21%

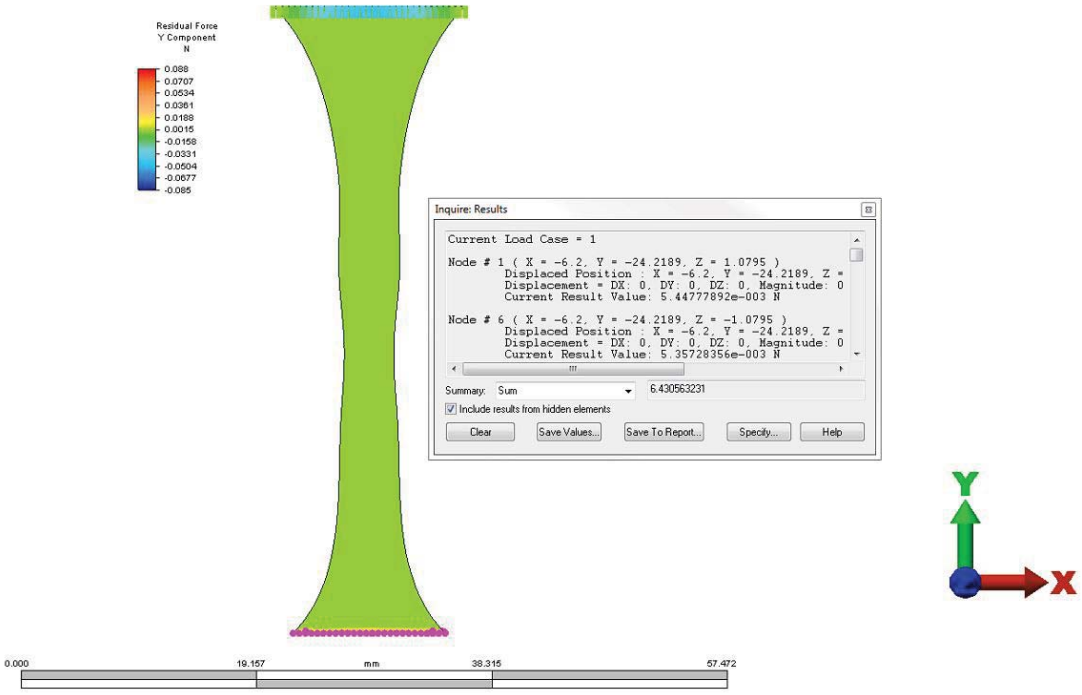

Figure 3.15: FEA Model of Tissue Sample 9A-4S

3.3.3 Discussion

(1) Mechanical Properties Only the thickness can be used as a comparison to the virgin tissue thickness since the widths were cut to specific dimensions. When looking at Figure 3.16, the data does not present a trend relating dosage to the thickness of the tissue. The cell concentration of 2.5 $x10^4$ cells/ml, the smallest dosage, had a thickness significantly lower than the concentrations of $5x10^4$ cells/ml and $2.5x10^5$cells/ml. All the cell concentrations had no significant difference in thicknesses when compared to the virgin tissue. Furthermore, concentrations of $1x10^5$cells/ml and $5x10^5$cells/ml had a thickness with no significant difference to the other concentrations.

The tensile strength (maximum stress) data did not seem to present any kind of a definitive trend either. Every cell concentration had a significantly higher maximum stress than the virgin tissue. The cell concentration of $5x10^5$cells/ml, the highest cell concentration, had the highest tensile strength, however, it was only significantly higher than the concentration of $5x10^4$ cells/ml and 2.5 x 10^5cells/ml. The concentration of 1 x 10^5cells/ml was also significantly higher than the concentration of 5 x 10^4cells/ml.

For the modulus of elasticity, only the cell concentrations of 2.5 x 10^5cells/ml and $5x10^5$cells/ml were significantly higher than the virgin tissue. Like with the maximum stress, the concentration of $5x10^5$cells/ml had the highest modulus of elasticity, but was only significantly higher than 2.5 x 10^4cells/ml, 5 x 10^4cells/ml, and 2.5 x 10^5cells/ml. The concentration of 1 x 10^5cells/ml was also significantly higher than the concentrations of 2.5 x 10^4cells/ml, 5 x 10^4cells/ml, and 2.5 x 10^5cells/ml. The was no significant difference

between concentration 1 x 10^5cells/ml and 5x10^5cells/ml or between the concentrations of 2.5 x 10^4cells/ml, 5 x 10^4cells/ml, and 2.5 x 10^5cells/ml.

There was no significance difference in the modulus of toughness between any of the cell concentration groups; however, there did seem to be a trend. For cell concentrations of 5x10^4 cells/ml, 1x10^5 cells/ml, 2.5x10^5 cell/ml, and 5x10^5cells/ml, the toughness value increased as the dosage concentration for the group increased. The cell concentration of 2.5 x10^4 cells/ml did not follow this trend as it had a higher modulus of toughness than the other four groups. The cell concentration groups were all significantly higher than the virgin tissue.

The results show that there could be a correlation between the amount of MSCs applied to the wound and the increase in the mechanical properties. With this being said, it would have to be assumed that the concentrations of 5 x10^4 cells/ml and 2.5x10^5 cell/ml were not accurate. This is because the concentration of 2.5 x10^5 cells/ml had properties similar to those of concentration 5x10^4, which was a much lower dosage, and should have had values between cell concentrations 1x10^5cells/ml and 5x10^5cells/ml. For the concentration of 2.5 x10^4 cells/ml, its mechanical properties were inconsistent and should have been the lowest of the five groups since it was the lowest dosage. However, it had the highest modulus of toughness, the lowest thickness, and was the third highest for maximum stress and modulus of elasticity. These results led to the repeat dosage study in which the concentrations of 2.5 x10^4 cells/ml, 2.5x10^5 cell/ml, and 5x10^5cells/ml would be repeated to verify the results.

(2) <u>Finite Element Models</u> Finite Element models of the samples in Table 3.12 were made and the reaction force in the Y-direction was compared to the load force recorded by

the Instron in order to verify the models. The percent difference of the forces ranged from 0% to 45% with a mean of 16%. The difference in the forces could be due to inaccurate dimensioning of the tissue. Unlike the finite element models in Section 3.2, these models had a percent difference and were not as accurate. This inaccuracy means that further work and modifications will be needed to make the models more accurate

3.4 Repeat of Dosage Trial

Since there were questions concerning the accuracy of cell concentrations of 2.5×10^4 cells/ml, 2.5×10^5 cell/ml, and 5×10^5 cells/ml of the dosage study, it was decided to repeat these three cell concentrations. Table 3.13 shows the groups and MSCs concentration for this trial. The results from these groups would be compared to the corresponding concentration group from the dosage trial in Section 3.3.

Table 3.13: Repeat Dosage Trial Groups

Experimental Group	Technique for Closure	Number of Rats
13R	Same as group 2 + MSCs at 2.5×10^4 cells/ml	7
11R	Same as group 2 + MSCs at 2.5×10^5 cells/ml	7
12R	Same as group 2 + MSCs at 5×10^5 cells/ml	7

3.4.1 Experimental Results

For the repeat dosage trial, there were a total of 42 samples. Table 3.14 shows the number of samples in each group, the average thickness, the average width, and the average area of the tissue. Individual samples measurements are in Tables A.13 – A.15 in Appendix A.

Table 3.14: Average Dimensions for Groups 11R – 13R

Group	Number of Samples	Width(mm)	Thickness(mm)	Area(mm^2)
13R	14	5.3 ± 0.84	1.83 ± 0.37	9.75 ± 2.78
11R	14	5.59 ± 0.67	2.34 ± 0.19	13.02 ± 1.33
12R	14	6.1 ± 1.07	1.97 ± 0.19	11.98 ± 2.15

Significant differences for the thickness can be seen in Figure 3.12. Figure 3.16 shows the thickness for the original concentration and the repeat concentration. Using the TTest function in Excel, significant differences were found when comparing the results for each dosage group.

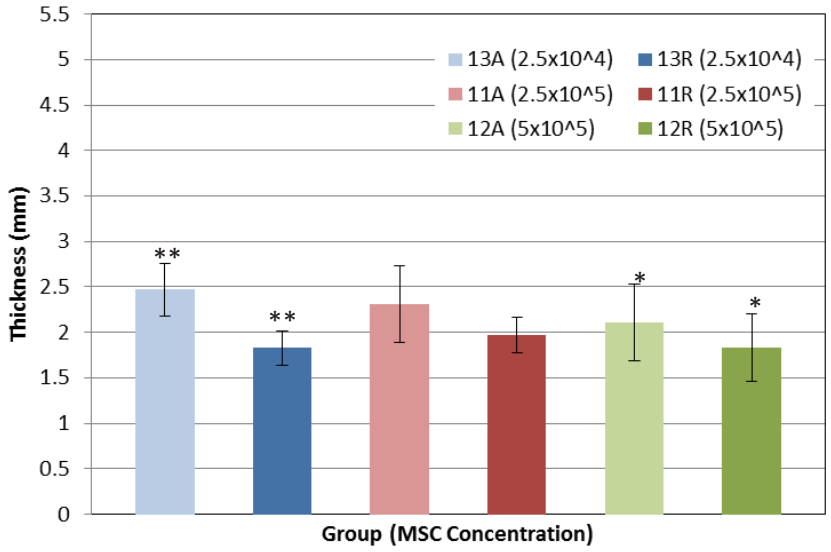

Figure 3.16: Average Thickness for Groups 11A, 11R, 12A, 12R, 13A, 13R, and VT. Error bars represent a 95% mean population. Statistical significance was found in the thickness of the two cell concentrations of 5 x 10^5cell/ml, (*: $p < 0.05$). There was also a significant difference in the thickness when comparing the two concentrations of 2.5 x 10^4cells/ml (**: $p < 0.05$). There was no significant difference when comparing the two concentrations of 2.5 x 10^5cells/ml.

The statistical analysis described in Section 2.11 was used to see if any of the mechanical property values should be discarded and a mean population of 95% was found. Table 3.15 shows maximum stress, maximum strain, modulus of elasticity, and modulus of toughness. Mechanical properties for each sample can be seen in Tables B.13 – B.15 in Appendix B.

Table 3.15: Mechanical Properties for Repeat Dosage Trial Groups

Group	95% Mean Population of Max Stress (kPa)	95% Mean Population of Max Strain (mm/mm)	95% Mean Population of Elasticity (kPa)	95% Mean Population of Toughness (kPa)
13R	1074 ± 137	0.234 ± 0.035	6240 ± 1065	140 ± 29
11R	677 ± 97	0.182 ± 0.028	4969 ± 709	75 ± 18
12R	702 ± 100	0.154 ± 0.024	6051 ± 751	65 ± 14

Significant differences for the mechanical properties can be seen in Figure 3.18 to 3.21. Table 3.16 shows the samples from each group that had a modulus of elasticity, modulus of toughness, max stress, and max strain which were within the mean population values. These samples were chosen to be the best representatives for their respective groups.

Table 3.16: Quality Samples for Repeat Dosage Study

Group	Sample
13R	3I
11R	2I, 5I, & 6I
12R	3S & 4S

Figure 3.17 shows the stress-strain curves that best represent groups 11R, 12R, and 13R. These samples had a modulus of elasticity and modulus of toughness within the mean population. Stress-strain curves for every sample in groups 11R, 12R, and 13R can be seen in Figures C.13 – C.15 in Appendix C.

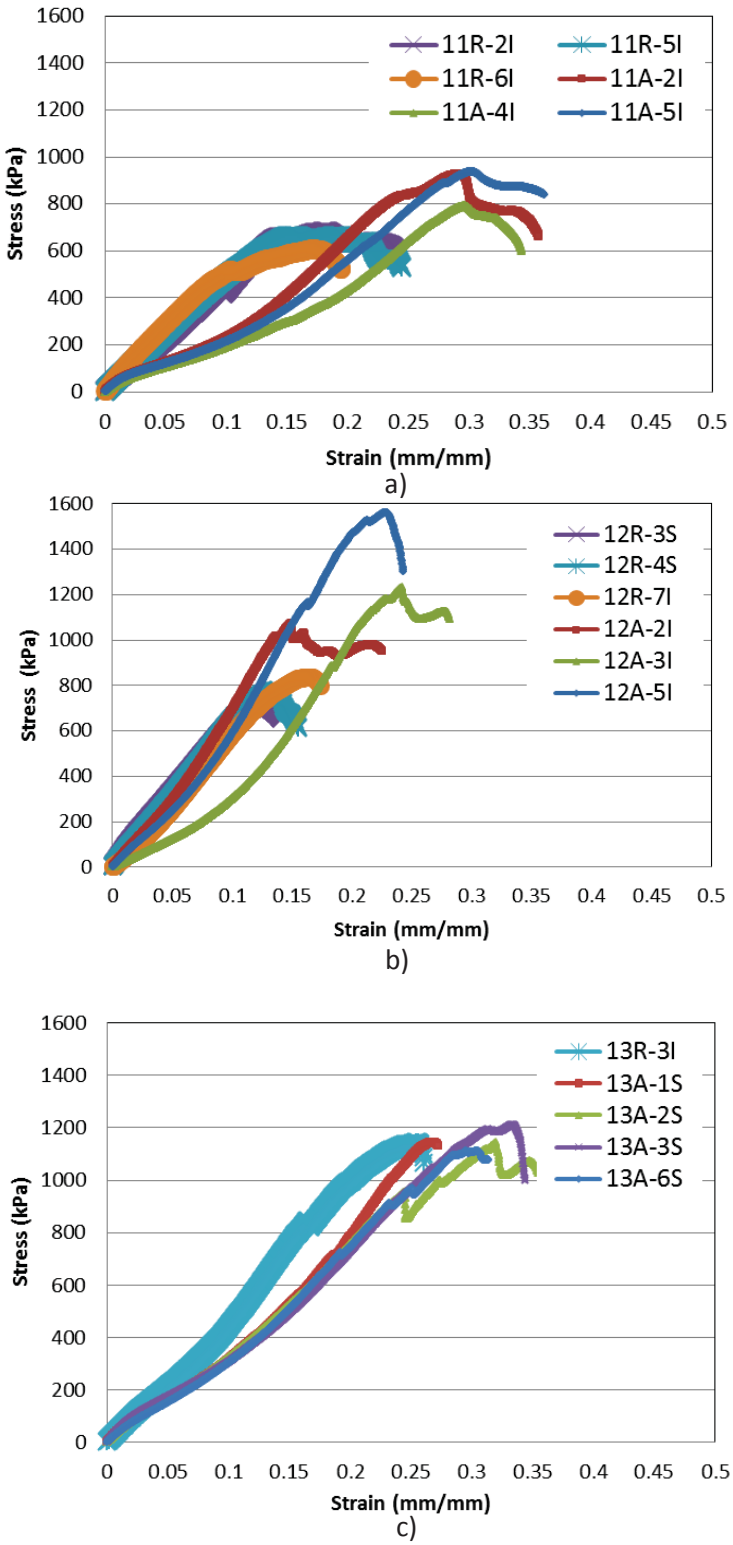

Figure 3.17: Stress-Strain Curves for Groups a) 11R, b) 12R, c) and 13R

Figure 3.18 shows the variation in the maximum stress, Figure 3.19 the maximum strain, Figure 3.20 the modulus of elasticity, and Figure 3.21 the modulus of toughness for the original concentration and repeat concentration.

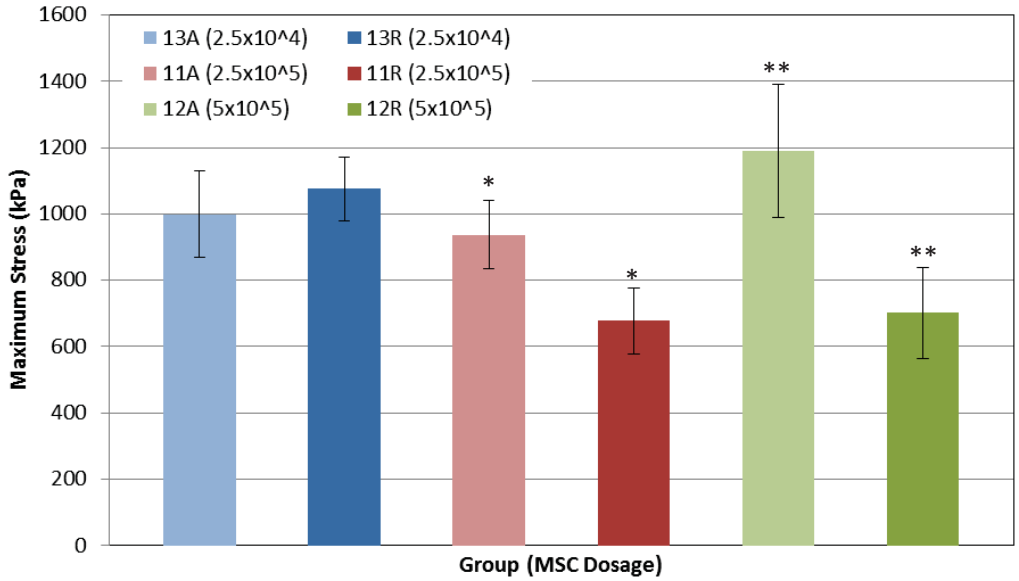

Figure 3.18: Comparison of the Maximum Stress between the two Cell Concentrations. Error bars represent a 95% mean population. Statistical significance was found in the maximum stress of the two cell concentrations of 2.5 x 10^5cell/ml, (*: $p < 0.05$). There was also a significant difference in the maximum stress when comparing the two concentrations of 5 x 10^5cells/ml (**: $p < 0.05$). There was no significant difference when comparing the two concentrations of 2.5 x 10^4cells/ml.

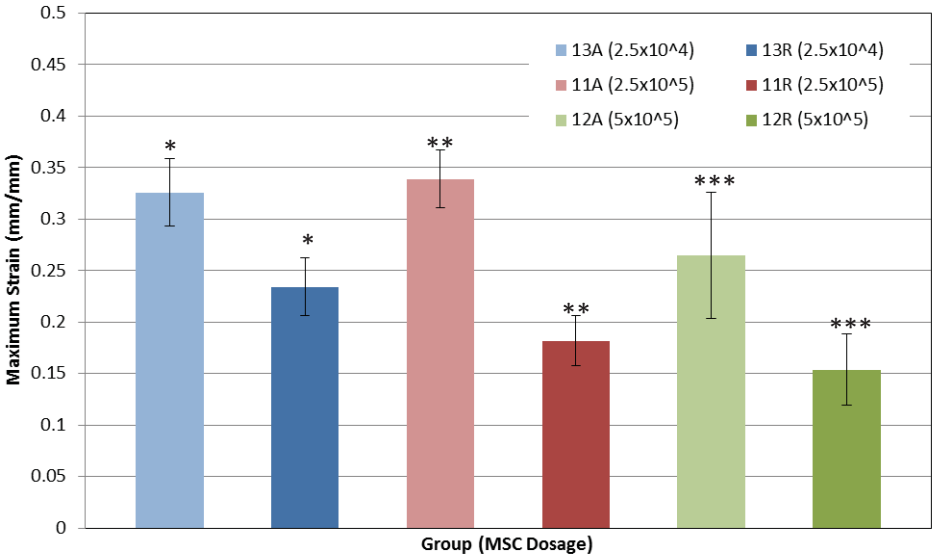

Figure 3.19: Comparison of the Maximum Strain between the two Cell Concentrations. Error bars represent a 95% mean population. Statistical significance was found in the maximum strain of the two cell concentrations of 2.5 x 10^4cell/ml, (*: $p = 0.007$). There was also a significant difference in the maximum strain when comparing the two concentrations of 2.5 x 10^5cells/ml (**: $p < 0.001$). There was no significant difference when comparing the two concentrations of 5 x 10^5cells/ml (***: $p < 0.001$).

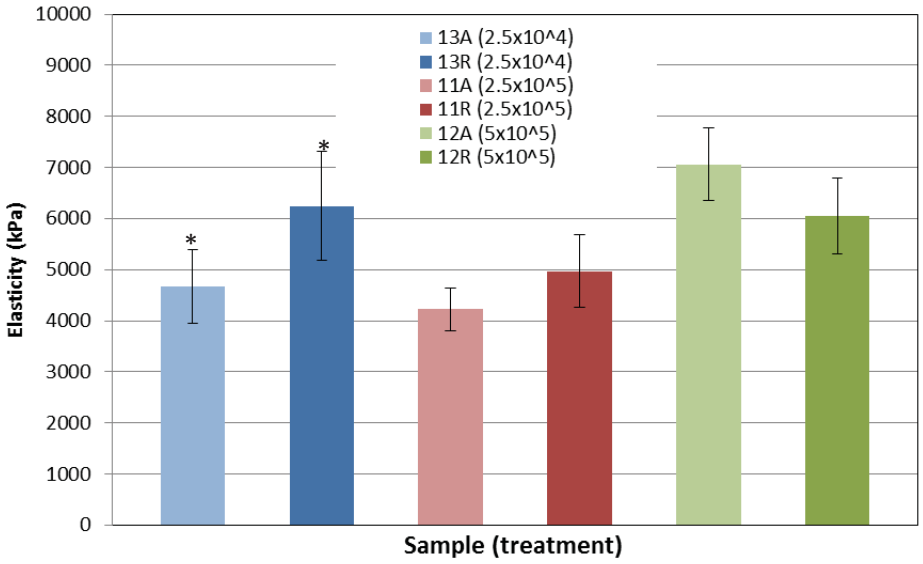

Figure 3.20: Comparison of the Modulus of Elasticity between the two Cell Concentrations. Error bars represent a 95% mean population. Statistical significance was found in the modulus of elasticity of the two cell concentrations of 2.5 x 10^4cell/ml, (*: $p < 0.05$). There was no significant difference when comparing the two concentrations of 2.5 x 10^5cells/ml or the two concentrations of 5 x 10^5cells/ml.

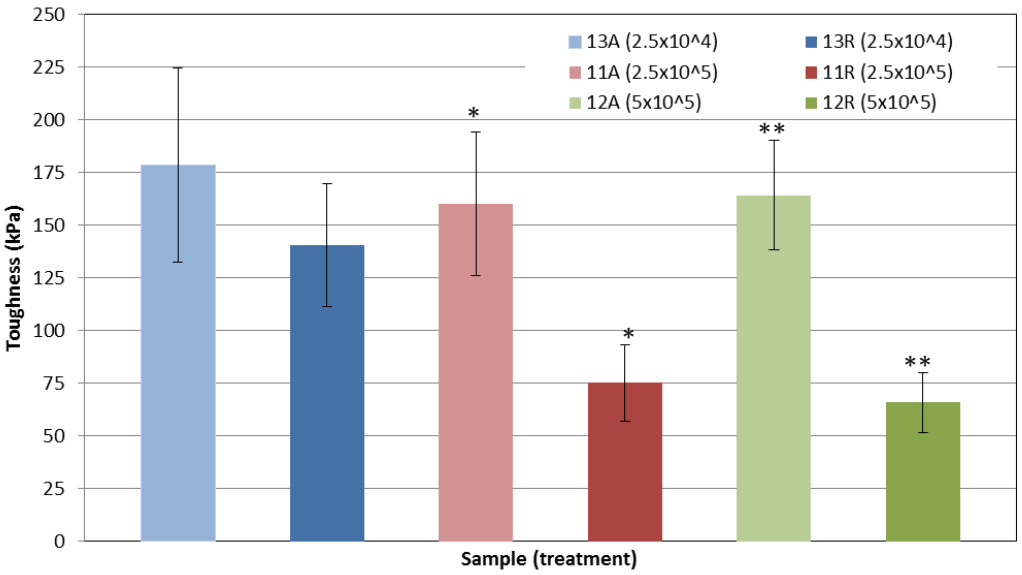

Figure 3.21: Comparison of the Modulus of Toughness between the two Cell Concentrations. Error bars represent a 95% mean population. Statistical significance was found in the modulus of toughness of the two cell concentrations of 2.5 x 10^5cell/ml, (*: $p < 0.05$). There was also a significant difference in the modulus of toughness when comparing the two concentrations of 5 x 10^5cells/ml (**: $p < 0.05$). There was no significant difference when comparing the concentration of 2.5 x 10^4cells/ml.

3.4.2 Discussion

(1) Mechanical Properties The repeat dosage study produced mixed results and only verified a few of the results from the previous dosage study. Each of the groups had thicknesses smaller than what was found in the previous study, but only the concentrations of 2.5 x 10^5cell/ml and 5 x 10^5cells/ml had a significant difference. The cell concentration of 2.5x10^4 cells/ml had the highest mechanical properties of the three groups, but had the lowest cell concentration. All of the cell concentrations had a decrease in modulus of toughness, but only the concentrations of 2.5x10^5 cell/ml and 5x10^5cells/ml were significantly lower. Concentrations of 2.5x10^5 cell/ml and 5x10^5cells/ml also had a significantly lower maximum strength than in the previous dosage study. It is also important to note that the modulus of

toughness for these two groups decreased by over 100%. The cell concentration of $2.5x10^4$cells/ml saw a significant increase in modulus of elasticity. Similar to the first dosage study, the concentration of 2.5×10^4 cell/ml had the highest modulus of toughness and there was no significant difference between the two studies. It is also important to note that for each group, the maximum strain was significantly less in the repeat dosage study when compared to the original dosage study maximum strain. The higher toughness for the concentration of 2.5×10^4 could reflect the difference resulting from a ratio between the platelet to the MSCs, but further testing would need to be performed to prove this hypothesis. Since this study didn't completely clear up the questions left after the original dosage study, it is still unclear if there is a definitive correlation between the dosage and the mechanical properties.

3.5 Results of both Dosage Studies Combined

For this section, the results for the two dosage studies, Section 3.3 and 3.4, were combined and looked at for trends.

3.5.1 Experimental Results

For the combined dosage study, there were a total of 112 samples. Table 3.17 shows the number of samples in each group, the average thickness, the average width, and the average area of the tissue. Significant differences for the thickness can be seen if Figure 3.22. "C" represents groups that contain data from both dosage studies.

Table 3.17: Average Dimensions for Groups 9 – 13

Group	Number of Samples	Width(mm)	Thickness(mm)	Area(mm^2)
13C	28	4.87 ± 0.82	1.97 ± 0.36	9.55 ± 2.17
9A	14	4.49 ± 0.58	2.47 ± 0.36	11.19 ± 2.53
10A	14	4.37 ± 0.74	2.29 ± 0.37	10.05 ± 2.76
11C	28	3.57 ± 1.03	2.42 ± 0.33	11.34 ± 2.42
12C	28	5.21 ± 1.29	2.14 ± 0.37	10.94 ± 1.97

Figure 3.22 shows the thickness for the combined dosage study. Using the TTest function in Excel, significant differences were found when comparing the results for each dosage group.

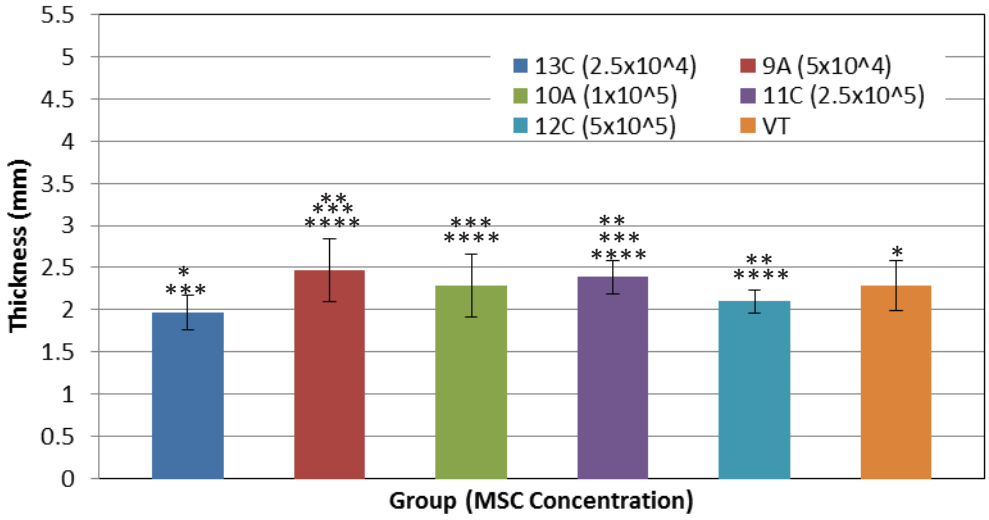

Figure 3.22: Average Thickness for Groups 13C, 9A, 10A, 11C, 12C, and VT. Error bars represent a 95% mean population. Statistical significance was found in the thickness of the cell concentrations of 2.5 x 10^4cell/ml and the virgin tissue (*: $p < 0.05$). There was also a significant difference in the thickness of the concentration of 5 x 10^4cells/ml and 2.5 x 10^5cells/ml when compared to the concentration of 5 x 10^5cells/ml (**: $p < 0.05$). Significant difference in the thickness of the concentration of 2.5 x 10^4cells/ml when compared to the concentrations of 5 x 10^4cells/ml, 1 x 10^5cells/ml, and 2.5 x 10^5cells/ml (***: $p < 0.05$). There was also a significant difference in the thickness of the concentration of 5 x 10^5cells/ml compared to the concentration of 5 x 10^4cells/ml, 1 x 10^5cells/ml, and 2.5 x 10^5cells/ml (****: $p < 0.05$).

The statistical analysis described in Section 2.11 was used to see if any of the mechanical property values should be discarded and a mean population of 95% was found. Table 3.18 shows maximum stress, maximum strain, modulus of elasticity, and modulus of toughness.

Table 3.18: Mechanical Properties of Combined Dosage Study

Group	95% Mean Population of Max Stress (kPa)	95% Mean Population of Max Strain (mm/mm)	95% Mean Population of Elasticity (kPa)	95% Mean Population of Toughness (kPa)
13C	1036 ± 87	0.280 ± 0.061	5455 ± 722	152 ± 26
9A	865 ± 131	0.305 ± 0.033	4274 ± 836	139 ± 24
10A	1050 ± 136	0.239 ± 0.021	6705 ± 1081	140 ± 24
11C	811 ± 24	0.260 ± 0.027	4596 ± 415	111 ± 21
12C	919 ± 125	0.209 ± 0.028	6556 ± 715	115 ± 23

Significant differences for the mechanical properties can be seen in Figure 3.23 to 3.26. “C” represents groups that contain data from both dosage studies. Figure 3.23 shows the variation in the maximum stress, Figure 3.14 the maximum strain, Figure 3.25 the modulus of elasticity, and Figure 3.26 the modulus of toughness for the combination of the dosage studies.

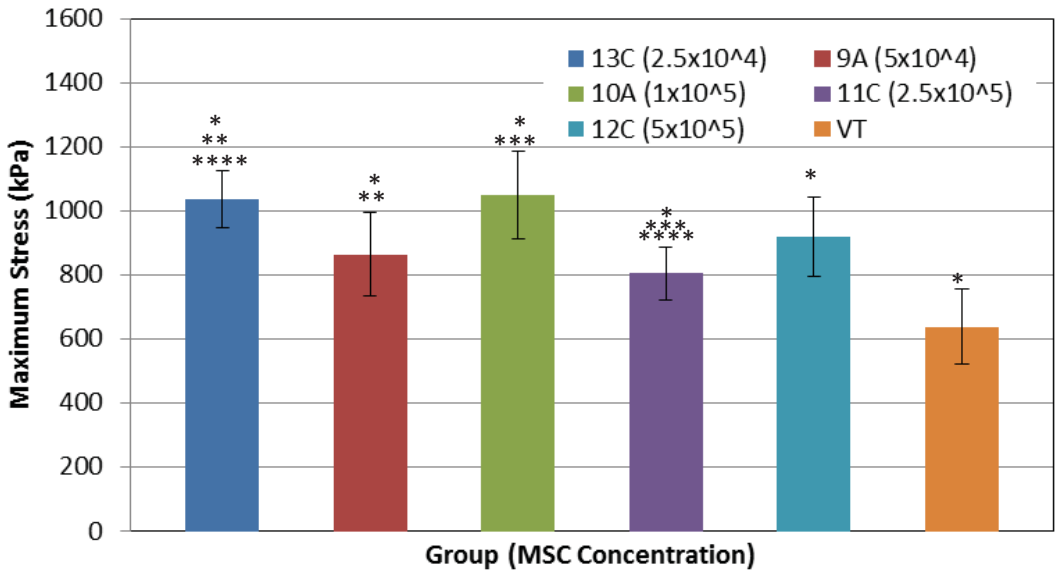

Figure 3.23: Average Maximum Stress for Groups 13C, 9A, 10A, 11C, 12C, and VT. Error bars represent a 95% mean population. Statistical significance was found in the maximum stress of all the cell concentrations when compared to the virgin tissue (*: $p < 0.05$). There was also a significant difference in the maximum stress of the concentration of 5 x 10^4cells/ml and 2.5 x 10^4cells/ml (**: $p < 0.05$). There was significant difference in the concentration of 2.5 x 10^5cells/ml when compared to the concentration of 1 x 10^5cells/ml (***: $p = 0.002$). There was also a significant difference in the thickness of the concentration of 2.5 x 10^4cells/ml compared to the concentration of and 2.5 x 10^5cells/ml (****: $p < 0.001$).

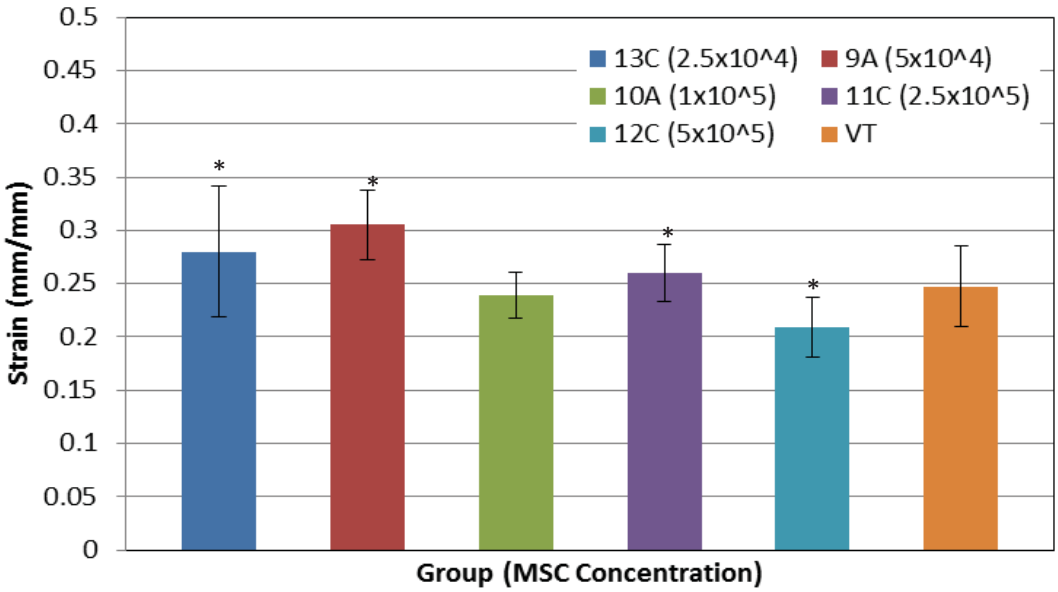

Figure 3.24: Average Maximum Strain for Groups 13C, 9A, 10A, 11C, 12C, and VT. Error bars represent a 95% mean population. Statistical significance was found in the maximum strain of the cell concentration of 5 x 10^5cell/ml when compared to 2.5 x 10^4cell/ml, 5 x 10^4cell/ml, and 2.5 x 10^5cell/ml (*: $p < 0.003$). There was no significant difference in the maximum strain between the dosage concentrations and the virgin tissue.

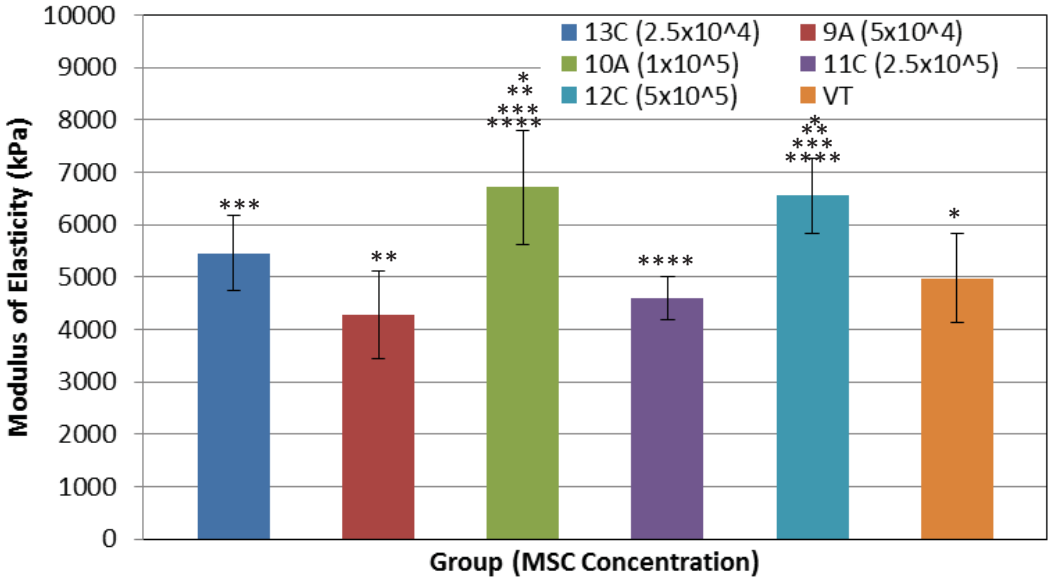

Figure 3.25: Average Modulus of Elasticity for Groups 13C, 9A, 10A, 11C, 12C, and VT. Error bars represent a 95% mean population. Statistical significance was found in the modulus of elasticity of the cell concentrations of 1 x 10^5cell/ml and 5 x 10^5cell/ml when compared to the virgin tissue (*: $p < 0.002$). There was also a significant difference in the modulus of elasticity of the concentration of 1 x 10^5cell/ml and 5 x 10^5cell/ml when comparing them to the concentration of 5 x 10^4cells/ml (**: $p < 0.001$), 2.5 x 10^4cells/ml (*** : $p < 0.01$), and 2.5 x 10^5cells/ml (**** : $p < 0.001$).

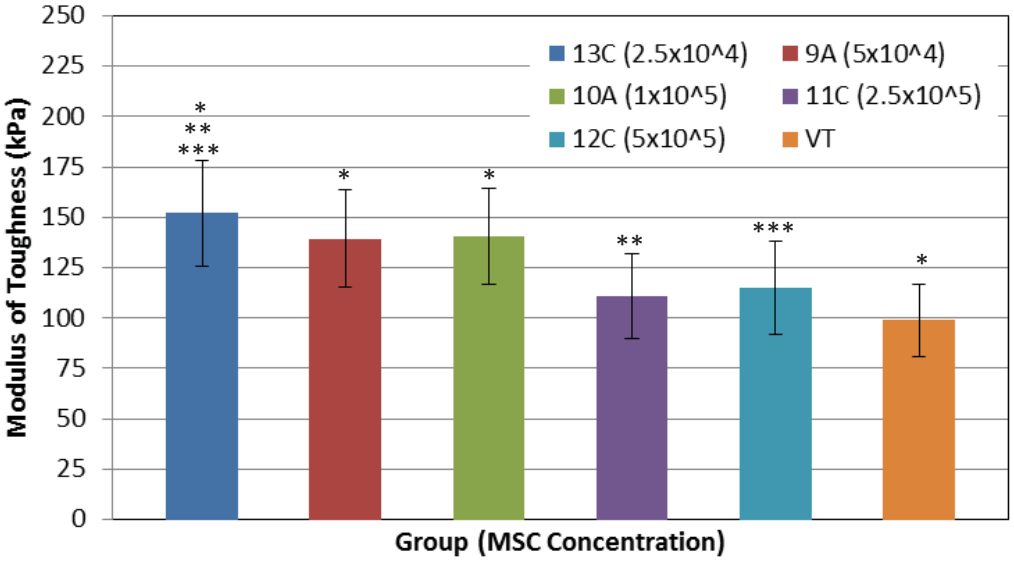

Figure 3.26: Average Modulus of Toughness for Groups 13C, 9A, 10A, 11C, 12C, and VT. Error bars represent a 95% mean population. Statistical significance was found in the modulus of toughness of the cell concentrations of 2.5 x 10^4cell/ml, 5 x 10^4cell/ml, and 1 x 10^5cell/ml when compared to the virgin tissue (*: $p < 0.05$). There was also a significant difference in the modulus of toughness of the concentration of 2.5 x 10^4cells/ml and 2.5 x 10^5cells/ml (**: $p < 0.01$). Significant difference was seen in the modulus of toughness of the concentration 2.5 x 10^4cells/ml when compared to the concentrations of 5 x 10^5cells/ml (***: $p < 0.01$).

3.5.2 Discussion

When looking at the combine data for the two dosage studies, there were several changes in which concentration had the best results. For the thickness, the concentration of 2.5 x 10^4cells/ml is now significantly lower than the virgin tissue. The maximum stresses for each concentration groups are still significantly higher than the virgin tissue. The concentration of 5 x 10^5cells/ml saw a significant decrease in maximum stress when comparing the original to the combined data ($p < 0.05$). Also, the concentration of 1 x 10^5cells/ml has the highest maximum stress. The only change in the modulus of elasticity values is that the concentration of 1 x 10^5cells/ml now has the highest value. For the modulus of toughness, all concentration dosages are still significantly higher than the virgin tissue. The concentration

of 2.5 x 10^4cells/ml is now significantly higher than the concentrations of 2.5 x 10^5cells/ml and 5 x 10^5cells/ml. There is also a new trend discovered when looking at the modulus of toughness values in that the toughness decreases as the cell concentration increases. This furthers the hypothesis made in Section 3.4.2 where the higher toughness for the concentration of 2.5 x 10^4 could reflect the difference resulting from a ratio between the platelet to the MSCs.

3.6 Non-Invasive Elastography

For some medical cases, absolute property values are required to make a proper diagnosis, such as the Young's modulus. This study is performed to investigate the feasibility of a strain elastogram as an alternative method to estimating the Young's modulus for in-vivo use.

3.6.1 Results

Four samples, 12A-3I, 12A-4I, H1, and H2, were used for comparing the strain obtained through the tensile test to the strain obtained through elastography. Figure 3.22 shows the stress-strain curves using tensile test strain and the elastography strain.

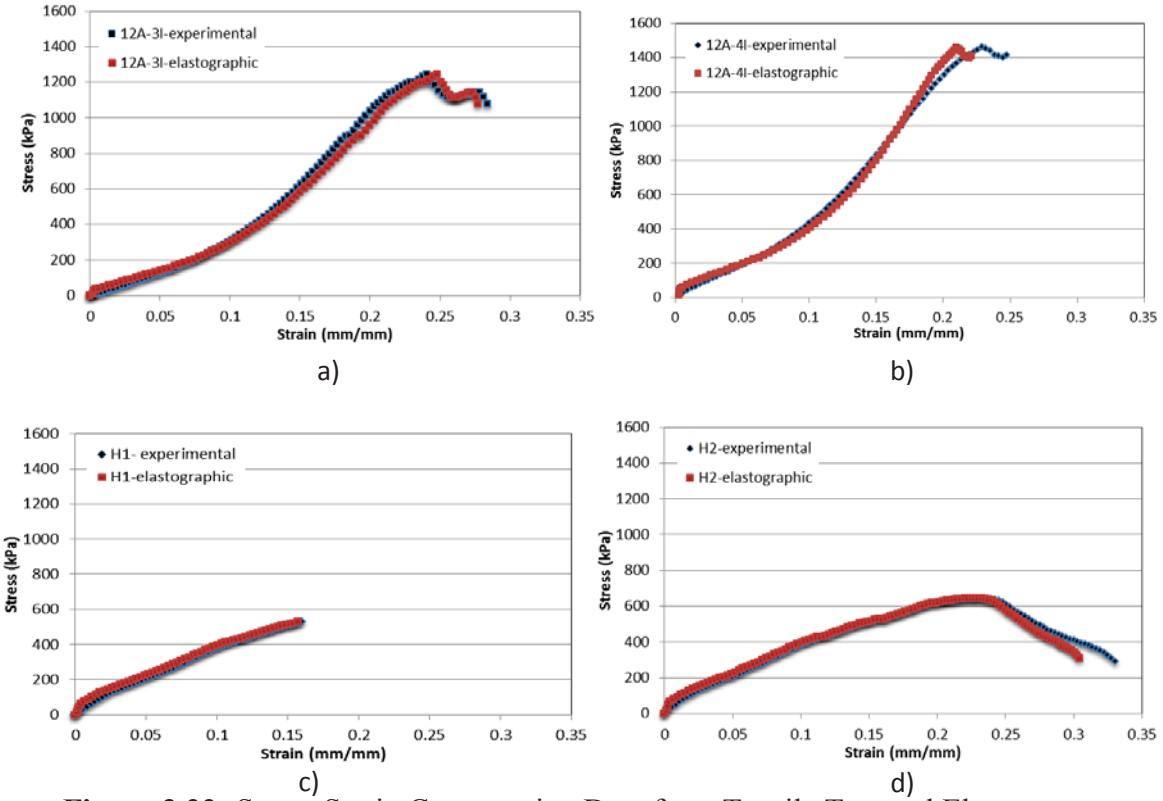

Figure 3.22: Stress-Strain Curves using Data from Tensile Test and Elastograms

a) 12A-3I b) 12A-4I c) H1 and d) H2

Table 3.19 shows the young's modulus for the elastography data and the tensile test data.

Table 3.19: Young's Modulus from Tensile Test and Elastogram

	12A-3I	**12A-4I**	**H1**	**H2**
Tensile Test (kPa)	2586	3739	3169	2971
Elastography (kPa)	2804	3404	3241	2877
Percent Difference (%)	8.4	9.8	2.3	3.3

Table 3.20 shows the modulus of toughness for the elastography data and the tensile test data.

Table 3.20: Modulus of Toughness from Tensile Test and Elastogram

	12A-3I	12A-4I	H1	H2
Tensile Test (kPa)	170	166	48	131
Elastography (kPa)	162	150	50	129
Percent Difference (%)	4.7	10.7	4.2	1.6

3.6.2 Discussion

Figure 3.13 shows that the elastography strain is similar to the tensile test strain. There are, however, two locations were the sets of data seem to differ. The first is in the beginning of the stress-strain curve. When looking at the graphs, one can see that each of the four elastography stress-strain curves have four or five points that are steeper than they should be. This error is due to the timing of the start of the Instron being a bit off from the start of the camera's recording. Since the camera is started slightly before the Instron begins stretching the tissue, the first couple of points in the elastography has a force associated to the same strain point, which is zero. The second point of error is when the tissue experiences plastic deformation. It seemed that once the linear climb in the stress-strain curve stops, the two stress-strain curves slowly diverged from one and another. It is not exactly known to why this error occurs. The properties of the tissue could change once failure occurs and the light reflects off the tissue differently because of this.

Table 3.19 shows that there was an 8.4%, 9.8%, 2.3% and 3.3% difference in the modulus of elasticity between the elastography data and tensile test data for samples 12A-3I, 12A-4I, H1, and H2. Table 3.20 gives 4.7%, 10.7%, 4.2%, and 1.6% difference in the modulus of

toughness for the same four samples. These low percent differences show that elastography can be used as a way to obtained strain data that can be used to find Young's modulus for in-vivo testing.

CHAPTER 4

CONCLUSION

Defects to the abdominal wall can improperly heal and have a 10% - 20% chance of leading to hernia formation. Even though there have been numerous techniques in decreasing hernia formation, no standard procedure has been established. Recently, the uses of mesenchymal stromal cells (MSCs) have been shown to decrease the healing time of skin wounds, tendons, muscles and ligaments. MSCs have the ability to differentiate into various cell types making them hard to be rejected by the site; they also have the ability to divide rapidly. These qualities have led MSCs to become very popular in the medical field. This study had two main objectives. The first objective was to determine if the additives of MSCs and platelet-rich plasma (PRP) on collagen tape led to increase in wound healing of the abdominal muscle and fascia in a rat model after four and eight weeks recovery period. The second study was to investigate the wound healing at different cell dosages. For both studies, the effects the MSCs and PRP were looked at by performing a histology analysis and tensile strength analysis on the samples. For the first study, the tensile test data and histology analysis showed the samples that had been treated with PRP and MSCs healed better than the PRP only group and the control group. For the dosage trial, a definitive healing trend could not be made from the tensile test and histological data and further studies will need to be performed.

4.1 Mechanical Properties vs. Histological Analysis

Collagen has been shown in studies by Ahmed et al. (2005), Boccafoschi et al. (2005), Jung et al. (2007), and Lin et al. (2006) to provide a scaffold for fibroblast migration and collagen deposition. This, in theory, could lead to an increase in the modulus of elasticity and toughness. In this current study however, only the preliminary trial had collagen contributions that matched up with the tensile test data. When looking at the histology report, (Heffner et al., 2012) and the mechanical properties of the combination of MSCs + PRP, group 3A and 3B, there seems to be a relation between the abundance and organization of collagen and the modulus of elasticity and toughness as this treatment had the highest histology scores and mechanical values at both four and eight weeks. This was also the case when comparing the PRP only treated group, 2A, with the control, group 1A, at four weeks recovery as the organization was similar for each group but the PRP treated group had significantly more abundance. However at eight weeks, the PRP group, 2B, had a slightly lower abundance and much lower organization of collagen despite higher mechanical properties. The PRP group also had significantly higher myocyte degeneration. According to Iwata et al. (2003), myocyte degeneration has been attributed to membrane defects such as an increase in brittleness in the mechanical stress. The higher degeneration in the PRP group could be why its' modulus of elasticity and toughness is only slightly higher than the control group even though the collagen abundance is significantly higher in the PRP group at four weeks.

The dosage study had mixed results when trying to relate the histology report, (Bown, 2013) to the tensile test data. The cell concentrations of $5x10^4$ cells/ml and $2.5x10^5$ cells/ml had similar Young's modulus, but different modulus of toughness's and his histology report

showed that they had similar collagen organization and abundance numbers. The difference in toughness could be explained by the concentration $2.5x10^5$ cells/ml having a higher degeneration than concentration $5x10^4$ cells/ml. For the cell concentrations of $2.5x10^4$ cells/ml, $1x10^5$ cells/ml, and $5x10^5$ cells/ml, there was little correlation between their mechanical properties and histology analysis. The concentration of $1x10^5$ cells/ml had the highest collagen organization and abundance scores and the lowest myocyte degeneration scores, but had lower modulus of elasticity and toughness than the $2.5x10^4$ cells/ml concentration group . The $2.5x10^4$ cells/ml concentration group had the lowest abundance of collagen and organization and highest degeneration scores, but had the third highest modulus of elasticity and the highest modulus of toughness. From the data collected from the tensile test, Bown hypothesis that the concentration of 1×10^5cells/ml is the optimal dosage could not be backed up by the mechanical properties. However, if the data for both dosage studies were to be combined as it was in Section 3.5.1, the concentration 1×10^5cells/ml would have the highest maximum stress and modulus of elasticity and would help Bown's hypothesis. This cannot be confirmed until the histology reports are analyzed for the repeat dosage study.

4.2 Mechanical Properties vs. Literature

Since no articles were found using PRP and MSCs, the comparison of mechanical properties obtained experimentally to those found in literature were based solely on MSC treatment studies.

In Young et al. (1998) study, he looked at how MSCs could improve the healing process of Achilles tendon repair. Like this current study, the MSC treated Achilles tendons had a significant increase in maximum force and modulus of toughness at four and eight weeks

over the control group. Another similarity between the studies was the drop in difference between the mechanical properties from four to eight weeks recovery. In Young's study, the modulus of elasticity was 60% greater than the control at four weeks but drops to 45% greater at eight weeks. The same pattern is seen with the modulus of toughness and maximum stress in which the toughness goes from 128% greater than the control at four weeks to 53% greater than the control at eight weeks. The maximum stress goes from being 83% greater than the control at four weeks to 45% greater than the control at eight weeks.

The drops in the current study, however, were much steeper as the modulus of elasticity is 280% greater than the control at four weeks and drops to 77% greater than the control at eight weeks. The same dramatic drop is seen in the toughness and maximum stress as the toughness goes from being 325% greater at four weeks to 142% greater at eight weeks and the maximum stress goes from being 400% greater at four to 217% greater at eight weeks. The difference in the drops in the two studies can be attributed to this study's MSCs + PRP treated tissue being closer to healed as the properties stayed similar from four to eight weeks. In Young's study, the MSCs treated Achilles' properties still were changing at even at twelve weeks.

Another trend that was made between the current study and Young's was that the control group's mechanical properties increased more than the treated groups from four to eight weeks. In Young's study, the modulus of elasticity, modulus of toughness, and maximum stress saw an increase of 86%, 13%, and 53% from four to eight weeks. The MSCs treated group saw an increase of 37% for the modulus of elasticity, 2.2% increase to the maximum stress, and a decrease of 32% in the modulus of toughness. The current study had no change in the modulus of elasticity for the treated group, a 10% increase maximum stress, and a 13%

increase in modulus of toughness. The control group saw around a 110% increase in all mechanical properties. This furthers the conclusion the rat hernia repairs faster with the addition of MSCs + PRP and is close to being completely healed.

In studies done by Liu et al. (2006) and Li et al. (2007), a similar trend in the difference from the MSCs treated group to the control group from seven to fourteen days was observed. Liu had a maximum stress that went from being 76% greater than the control at seven days to 39% greater at fourteen days. Li saw the same decrease in maximum stress percent difference from four to eight weeks of 82% to 13% respectively. Thus these other studies confirm the findings in this study that the addition of MSCs decreases the time it takes to heal from hernia repair.

However, since this study did not investigate the effects of just MSCs, no direct comparison can be made to the literature articles that were found. Since data that was able to be compared matched up with the data found in literature, it can be concluded that combination of MSCs and PRP added to the significant increase to the mechanical properties over the control's properties. A study to determine just how much the PRP contributed is warranted. It is also unclear to why in literature none of the samples mechanical properties surpassed those of virgin tissue; while the current study, any group with PRP and MSCs had properties greater than the virgin tissue samples.

4.3 Finite Element Models vs. Literature

Niebur et. al (2000) and Davis et al. (2013) both developed finite element models to simulate soft tissue tension test. The finite element models in both studies produced similar results to

the experimental data. Niebur study had a 3.6% difference in maximum tensile stress and Davis had percent difference of the peak tensile stress of 13%, 12%, 24%, and 50% at strain rates of 10 mm/s, 1 mm/s, 0.1 mm/s, and 0.01mm/s. This study's models had an average percent difference of 15%, falling in line with Niebur's study and adds to the validation of the finite element model.

4.4 Future Work

For future work, the four studies would be suggested. The first study would be to investigate how treating the hernia rupture with just MSCs affected the biomechanics properties and histological analysis of the tissue during healing. From the studies done so far, it was shown that MSCs + PRP greatly enhanced the biomechanics properties and histological analysis. It needs to be determined how much of this was due to the MSCs, and if the PRP enhances the healing effects of MSCs. The second study would be another dosage study, but with the dosages varying by at least a million each. By having a greater separation between dosages, the error in counting the amount of MSCs in each injection would not be as significant as when the dosages are only a quarter of a million different. A third suggested study would be a fatigue test. After a prescribed number of cycles centered on a mean load, the tissue would then be stretched to failure. This would be done in-order to simulate the actual stretching the tissue would undergo in the body. The mean load, amplitude of the cyclic load, and frequency of the load would have to be determined. A time study would be the fourth suggested study needed to be done. This study would require samples to be collected six to eight times within the four week period to see how quickly the MSCs work, and if the herniated tissue is healed before four weeks.

Investigating to see if elastography could be used as a way to find the strain in specific regions of the tissue would be another area of interest. It is believed that the tissue sample's modulus of elasticity increases as it gets nearer to the scar area. Unfortunately, these values cannot be found through experimental testing, and Literature only indicates that this can be done by drawing a grid on the sample being tested and measuring how much this grid deforms after testing. Elastography would provide a non-invasive way of calculating localized strains that can be done at multiple locations. By obtaining localized strains, the finite element models would become more accurate and a greater understanding of how the mechanical properties are affected once the abdominal wall has had an incision made on it. Localized strain values through elastography would also allow a comparison to virgin tissue to see if the strain regions match up.

APPENDIX A

Individual Sample Measurements

Table A.1: Dimensions for Virgin Tissue

VT	Width(mm)	Thickness(mm)	Area(mm^2)
10I	6.88	2.13	14.6544
10S	5.68	1.88	10.6784
11I	6.23	1.88	11.7124
12I	5.63	2.25	12.6675
12S	5.36	2.48	13.2928
13I	6.56	2.56	16.7936
13S	5.49	2.24	12.2976
14I	6.01	2.41	14.4841
14S	7.16	2.76	19.7616

Table A.2: Dimensions for Group 1A

1A	Width(mm)	Thickness(mm)	Area(mm^2)
1I	9.14	3.8	34.732
1S	10.46	1.8	18.828
2I	8.14	4.5	36.63
2S	8.1	3.95	31.995
3I	9.09	4.02	36.5418
3S	6.97	4.5	31.365
4I	9.59	3.87	37.1133
4S	7.58	3.77	28.5766
5I	9.7	4.7	45.59
5S	6.11	4.23	25.8453
6I	9.84	3.51	34.5384
6S	5.74	3.57	20.4918
7I	8.43	4.01	33.8043
7S	8.29	4.31	35.7299

Table A.3: Dimensions for Group 1B

1B	Width(mm)	Thickness(mm)	Area(mm^2)
1I	7.68	3.44	26.4192
1S	7.43	3.91	29.0513
2I	5.82	3.77	21.9414
2S	7.39	3.06	22.6134
3I	8.32	4.01	33.3632
3S	4.89	4.32	21.1248
4I	7.81	3.23	25.2263
4S	5.18	3.81	19.7358
5I	7.17	3.9	27.963
5S	4.46	3.95	17.617
6I	7.52	4.69	35.2688
6S	5.28	4.33	22.8624
7I	6.65	4.65	30.9225
7S	4.47	3.73	16.6731

Table A.4: Dimensions for Group 2A

2A	Width(mm)	Thickness(mm)	Area(mm^2)
1I	6.25	4.08	25.5
1S	7.37	3.96	29.1852
2I	6.76	3.5	23.66
2S	7.13	3.71	26.4523
3I	6.95	4.42	30.719
3S	6.84	4.24	29.0016
4I	5.94	4.02	23.8788
4S	6.06	4.8	29.088
5I	5.14	3.59	18.4526
5S	8.98	4.69	42.1162
6I	7.63	3.67	28.0021
6S	6.79	4.29	29.1291
7I	7	2.83	19.81
7S	6.22	4.52	28.1144

Table A.5: Dimensions for Group 2B

2B	Width(mm)	Thickness(mm)	Area(mm^2)
1I	5.87	2.77	16.2599
1S	6.36	2.94	18.6984
2I	7.01	3.12	21.8712
2S	5.78	2.65	15.317
3I	5.84	2.95	17.228
3S	6.16	3.53	21.7448
4I	5.52	2.95	16.284
4S	5.66	3.09	17.4894
5I	6.47	3.24	20.9628
5S	4.44	3.55	15.762
6I	5.56	3.04	16.9024
6S	6.65	3.12	20.748
7I	6.53	3.3	21.549
7S	7.53	3.86	29.0658

Table A.6: Dimensions for Group 3A

3A	Width(mm)	Thickness(mm)	Area(mm^2)
1I	7.4	2.75	20.35
1S	6.13	3.28	20.1064
2I	5.31	2.47	13.1157
2S	6.17	2.78	17.1526
3I	6.54	2.68	17.5272
3S	5.57	2.23	12.4211
4I	5.24	3.33	17.4492
4S	4.76	2.33	11.0908
5I	5.54	2.88	15.9552
5S	4.44	3.03	13.4532
6I	5.03	2.54	12.7762
6S	3.97	3.95	15.6815
7I	4.81	2.11	10.1491
7S	4.8	2.25	10.8

Table A.7: Dimensions for Group 3B

3B	Width(mm)	Thickness(mm)	Area(mm^2)
1I	7.57	2.97	22.4829
1S	5.51	2.79	15.3729
2I	5.6	2.75	15.4
2S	4.98	3.12	15.5376
3I	6.86	2.41	16.5326
3S	7.28	2.23	16.2344
4I	6.39	2.4	15.336
4S	5.7	2.51	14.307
5I	6.4	2.42	15.488
5S	5.3	2.33	12.349
6I	6.17	2.81	17.3377
6S	5.68	3.05	17.324

Table A.8: Dimensions for Group 9A

9A	Width(mm)	Thickness(mm)	Area(mm^2)
1I	4.54	2.49	11.3046
1S	4.19	1.9	7.961
2I	4.6	3.07	14.122
2S	4.07	2.39	9.7273
3I	3.96	2.31	9.1476
3S	3.97	2.29	9.0913
4I	5.15	2.74	14.111
4S	4.13	2.16	8.9208
5I	5.46	2.97	16.2162
5S	5.16	2.18	11.2488
6I	5.4	2.51	13.554
6S	4.12	3.05	12.566
7I	3.73	2.36	8.8028
7S	4.43	2.23	9.8789

Table A.9: Dimensions for Group 10A

10A	Width(mm)	Thickness(mm)	Area(mm^2)
1I	5.09	2.87	14.6083
1S	3.9	2.18	8.502
2I	4.22	2.13	8.9886
2S	3.09	2.23	6.8907
3I	4.1	1.88	7.708
3S	5.37	2.31	12.4047
4I	5.3	2.77	14.681
4S	4.14	2.18	9.0252
5I	4.95	2.82	13.959
5S	4.55	2.18	9.919
6I	4.9	1.52	7.448
6S	3.99	2.08	8.2992
7I	4.57	2.32	10.6024
7S	3	2.56	7.68

Table A.10: Dimensions for Group 11A

11A	Width(mm)	Thickness(mm)	Area(mm^2)
1I	4.74	3	14.22
1S	3.8	3.48	13.224
2I	4.35	2.29	9.9615
2S	4.53	2.59	11.7327
3I	3.8	2.21	8.398
3S	4.04	2.16	8.7264
4I	4.26	2.67	11.3742
4S	3.92	2.79	10.9368
5I	3.85	2.11	8.1235
5S	3.43	2.82	9.6726
6I	3.15	2.69	8.4735
6S	3.45	2.03	7.0035
7I	3.24	2.16	6.9984
7S	3.57	2.16	7.7112

Table A.11: Dimensions for Group 12A

12A	Width(mm)	Thickness(mm)	Area(mm^2)
1I	5.45	3.2	17.44
1S	4.3	2.44	10.492
2I	5.33	1.78	9.4874
2S	3.61	2.74	9.8914
3I	4.99	1.85	9.2315
3S	3.37	2.39	8.0543
4I	4.37	1.8	7.866
4S	3.7	2.54	9.398
5I	4.38	1.98	8.6724
5S	3.35	2.49	8.3415
6I	4.12	2.18	8.9816
6S	3.76	2.39	8.9864
7I	5.92	1.85	10.952
7S	4.03	2.72	10.9616

Table A.12: Dimensions for Group 13A

13A	Width(mm)	Thickness(mm)	Area(mm^2)
1I	4.99	2.54	12.6746
1S	3.85	2.16	8.316
2I	4.39	2.26	9.9214
2S	4.12	2.69	11.0828
3I	4.01	2.06	8.2606
3S	3.77	2.16	8.1432
4I	4.93	2.26	11.1418
4S	3.59	2.31	8.2929
5I	5.09	1.78	9.0602
5S	4.44	1.8	7.992
6I	4.49	1.8	8.082
6S	5.37	1.8	9.666
7I	5.02	1.8	9.036
7S	4.27	2.18	9.3086

Table A.13: Dimensions for Group 11R

11R	Width(mm)	Thickness(mm)	Area(mm^2)
1I	4.68	2.61	12.2148
1S	5.79	2.44	14.1276
2I	5.33	2.47	13.1651
2S	4.91	2.54	12.4714
3I	6.78	2.37	16.0686
3S	5.58	2.31	12.8898
4I	6.7	2.14	14.338
4S	5.16	2.13	10.9908
5I	6.46	2.13	13.7598
5S	5.53	2.32	12.8296
6I	5.88	2.24	13.1712
6S	4.84	2.73	13.2132
7I	5.34	2.22	11.8548
7S	5.23	2.13	11.1399

Table A.14: Dimensions for Group 12R

12R	Width(mm)	Thickness(mm)	Area(mm^2)
1I	5.63	1.87	10.5281
1S	4.44	1.94	8.6136
2I	6.01	2.21	13.2821
2S	6.04	2.18	13.1672
3I	8.62	1.87	16.1194
3S	4.82	2.34	11.2788
4I	7.23	2.01	14.5323
4S	5.9	1.61	9.499
5I	6.75	1.94	13.095
5S	5.54	1.81	10.0274
6I	6.17	2.17	13.3889
6S	6.18	1.95	12.051
7I	7.01	1.79	12.5479
7S	5.07	1.88	9.5316

Table A.15: Dimensions for Group 13R

13R	Width(mm)	Thickness(mm)	Area(mm^2)
1I	5.85	2.08	12.168
1S	4.56	1.82	8.2992
2I	5.15	2.39	12.3085
2S	4.59	1.43	6.5637
3I	5.07	2.05	10.3935
3S	5.74	1.53	8.7822
4I	4.19	1.87	7.8353
4S	6.65	1.59	10.5735
5I	5.02	1.09	5.4718
5S	5.74	2.03	11.6522
6I	5.57	1.9	10.583
6S	6.31	2.47	15.5857
7I	6.03	1.69	10.1907
7S	3.67	1.67	6.1289

APPENDIX B

Individual Sample Mechanical Properties

Table B.1: Mechanical Properties for Samples of Group VT

VT	High Stress (kPa)	Max Strain (mm/mm)	Mod of Elasticity (kPa)	Mod of Toughness (kPa)
10I	739	0.214	5335	103.13
10S	1031	0.206	4410	108.49
11I	825	0.176	7329	83.72
12I	620	0.33	5613	152.81
12S	597	0.19	5258	75.78
13I	536	0.287	3924	108.31
13S	649	0.293	5626	118.54
14I	580	0.281	4707	105.89
14S	247	0.249	4136	45.84
AVE	647	0.247	5149	100.28
ST. DEV.	214	0.053	1031	29.8

Table B.2: Mechanical Properties for Samples of Group 1A

1A	High Stress (kPa)	Max Strain (mm/mm)	Mod of Elasticity (kPa)	Mod of Toughness (kPa)
1I	180	0.226	836	24.48
1S	201	0.327	1077	42.52
2I	246	0.23	1606	33.06
3I	172	0.25	1131	36.7
3S	242	0.2	1608	24.18
4I	220	0.3	1028	37.71
4S	205	0.223	1218	25.55
5I	167	0.202	1252	21.54
5S	162	0.152	1653	15.76
6I	181	0.193	1171	19.5
6S	218	0.162	1634	22.89
7I	242	0.236	1518	35.96
7S	216	0.2	1606	27.74
AVE	204	0.223	1333.75	28.28
St. DEV	30	0.049	280.54	8.12

Table B.3: Mechanical Properties for Samples of Group 1B

1B	High Stress (kPa)	Max Strain (mm/mm)	Mod of Elasticity (kPa)	Mod of Toughness (kPa)
1S	308	0.127	3001	23.82
2I	402	0.254	2046	51.27
2S	461	0.18	3781	111.29
3I	390	0.258	2377	83.6
3S	400	0.139	3673	24.49
4I	295	0.253	1538	44.09
4S	562	0.206	3428	58.95
5I	384	0.333	1701	79.16
5S	525	0.227	4289	71.9
6I	421	0.298	2050	73.89
6S	570	0.229	3933	56.6
7I	344	0.221	2567	42.89
AVE	421.83	0.227	2865	60.16
ST DEV.	91.55	0.06	943	25.39

Table B.4: Mechanical Properties for Samples of Group 2A

2A	High Stress (kPa)	Max Strain (mm/mm)	Mod of Elasticity (kPa)	Mod of Toughness (kPa)
1I	528.5	0.32	2506	104.08
1S	475	0.27	1859	59.25
2I	385	0.24	2391	46.28
3I	473	0.29	2127	77.68
3S	367	0.32	2383	77.52
4I	377	0.26	2188	50.84
4S	376	0.22	2577	50.37
5I	511	0.23	3088	47.91
5S	335	0.29	1949	54.40
6I	315	0.20	1718	33.44
6S	417	0.26	2172	59.33
7I	352	0.32	1410	64.17
7S	413	0.34	1959	89.13
AVE	410	0.272	2179	62.65
St. DEV.	68	0.044	427	19.55

Table B.5: Mechanical Properties for Samples of Group 2B

2B	High Stress (kPa)	Max Strain (mm/mm)	Mod of Elasticity (kPa)	Mod of Toughness (kPa)
1S	437	0.16	4810	42.01
2I	520	0.3	3427	97.11
2S	590	0.239	3187	112.58
3I	708	0.315	4382	135.04
3S	639	0.385	5157	162.85
4S	629	0.281	3824	90.78
5I	547	0.331	2874	216.56
5S	751	0.234	4596	133.59
6I	560	0.21	3095	54.48
7I	547	0.353	2809	120.56
7S	476	0.218	3200	55.99
AVE	582	0.275	3760	111.05
ST. DEV.	94	0.069	838	51.57

Table B.6: Mechanical Properties for Samples of Group 3A

3A	High Stress (kPa)	Max Strain (mm/mm)	Mod of Elasticity (kPa)	Mod of Toughness (kPa)
1I	673	0.177	6296	76.11
1S	804	0.2	4984	79.33
2S	730	0.155	6099	63.2
3I	604	0.36	2889	137.47
3S	1044	0.25	6510	146.95
4I	768	0.321	3835	141.45
4S	1053	0.236	7156	182.22
5I	634	0.326	3750	127.25
5S	853	0.22	4266	108.01
6I	718	0.24	2750	88.13
6S	861	0.168	7469	86.33
7I	697	0.34	3181	157.53
7S	1184	0.24	6928	151.03
AVE	817	0.249	5086	118.85
ST. DEV	178	0.068	1728	37.49

Table B.7: Mechanical Properties for Samples of Group 3B

3B	High Stress (kPa)	Max Strain (mm/mm)	Mod of Elasticity (kPa)	Mod of Toughness (kPa)
1I	654	0.252	4724	113.05
1S	1026	0.226	6321	120.94
2I	1010	0.4	3256	212.51
2S	1095	0.267	6560	148.91
3I	952	0.36	3589	185.73
3S	912	0.277	5835	133.21
4I	834	0.287	5404	146.84
4S	917	0.217	6342	115.49
5I	817	0.293	4410	147.1
5S	1078	0.28	5314	136.3
6I	948	0.282	5399	143.94
6S	763	0.332	3760	141.22
AVE	917	0.289	5076	145.44
ST. DEV.	131	0.053	1129	28.51

Table B.8: Mechanical Properties for Samples of Group 9A

9A	High Stress (kPa)	Max Strain (mm/mm)	Mod of Elasticity (kPa)	Mod of Toughness (kPa)
1I	844	0.313	4468	148.84
1S	1291	0.333	6351	234.36
2I	556	0.306	3273	90.96
2S	1010	0.234	5494	112.01
3I	1030	0.249	5172	148.98
3S	1154	0.234	7240	141.83
4I	704	0.269	3268	86.39
4S	976	0.283	3995	138.85
5I	733	0.337	3536	115.13
5S	546	0.263	2906	91.49
6I	676	0.365	2882	142.1
6S	725	0.45	2223	205.39
7I	952	0.306	5219	133.2
7S	917	0.335	3806	162.31
AVE	865	0.305	4274	139.42
ST. DEV.	220	0.058	1447	41.99

Table B.9: Mechanical Properties for Samples of Group 10A

10A	High Stress (kPa)	Max Strain (mm/mm)	Mod of Elasticity (kPa)	Mod of Toughness (kPa)
1I	779	0.226	4620	98.61
1S	1029	0.193	8622	122.03
2I	1257	0.246	8759	192.34
2S	1442	0.214	9785	187.29
3I	1099	0.21	7673	126.1
3S	814	0.212	5728	86.89
4I	655	0.273	4470	122.46
4S	1251	0.318	6191	220.35
5I	848	0.21	5351	75.74
5S	1135	0.214	8194	128.53
6I	1332	0.22	8745	158.54
6S	1025	0.265	4736	156.7
7I	824	0.302	4565	146.2
7S	1204	0.25	6430	145.77
AVE	1050	0.24	6705	140.54
ST. DEV.	237	0.038	1873	40.89

Table B.10: Mechanical Properties for Samples of Group 11A

11A	High Stress (kPa)	Max Strain (mm/mm)	Mod of Elasticity (kPa)	Mod of Toughness (kPa)
1I	707	0.295	3743	122.86
1S	656	0.322	3050	111.96
2I	926	0.313	4443	146.8
2S	1030	0.321	4847	167.96
3I	860	0.277	3714	97.41
3S	1146	0.441	4329	230.07
4I	789	0.326	4221	123.05
4S	904	0.316	4864	159.36
5I	933	0.354	4130	172.95
5S	1069	0.306	5529	154.57
6I	907	0.384	3457	178.53
6S	1243	0.431	4576	306.52
7I	854	0.333	3071	127.4
7S	1082	0.322	5151	144.56
AVE	936	0.339	4223	160.28
ST. DEV.	165	0.048	751	53.66

Table B.11: Mechanical Properties for Samples of Group 12A

12A	High Stress (kPa)	Max Strain (mm/mm)	Mod of Elasticity (kPa)	Mod of Toughness (kPa)
1I	409	0.289	2246	77.86
1S	937	0.194	7335	98.84
2I	1071	0.22	8955	144.4
2S	1043	0.262	6361	150.74
3I	1229	0.272	7914	158.19
3S	1356	0.247	9231	188.69
4I	1459	0.245	9266	166.38
4S	1251	0.314	5135	229.64
5I	1560	0.241	8194	191.82
5S	1435	0.278	9076	213.05
6I	1054	0.308	6557	222.77
6S	1189	0.19	9179	122.04
7I	860	0.367	4492	177.31
7S	1038	0.289	4918	155.68
AVE	1135	0.265	7061	164.1
ST. DEV.	293	0.048	2195	44.57

Table B.12: Mechanical Properties for Samples of Group 13A

13A	High Stress (kPa)	Max Strain (mm/mm)	Mod of Elasticity (kPa)	Mod of Toughness (kPa)
1I	658	0.318	2932	102.27
1S	1124	0.264	5361	132.19
2I	853	0.262	3555	95.98
2S	1099	0.348	4507	212.78
3I	966	0.444	3078	231.8
3S	1211	0.342	4372	211.96
4I	603	0.251	3390	82.51
4S	1034	0.206	6584	126.09
5I	747	0.407	2398	174.94
5S	1133	0.558	5472	357.53
6I	1384	0.413	5451	309.48
6S	1108	0.301	3966	163.07
7I	1017	0.249	7027	150.03
7S	1050	0.197	7291	147.9
AVE	999	0.326	4670	178.47
ST. DEV.	273	0.101	2069	84.8

Table B.13: Mechanical Properties for Samples of Group 11R

11R	High Stress (kPa)	Max Strain (mm/mm)	Mod of Elasticity (kPa)	Mod of Toughness (kPa)
1I	750	0.237	4781	115.91
1S	955	0.217	5504	120.85
2I	680	0.207	4589	88.6
2S	829	0.212	5703	100.74
3I	524	0.231	3155	70.55
3S	721	0.146	6428	61.84
4I	319	0.131	2710	24.99
4S	935	0.207	4773	104.61
5I	665	0.208	5011	91.92
5S	622	0.232	3305	74.12
6I	607	0.19	5371	79.15
6S	530	0.112	5556	33.45
7I	610	0.117	5644	41.36
7S	726	0.1	7049	44.4
AVE	677	0.182	4970	75.18
ST. DEV.	167	0.049	1229	30.75

Table B.14: Mechanical Properties for Samples of Group 12R

12R	High Stress (kPa)	Max Strain (mm/mm)	Mod of Elasticity (kPa)	Mod of Toughness (kPa)
1I	457	0.111	5414	33.12
1S	682	0.167	5075	70.8
2I	684	0.211	4557	97.79
2S	674	0.119	5858	40.36
3I	478	0.217	4145	69.82
3S	705	0.14	6287	60.29
4I	722	0.198	4670	89.44
4S	777	0.155	6638	70.72
5I	726	0.189	5522	88.57
5S	999	0.154	7032	81.98
6I	443	0.093	6629	25.24
6S	1007	0.132	9108	80.32
7I	836	0.171	6651	80.05
7S	642	0.096	7136	32.67
AVE	702	0.154	6051	65.8
ST. DEV.	173	0.041	1302	23.75

Table B.15: Mechanical Properties for Samples of Group 13R

13R	High Stress (kPa)	Max Strain (mm/mm)	Mod of Elasticity (kPa)	Mod of Toughness (kPa)
1I	1192	0.272	6121	176.81
1S	850	0.148	7223	74.91
2I	1389	0.162	10135	119.93
2S	780	0.179	6006	67.89
3I	1143	0.263	6303	163.47
3S	973	0.134	6607	64.34
4I	1275	0.234	7724	152.96
4S	1383	0.264	8034	208.54
5I	1102	0.265	3580	149.25
5S	983	0.215	4970	115.83
6I	576	0.331	2969	126.43
6S	1090	0.315	5284	221.24
7I	1316	0.236	7256	191
7S	992	0.262	5159	135.55
AVE	1075	0.234	6241	140.58
ST. DEV.	236	0.06	1845	49.93

APPENDIX C

Stress-Strain Curves for each Sample

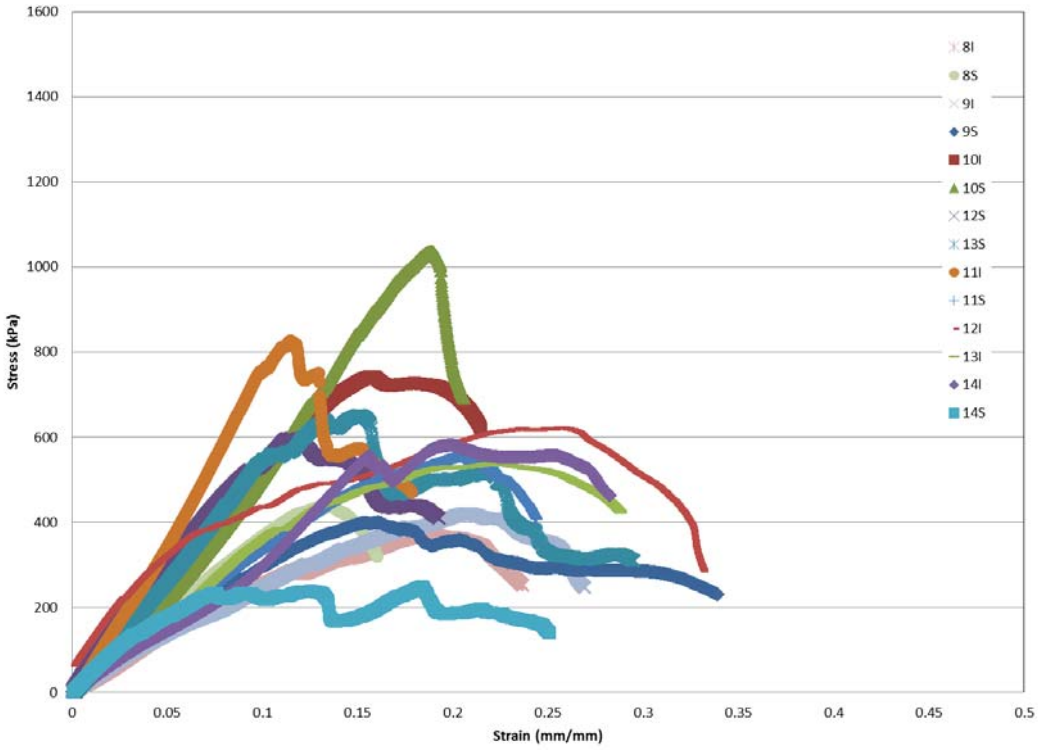

Figure C.1: Stress – Strain Curves for Virgin Tissue Samples

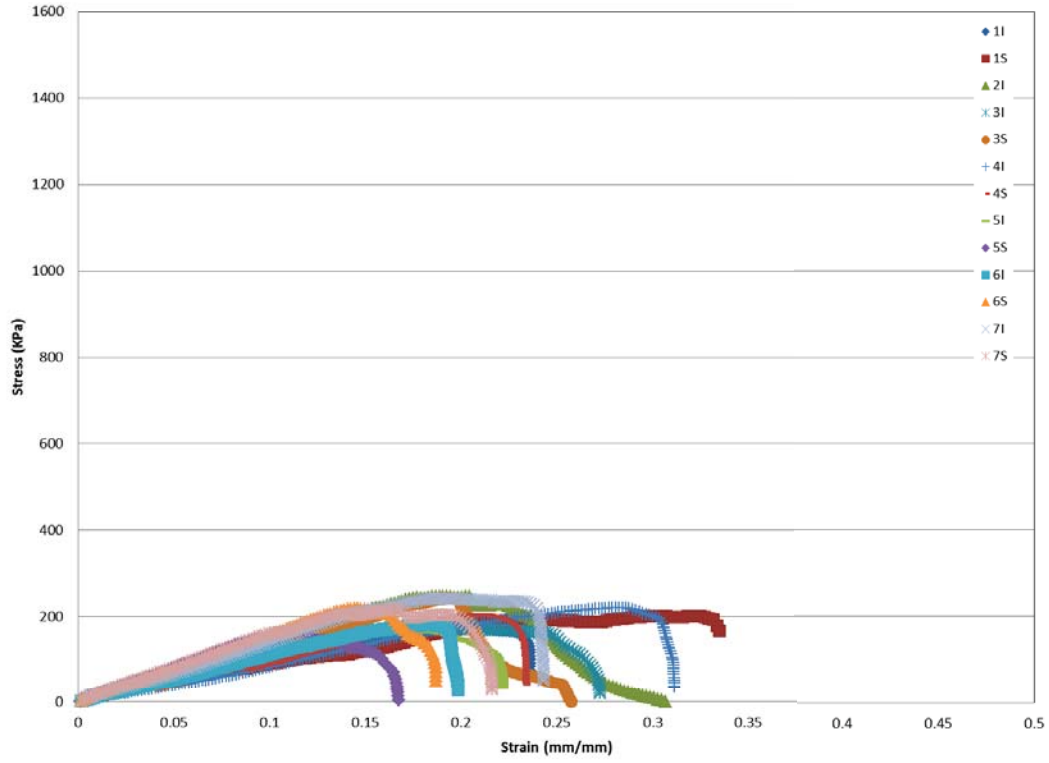

Figure C.2: Stress – Strain Curves for Group 1A Samples

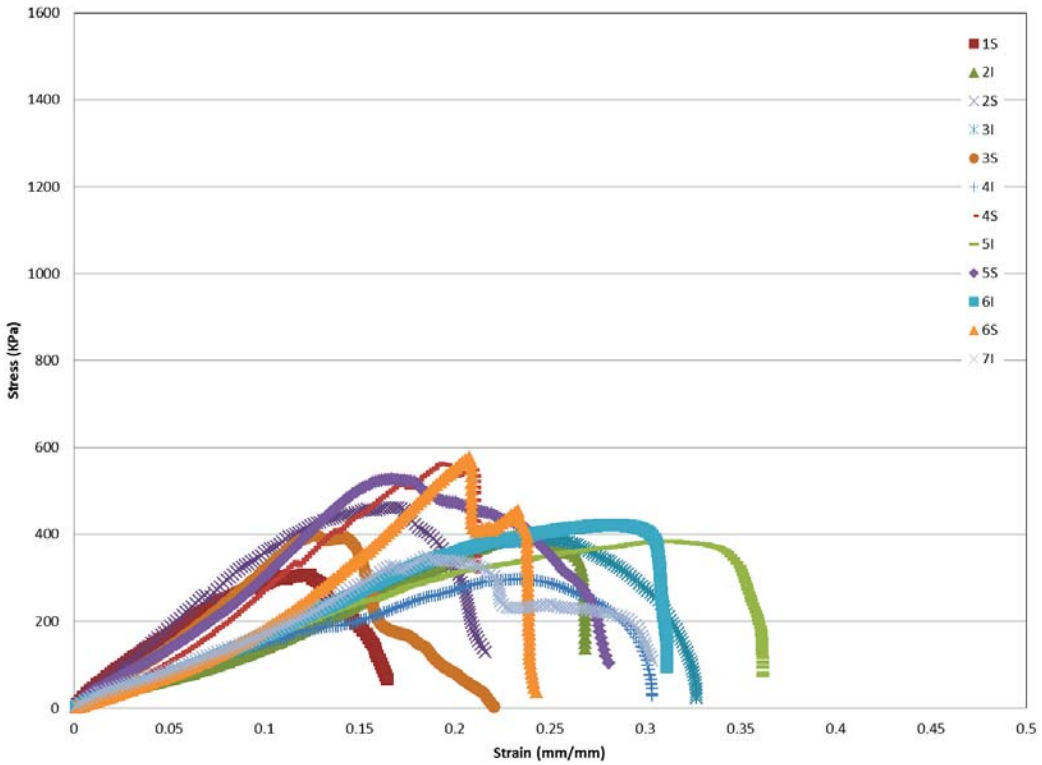

Figure C.3: Stress – Strain Curves for Group 1B Samples

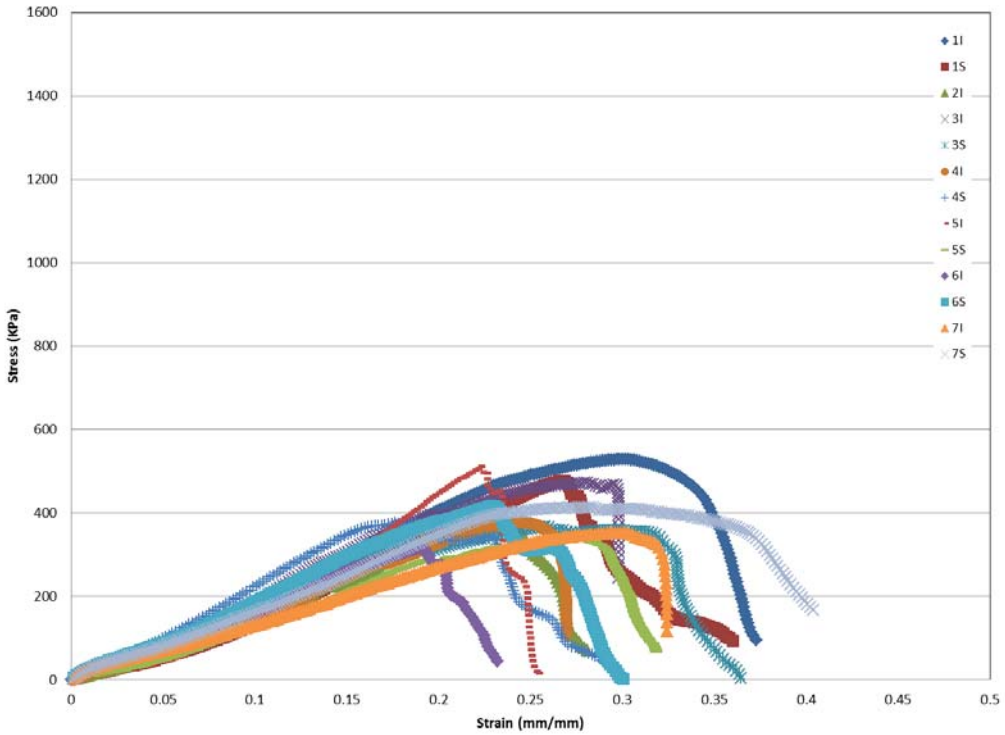

Figure C.4: Stress – Strain Curves for Group 2A Samples

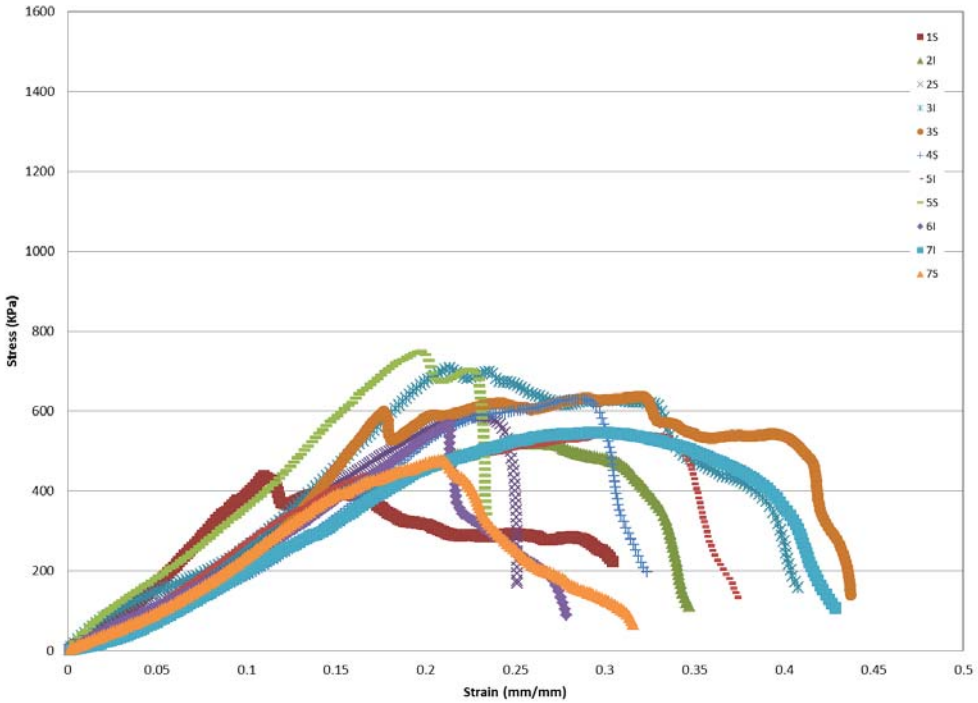

Figure C.5: Stress – Strain Curves for Group 2B Samples

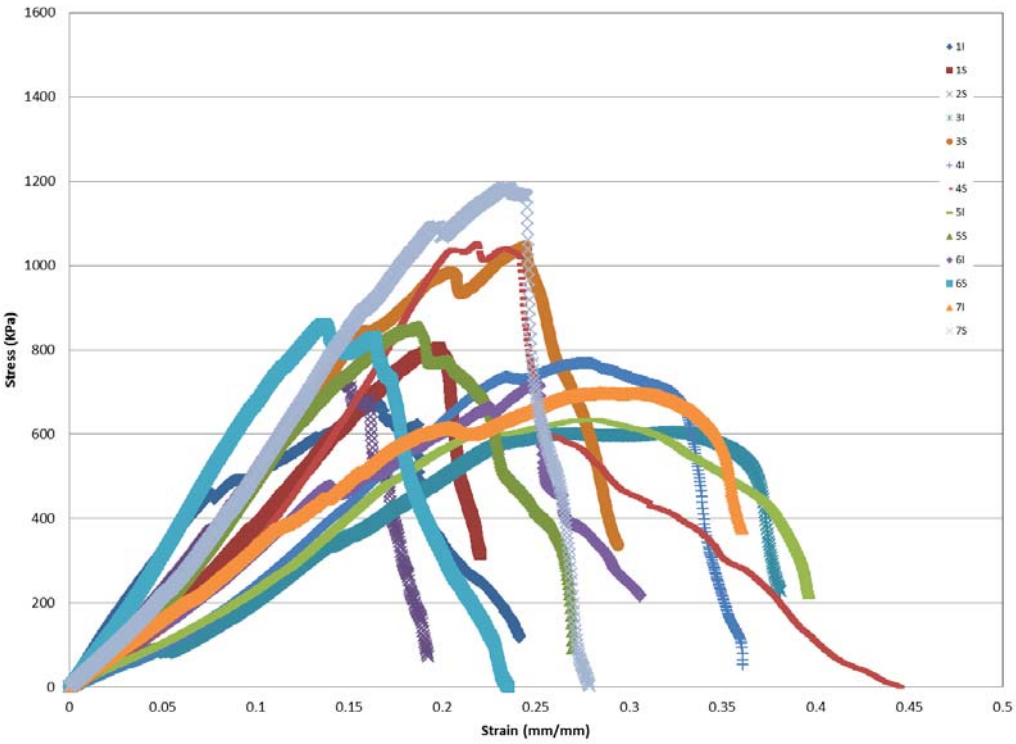

Figure C.6: Stress – Strain Curves for Group 3A Samples

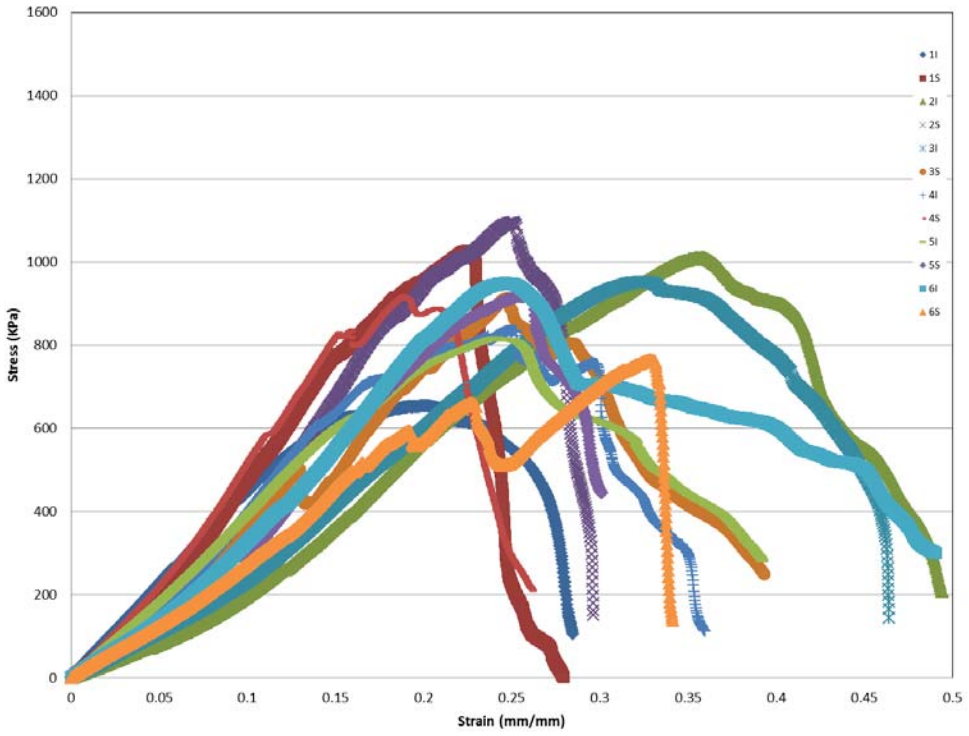

Figure C.7: Stress – Strain Curves for Group 3B Samples

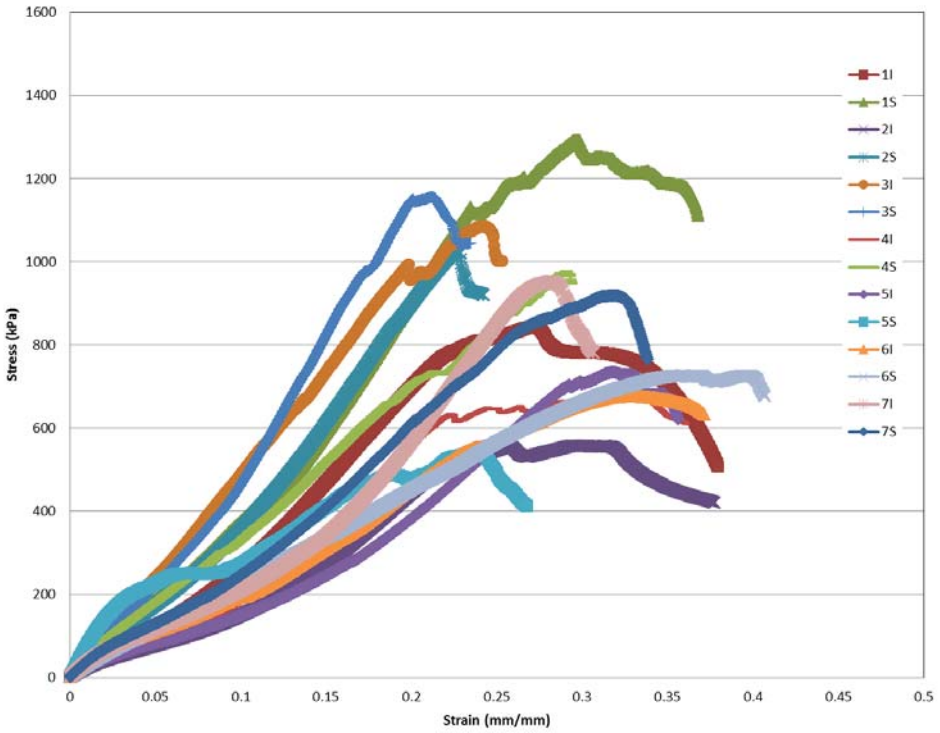

Figure C.8: Stress – Strain Curves for Group 9A Samples

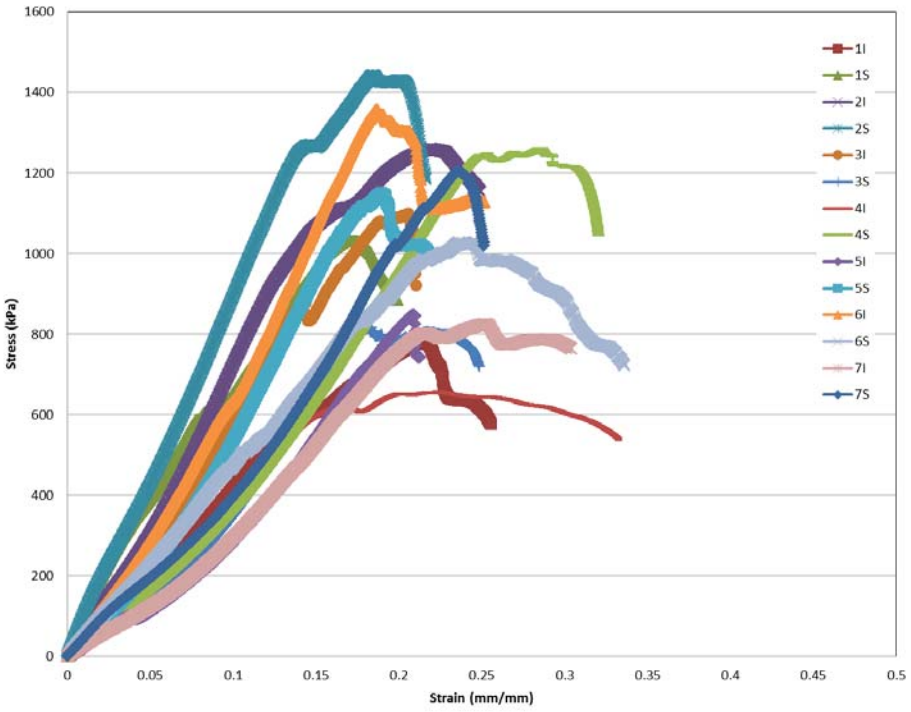

Figure C.9: Stress – Strain Curves for Group 10A Samples

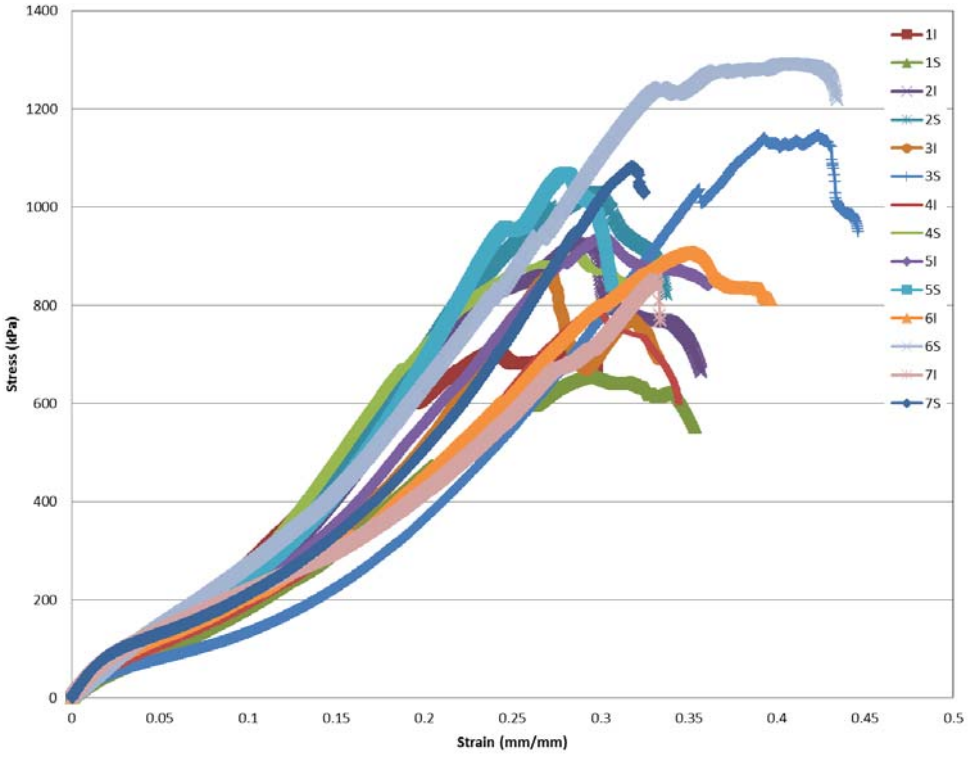

Figure C.10: Stress – Strain Curves for Group 11A Samples

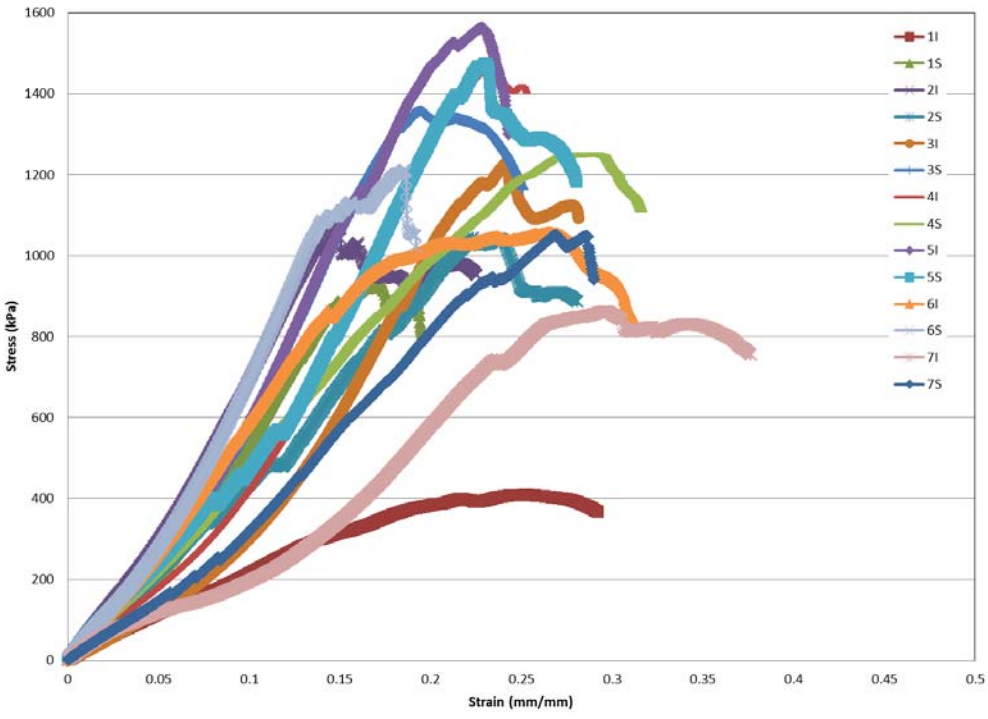

Figure C.11: Stress – Strain Curves for Group 12A Samples

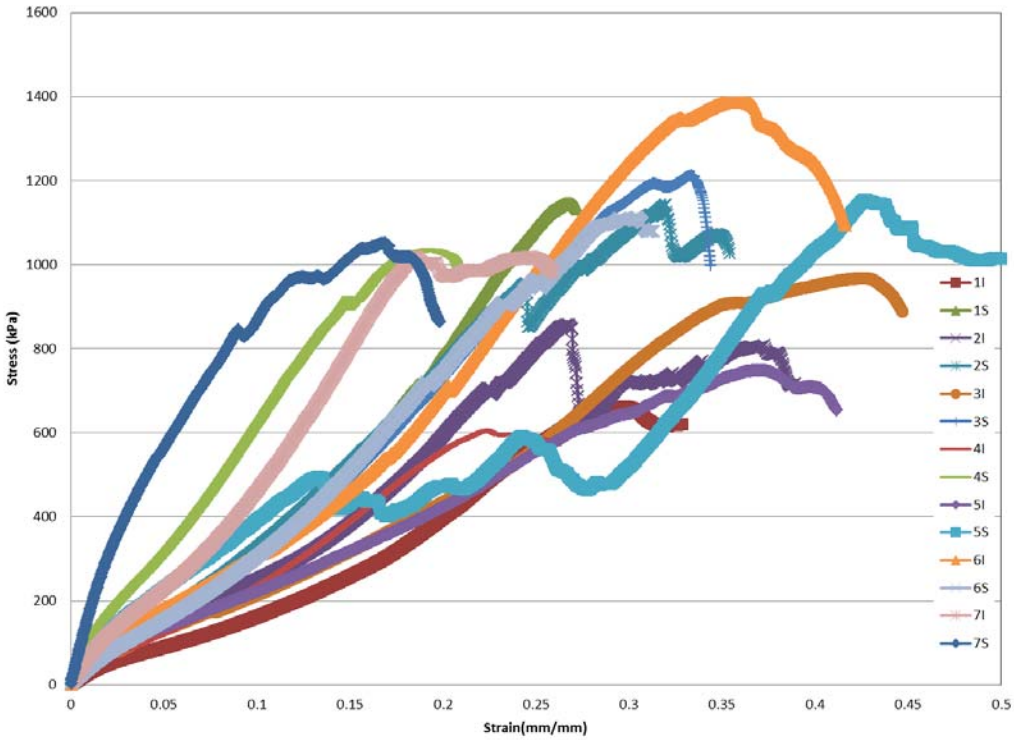

Figure C.12: Stress – Strain Curves for Group 13A Samples

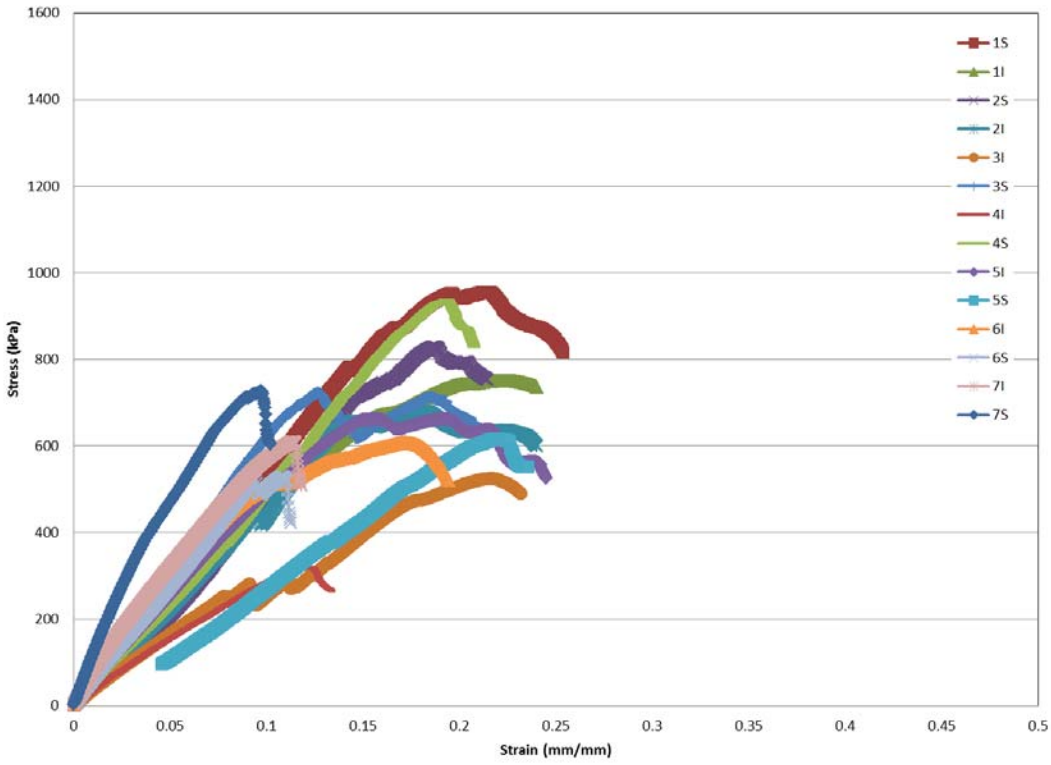

Figure C.13: Stress – Strain Curves for Group 11R Samples

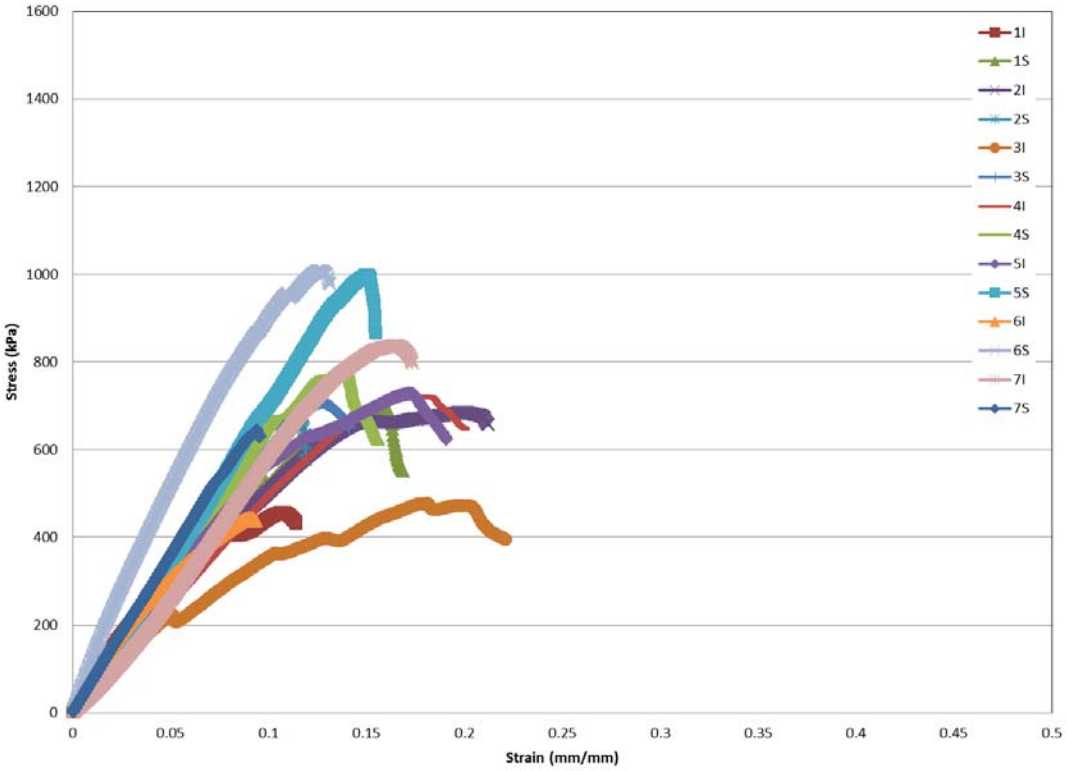

Figure C.14: Stress – Strain Curves for Group 12R Samples

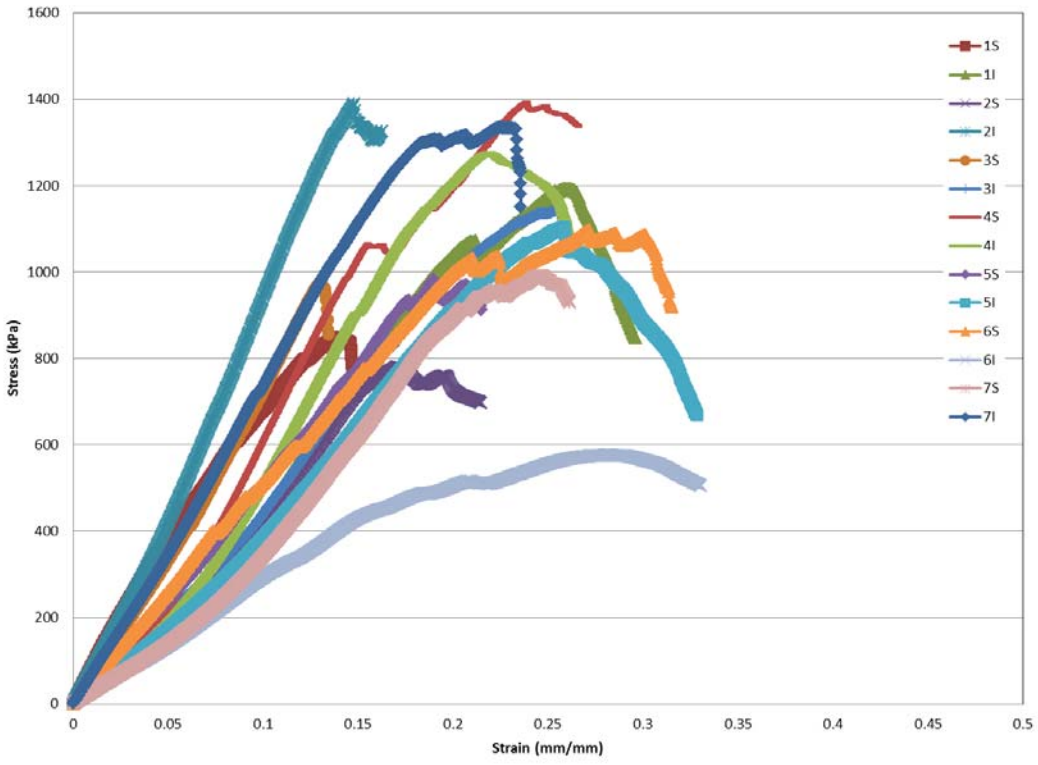

Figure C.15: Stress – Strain Curves for Group 13R Samples

REFERENCES

Ahmed, M. R., Vairamuthu, S., Shafiuzama, M. D., Basha, S. H., & Jayakumar, R. (2005). Microwave irradiated collagen tubes as a better matrix for peripheral nerve regeneration. *Brain research*, *1046*(1), 55-67.

Annandale, T. (1876). Case in which a reducible oblique and direct inguinal and femoral hernia existed on the same side and were successfully treated by operation. *Edinb Med J*, *21*, 1087-1091.

Askar, O. M. (1984). Aponeurotic hernias. Recent observations upon paraumbilical and epigastric hernias. *The Surgical clinics of North America*,*64*(2), 315-333.

Arnaud, J. P., Eloy, R., Adloff, M., & Grenier, J. F. (1977). Critical evaluation of prosthetic materials in repair of abdominal wall hernias: new criteria of tolerance and resistance. *The American Journal of Surgery*, *133*(3), 338-345.

Arroyo, A., Garcia, P., Perez, F., Andreu, J., Candela, F., & Calpena, R. (2001). Randomized clinical trial comparing suture and mesh repair of umbilical hernia in adults. *British journal of surgery*, *88*(10), 1321-1323.

Arslan, O. E. (2005). Anatomy of the abdominal wall. In *Aesthetic Surgery of the Abdominal Wall* (pp. 1-28). Springer Berlin Heidelberg.

Bassini, E. (1887). Nuova technica per la cura radicale dell'ernia. In *Atti del Associazione Medica Italiano Congresso* (Vol. 2, pp. 179-82).

Bassini, E. (1890). Ueber die behandlung des leistenbruches. *Arch Klin Chir*,*40*, 429-476.

Bendavid, R. (Ed.). (2001). *Abdominal wall hernias: principles and management*. Springer.

Black, M. J., & Anandan, P. (1996). The robust estimation of multiple motions: Parametric and piecewise-smooth flow fields. *Computer vision and image understanding*, *63*(1), 75-104.

Blumberg, N. A. (1980). Infantile umbilical hernia. *Surgery, gynecology & obstetrics*, *150*(2), 187-192.

Boccafoschi, F., Habermehl, J., Vesentini, S., & Mantovani, D. (2005). Biological performances of collagen-based scaffolds for vascular tissue engineering. *Biomaterials*, *26*(35), 7410-7417.

Brewer, L. A. (1980). History of surgery of the esophagus. *The American Journal of Surgery*, *139*(6), 730-743.

Bown, A. B. (2013). *The Utilization of Multipotent Mesenchymal Stromal Cell Transplantation to Improve Fascia Repair* (Doctoral dissertation, Youngstown State University).

Burcharth, J., Pommergaard, H. C., & Rosenberg, J. (2013). The inheritance of groin hernia: a systematic review. *Hernia*, *17*(2), 183-189.

Caix, P. (1999, August). [Anatomy of the abdominal wall]. In *Annales de chirurgie plastique et esthetique* (Vol. 44, No. 4, pp. 289-311).

Catlin, Brian. Fabricant, Arnold. Lyons, John. "Inguinal ligament, inguinal canal, and layers of scrotum". Photograph. 2009. Basic Human Anatomy. Dartmouth. 10 Apr. 2014. http://www.dartmouth.edu/~humananatomy/Figures/chapter_25/25-7.HTM

Chaudhury, S. (2012). Mesenchymal stem cell applications to tendon healing.*Muscles, Ligaments and Tendons Journal*, *2*(3), 222.

Cheatle, G. L. (1920). An operation for the radical cure of inguinal and femoral hernia. *British medical journal*, *2*(3107), 68.

Chen, L., Dong, S. W., Liu, J. P., Tao, X., Tang, K. L., & Xu, J. Z. (2012). Synergy of tendon stem cells and platelet-rich plasma in tendon healing.*Journal of Orthopaedic Research*, *30*(6), 991-997.

Che6rel, J. P. (1998). Hernia and Surgery of the Abdominal Wall.

COLVILLE, J. A., POWER, R. E., HICKEY, D. P., LANE, B. E., & O'MALLEY, K. J. (2000). Intermittent anuria secondary to a stone in a ureterofemoral hernia. *The Journal of urology*, *164*(2), 440-441.

Czerny, V., & Billroth, T. (Eds.). (1878). *Beiträge zur operativen Chirurgie: Herrn Hofrath Professor Dr. Theodor Billroth in Wien zu seinem fünfundzwanzigjährigen Doctor-Jubiläum gewidmet und herausgegeben*. Enke.

Dahlstrand, U., Wollert, S., Nordin, P., Sandblom, G., & Gunnarsson, U. (2009). Emergency femoral hernia repair: a study based on a national register.*Annals of surgery*, *249*(4), 672-676.

Davies, T. W., Williams, D. R. R., & WHITAKER, A. (1986). Risk factors for undescended testis. *International journal of epidemiology*, *15*(2), 197-201.

Davis, M. L., Moreno, D. P., Vavalle, N. A., & Gayzik, F. S. (2012). Human liver finite element model validation using compressive and tensile experimental data-biomed 2013. *Biomedical sciences instrumentation*, *49*, 289-296.

de Garengeot, R. J. C. (1748). *Traite des operations de chirurgie*.

Desarda, M. P. (2003). Surgical physiology of inguinal hernia repair-a study of 200 cases. *BMC surgery*, *3*(1), 2.

Desarda, M. P. (2001). New method of inguinal hernia repair: A new solution.*ANZ journal of surgery*, *71*(4), 241-244.

Deveney, K. E. (1994). Hernias and other lesions of the abdominal wall. *Way LW. Surgical diagnosis and treatment. Connecticut: Appleton & Lange Pubs*, 712-22.

Ding, D. C., Shyu, W. C., & Lin, S. Z. (2010). Mesenchymal stem cells. *Cell transplantation*, *20*(1), 5-14.

Dong, Y., Zhang, Q., Li, Y., Jiang, J., & Chen, S. (2012). Enhancement of Tendon–Bone Healing for Anterior Cruciate Ligament (ACL) Reconstruction Using Bone Marrow-Derived Mesenchymal Stem Cells Infected with BMP-2.*International journal of molecular sciences*, *13*(10), 13605-13620.

Franklin Jr, M. E., Trevino, J. M., Portillo, G., Vela, I., Glass, J. L., & González, J. J. (2008). The use of porcine small intestinal submucosa as a prosthetic material for laparoscopic hernia repair in infected and potentially contaminated fields: long-term follow-up. *Surgical endoscopy*, *22*(9), 1941-1946.

García, C. M., Ruiz, S. G., & Franco, C. C. (2014). Anatomy of the Abdominal Wall. In *Advances in Laparoscopy of the Abdominal Wall Hernia* (pp. 7-22). Springer London.

Ge, Z., Goh, J. C. H., & Lee, E. H. (2005). The effects of bone marrow-derived mesenchymal stem cells and fascia wrap application to anterior cruciate ligament tissue engineering. *Cell transplantation*, *14*(10), 763-773.

Gilbert, A. I. (1989). An anatomic and functional classification for the diagnosis and treatment of inguinal hernia. *The American journal of surgery*, *157*(3), 331-333.

Gulotta, L. V., Kovacevic, D., Ehteshami, J. R., Dagher, E., Packer, J. D., & Rodeo, S. A. (2009). Application of bone marrow-derived mesenchymal stem cells in a rotator cuff repair model. *The American journal of sports medicine*,*37*(11), 2126-2133.

Hay, J. M., Boudet, M. J., Fingerhut, A., Poucher, J., Hennet, H., Habib, E., ... & Flamant, Y. (1995). Shouldice inguinal hernia repair in the male adult: the gold standard? A multicenter controlled trial in 1578 patients. *Annals of surgery*, *222*(6), 719.

Heffner, J. J., Holmes, J. W., Ferrari, J. P., Krontiris-Litowitz, J., Marie, H., Fagan, D. L., ... & Dorion, H. A. (2012). Bone marrow-derived mesenchymal stromal cells and platelet-rich plasma on a collagen matrix to improve fascial healing. *Hernia*, *16*(6), 677-687.

Henry, A. (1936). Operation for femoral hernia by a midline extraperitoneal approach: with a preliminary note on the use of this route for reducible inguinal hernia. *The Lancet*, *227*(5871), 531-533.

Höer, J., Lawong, G., Klinge, U., & Schumpelick, V. (2002). [Factors influencing the development of incisional hernia. A retrospective study of 2,983 laparotomy patients over a period of 10 years]. *Der Chirurg; Zeitschrift fur alle Gebiete der operativen Medizen*, *73*(5), 474-480.

Horn, B. K., & Schunck, B. G. (1981, November). Determining optical flow. In*1981 Technical Symposium East* (pp. 319-331). International Society for Optics and Photonics.

Iwata, Y., Katanosaka, Y., Arai, Y., Komamura, K., Miyatake, K., & Shigekawa, M. (2003). A novel mechanism of myocyte degeneration involving the Ca2+-permeable growth factor–regulated channel. *The Journal of cell biology*, *161*(5), 957-967.

Jackson, O. J., & Moglen, L. H. (1970). Umbilical Hernia—A Retrospective Study. *California medicine*, *113*(4), 8.

Joun, M., Choi, I., Eom, J., & Lee, M. (2007). Finite element analysis of tensile testing with emphasis on necking. *Computational Materials Science*, *41*(1), 63-69.

Ju, Y. J., Muneta, T., Yoshimura, H., Koga, H., & Sekiya, I. (2008). Synovial mesenchymal stem cells accelerate early remodeling of tendon-bone healing.*Cell and tissue research*, *332*(3), 469-478.

Jung, U. W., Kim, S. K., Kim, C. S., Cho, K. S., Kim, C. K., & Choi, S. H. (2007). Effect of chitosan with absorbable collagen sponge carrier on bone regeneration in rat calvarial defect model. *Current Applied Physics*, *7*, e68-e70.

Kapiris, S. A., Brough, W. A., Royston, C. M. S., O'Boyle, C., & Sedman, P. C. (2001). Laparoscopic transabdominal preperitoneal (TAPP) hernia repair.*Surgical endoscopy*, *15*(9), 972-975.

Kavic, M. S. (1993). Laparoscopic hernia repair. *Surgical endoscopy*, *7*(3), 163-167.

Kawaguchi, H., Hirachi, A., Hasegawa, N., Iwata, T., Hamaguchi, H., Shiba, H., ... & Kurihara, H. (2004). Enhancement of periodontal tissue regeneration by transplantation of bone marrow mesenchymal stem cells. *Journal of periodontology*, *75*(9), 1281-1287.

Keith, A. (1924). On the origin and nature of hernia. *British Journal of Surgery*,*11*(43), 455-475.

Kemper, A., Santago, A., Sparks, J., Stitzel, J., & Duma, S. (2011). Multi-Scale biomechanical characterization of human liver and spleen. In *Proceedings of the 22nd Enhanced Safety of Vehicles Conference* (Vol. 11, p. 0195).

Kingsnorth, A. N. (2013). General Introduction and History of Hernia Surgery. In *Management of Abdominal Hernias* (pp. 1-23). Springer London.

Kingsnorth, A. N., LeBlanc, K. A., & Kingsnorth, A. N. (2003). *Management of abdominal hernias* (pp. 217-227). London: Arnold.

Kitoh, H., Kitakoji, T., Tsuchiya, H., Mitsuyama, H., Nakamura, H., Katoh, M., & Ishiguro, N. (2004). Transplantation of marrow-derived mesenchymal stem cells and platelet-rich plasma during distraction osteogenesis—a preliminary result of three cases. *Bone*, *35*(4), 892-898.

Klinge, U., Prescher, A., Klosterhalfen, B., & Schumpelick, V. (1997). Entstehung und Pathophysiologie der Bauchwanddefekte. *Der Chirurg*, *68*(4), 293-303.

Krampera, M., Glennie, S., Dyson, J., Scott, D., Laylor, R., Simpson, E., & Dazzi, F. (2003). Bone marrow mesenchymal stem cells inhibit the response of naive and memory antigen-specific T cells to their cognate peptide. *Blood*,*101*(9), 3722-3729.

Krishna, A., Misra, M. C., Bansal, V. K., Kumar, S., Rajeshwari, S., & Chabra, A. (2012). Laparoscopic inguinal hernia repair: transabdominal preperitoneal (TAPP) versus totally extraperitoneal (TEP) approach: a prospective randomized controlled trial. *Surgical endoscopy*, *26*(3), 639-649.

Krishna, A., Misra, M. C., Bansal, V. K., Kumar, S., Rajeshwari, S., & Chabra, A. (2012). Laparoscopic inguinal hernia repair: transabdominal preperitoneal (TAPP) versus totally extraperitoneal (TEP) approach: a prospective randomized controlled trial. *Surgical endoscopy*, *26*(3), 639-649.

Kwon, D. S., Gao, X., Liu, Y. B., Dulchavsky, D. S., Danyluk, A. L., Bansal, M., ... & Gautam, S. C. (2008). Treatment with bone marrow-derived stromal cells accelerates wound healing in diabetic rats. *International wound journal*,*5*(3), 453-463.

Lang, B., Lau, H., & Lee, F. (2002). Epigastric hernia and its etiology. *Hernia*,*6*(3), 148-150.

LeBlanc, K. A., & Booth, W. V. (1993). Laparoscopic repair of incisional abdominal hernias using expanded polytetrafluoroethylene: preliminary findings. *Surgical Laparoscopy Endoscopy & Percutaneous Techniques*, *3*(1), 39-41.

Lee, J. C., Min, H. J., Park, H. J., Lee, S., Seong, S. C., & Lee, M. C. (2013). Synovial Membrane–Derived Mesenchymal Stem Cells Supported by Platelet-Rich Plasma Can Repair Osteochondral Defects in a Rabbit Model.*Arthroscopy: The Journal of Arthroscopic & Related Surgery*, *29*(6), 1034-1046.

Lemmer, J. H., Strodel, W. E., Knol, J. A., & Eckhauser, F. E. (1983). Management of spontaneous umbilical hernia disruption in the cirrhotic patient.*Annals of surgery*, *198*(1), 30.

Li, W. J., Tuli, R., Okafor, C., Derfoul, A., Danielson, K. G., Hall, D. J., & Tuan, R. S. (2005). A three-dimensional nanofibrous scaffold for cartilage tissue engineering using human mesenchymal stem cells. *Biomaterials*, *26*(6), 599-609.

Lichtenstein, I. L., & Shore, J. M. (1974). Simplified repair of femoral and recurrent inguinal hernias by a “plug” technic. *The American Journal of Surgery*, *128*(3), 439-444.

Lichtenstein, I. L. (1987). Herniorrhaphy: a personal experience with 6,321 cases. *The American journal of surgery*, *153*(6), 553-559.

Lin, H., Chen, B., Sun, W., Zhao, W., Zhao, Y., & Dai, J. (2006). The effect of collagen-targeting platelet-derived growth factor on cellularization and vascularization of collagen scaffolds. *Biomaterials*, *27*(33), 5708-5714.

Liu, Y., Dulchavsky, D. S., Gao, X., Kwon, D., Chopp, M., Dulchavsky, S., & Gautam, S. C. (2006). Wound repair by bone marrow stromal cells through growth factor production. *Journal of surgical research*, *136*(2), 336-341.

Lockwood, C. B. (1893). THE RADICAL CURE OF FEMORAL AND INGUINAL HERNIA. *The Lancet*, *142*(3665), 1297-1302.

Lucarelli, E., Beccheroni, A., Donati, D., Sangiorgi, L., Cenacchi, A., Del Vento, A. M., ... & Picci, P. (2003). Platelet-derived growth factors enhance proliferation of human stromal stem cells. *Biomaterials*, *24*(18), 3095-3100.

Maekawa, Y., Yagi, K., Nonomura, A., Kuraoku, R., Nishiura, E., Uchibori, E., & Takeuchi, K. (2003). A tetrazolium-based colorimetric assay for metabolic activity of stored blood platelets. *Thrombosis research*, *109*(5), 307-314.

Marie, H., Zhang, Y., Heffner, J., Dorion, H. A., & Fagan, D. L. (2010). Biomechanical and elastographic analysis of mesenchymal stromal cell treated tissue following surgery. *Journal of biomechanical engineering*, *132*(7), 074503.

McCormack, K., Wake, B. L., Fraser, C., Vale, L., Perez, J., & Grant, A. (2005). Transabdominal pre-peritoneal (TAPP) versus totally extraperitoneal (TEP) laparoscopic techniques for inguinal hernia repair: a systematic review.*Hernia*, *9*(2), 109-114.

McEvedy, P. G. (1950). Femoral Hernia: Lecture delivered at the Royal College of Surgeons of England on 11th October, 1950. *Annals of the Royal College of Surgeons of England*, *7*(6), 484.

McEwen, Andrew. "FEMORAL NERVE BLOCK: LANDMARK APPROACH";2012 http://www.frca.co.uk/Documents/249%20Femoral%20Nerve%20Block-%20Landmark%20approach.pdf

McFarlin, K., Gao, X., Liu, Y. B., Dulchavsky, D. S., Kwon, D., Arbab, A. S., ... & Gautam, S. C. (2006). Bone marrow-derived mesenchymal stromal cells accelerate wound healing in the rat. *Wound Repair and Regeneration*, *14*(4), 471-478.

Menon, V. S., & Brown, T. H. (2003). Umbilical hernia in adults: day case local anaesthetic repair. *Journal of postgraduate medicine*, *49*(2), 132.

Merritt, E. K., Cannon, M. V., Hammers, D. W., Le, L. N., Gokhale, R., Sarathy, A., ... & Farrar, R. P. (2010). Repair of traumatic skeletal muscle injury with bone-marrow-derived mesenchymal stem cells seeded on extracellular matrix. *Tissue Engineering Part A*, *16*(9), 2871-2881.

Mishra, A., Tummala, P., King, A., Lee, B., Kraus, M., Tse, V., & Jacobs, C. R. (2009). Buffered platelet-rich plasma enhances mesenchymal stem cell proliferation and chondrogenic differentiation. *Tissue Engineering Part C: Methods*, *15*(3), 431-435.

Moore, D. S., & McCabe, G. P. (1989). *Introduction to the Practice of Statistics*. WH Freeman/Times Books/Henry Holt & Co.

Morigi, M., Imberti, B., Zoja, C., Corna, D., Tomasoni, S., Abbate, M., ... & Remuzzi, G. (2004). Mesenchymal stem cells are renotropic, helping to repair the kidney and improve function in acute renal failure. *Journal of the American Society of Nephrology*, *15*(7), 1794-1804.

Muschaweck, U. (2003). Umbilical and epigastric hernia repair. *Surgical Clinics of North America*, *83*(5), 1207-1221.

Nakagawa, H., Akita, S., Fukui, M., Fujii, T., & Akino, K. (2005). Human mesenchymal stem cells successfully improve skin-substitute wound healing.*British Journal of Dermatology*, *153*(1), 29-36.

Niebur, G. L., Feldstein, M. J., Yuen, J. C., Chen, T. J., & Keaveny, T. M. (2000). High-resolution finite element models with tissue strength asymmetry accurately predict failure of trabecular bone. *Journal of Biomechanics*, *33*(12), 1575-1583.

Ouyang, H. W., Goh, J. C., & Lee, E. H. (2004). Use of Bone Marrow Stromal Cells for Tendon Graft-to-Bone Healing Histological and Immunohistochemical Studies in a Rabbit Model. *The American journal of sports medicine*, *32*(2), 321-327.

Pacini, S., Spinabella, S., Trombi, L., Fazzi, R., Galimberti, S., Dini, F., ... & Petrini, M. (2007). Suspension of bone marrow-derived undifferentiated mesenchymal stromal cells for repair of superficial digital flexor tendon in race horses. *Tissue engineering*, *13*(12), 2949-2955.

Papanikitas, J., Sutcliffe, R. P., Rohatgi, A., & Atkinson, S. (2008). Bilateral retrovascular femoral hernia. *Annals of the Royal College of Surgeons of England*, *90*(5), 423.

Paquet, M., Penney, J., & Boerboom, D. (2008). Lateral femoral hernias in a line of FVB/NHsd mice: a new confounding lesion linked to genetic background *Comparative medicine*, *58*(4), 395.

Paulino, G. H., Carpenter, R. D., Liang, W. W., Munir, Z. A., & Gibeling, J. C. (2001). Fracture testing and finite element modeling of pure titanium.*Engineering Fracture Mechanics*, *68*(12), 1417-1432.

Pieri, F., Lucarelli, E., Corinaldesi, G., Fini, M., Aldini, N. N., Giardino, R., ... & Marchetti, C. (2009). Effect of mesenchymal stem cells and platelet-rich plasma on the healing of standardized bone defects in the alveolar ridge: a comparative histomorphometric study in minipigs. *Journal of Oral and Maxillofacial Surgery*, *67*(2), 265-272.

Ramirez, O. M., Ruas, E., & Dellon, A. L. (1990). " Components separation" method for closure of abdominal-wall defects: an anatomic and clinical study.*Plastic and reconstructive surgery*, *86*(3), 519-526.

Read, R. C. (2004). Milestones in the history of hernia surgery: prosthetic repair. *Hernia*, *8*(1), 8-14.

Rives, J., Pire, J. C., Flament, J. B., & Convers, G. (1977). [Treatment of large eventrations (apropos of 133 cases)]. *Minerva chirurgica*, *32*(11), 749-756.

Robin, A. P. (1995). Epigastric hernia. *Hernia, 4th ed. Philadelphia: Nyhus and Condon*.

Rojas, M., Xu, J., Woods, C. R., Mora, A. L., Spears, W., Roman, J., & Brigham, K. L. (2005). Bone marrow–derived mesenchymal stem cells in repair of the injured lung. *American journal of respiratory cell and molecular biology*,*33*(2), 145.

Rosemar, A., Angerås, U., Rosengren, A., & Nordin, P. (2010). Effect of body mass index on groin hernia surgery. *Annals of surgery*, *252*(2), 397-401.

Rosenbaum, A. J., Grande, D. A., & Dines, J. S. (2008). The use of mesenchymal stem cells in tissue engineering. *Organogenesis*, *4*(1), 23-27.

Runyon, B. A., & Juler, G. L. (1985). Natural history of repaired umbilical hernias in patients with and without ascites. *American Journal of Gastroenterology*, *80*(1).

Rutkow, I. M. (1992). Laparoscopic hernia repair: the socioeconomic tyranny of surgical technology. *Archives of Surgery*, *127*(11), 1271-1271.

Rutkow, I. M., & Robbins, A. W. (1998). Classification systems and groin hernias. *Surgical Clinics of North America*, *78*(6), 1117-1127.

Rutkow, I. M., & Robbins, A. W. (1993). " Tension-free" inguinal herniorrhaphy: a preliminary report on the" mesh plug" technique. *Surgery*, *114*(1), 3-8.

Samur, E., Sedef, M., Basdogan, C., Avtan, L., & Duzgun, O. (2007). A robotic indenter for minimally invasive measurement and characterization of soft tissue response *Medical Image Analysis*, *11*(4), 361-373.

Satar, B., Karahatay, S., Kurt, B., Ural, A. U., Safali, M., Avcu, F., ... & Kucuktag, Z. (2009). Repair of transected facial nerve with mesenchymal stromal cells: histopathologic evidence of superior outcome. *The Laryngoscope*, *119*(11), 2221-2225.

Sauerland, S., Korenkov, M., Kleinen, T., Arndt, M., & Paul, A. (2004). Obesity is a risk factor for recurrence after incisional hernia repair. *Hernia*, *8*(1), 42-46.

Sheehan, V. (1955). The surgical approaches to femoral hernia. *Irish Journal of Medical Science (1926-1967)*, *30*(4), 166-175.

Shulman, A. G., Amid, P. K., & Lichtenstein, I. L. (1992). Prosthetic mesh plug repair of femoral and recurrent inguinal hernias: the American experience.*Annals of the Royal College of Surgeons of England*, *74*(2), 97.

Shouldice, E. E. (1953). Obesity and ventral hernia repair. *Modern Medicine of Canada. p*, *89*.

Smith, Rick G.; Gassmann, Craig J.; Campbell, Mark S.; Platelet-Rich Plasma: Properties and Clinical Applications. The journal of Lancaster General Hospital, 2007, p73-78.

Smith, R. K. W., & Webbon, P. M. (2005). Harnessing the stem cell for the treatment of tendon injuries: heralding a new dawn?. *British journal of sports medicine*, *39*(9), 582-584.

Socin, A. "Femoral hernia." Arch Klin Chir 24 (1879): 391.

Stoff, A., Rivera, A. A., Sanjib Banerjee, N., Moore, S. T., Michael Numnum, T., Espinosa-de-los-Monteros, A., ... & Curiel, D. T. (2009). Promotion of incisional wound repair by human mesenchymal stem cell transplantation.*Experimental dermatology*, *18*(4), 362-369.

Stoppa, R. E., Rives, J. L., Warlaumont, C., Palot, J. P., Verhaeghe, P. J., & Delattre, J. F. (1984). The use of Dacron in the repair of hernias of the groin.*The Surgical clinics of North America*, *64*(2), 269-285.

Tamme, C., Scheidbach, H., Hampe, C., Schneider, C., & Köckerling, F. (2003). Totally extraperitoneal endoscopic inguinal hernia repair (TEP). *Surgical Endoscopy and Other Interventional Techniques*, *17*(2), 190-195.

Tae, S. K., Lee, S. H., Park, J. S., & Im, G. I. (2006). Mesenchymal stem cells for tissue engineering and regenerative medicine. *Biomedical Materials*,*1*(2), 63.

Tsutsumi, S., Shimazu, A., Miyazaki, K., Pan, H., Koike, C., Yoshida, E., ... & Kato, Y. (2001). Retention of multilineage differentiation potential of mesenchymal cells during proliferation in response to FGF. *Biochemical and biophysical research communications*, *288*(2), 413-419.

USHER, F. C. (1962). Hernia repair with Marlex mesh: an analysis of 541 cases. *Archives of Surgery*, *84*(3), 325.

Van Pham, P., Bui, K. H., Ngo, D. Q., Vu, N. B., Truong, N. H., Phan, N. L., ... & Phan, N. K. (2013). Activated platelet-rich plasma improves adipose-derived stem cell transplantation efficiency in injured articular cartilage. *Stem Cell Res Ther*, *4*, 91.

Williams M, Frankel S, Nanchalal K, Coast J, Donovan J. Hernia repair: epidemiologically based needs assessment. Bristol: Health Care Evaluation Unit, University of Bristol Print Services; 1992.

Wood, J. (1863). *On rupture, inguinal, crural, and umbilical*. JW Davies.

Wu, Y., Chen, L., Scott, P. G., & Tredget, E. E. (2007). Mesenchymal stem cells enhance wound healing through differentiation and angiogenesis. *Stem cells*, *25*(10), 2648-2659.

Xie, X., Wang, Y., Zhao, C., Guo, S., Liu, S., Jia, W., ... & Zhang, C. (2012). Comparative evaluation of MSCs from bone marrow and adipose tissue seeded in PRP-derived scaffold for cartilage regeneration. *Biomaterials*, *33*(29), 7008-7018.

Young, R. G., Butler, D. L., Weber, W., Caplan, A. I., Gordon, S. L., & Fink, D. J. (1998). Use of mesenchymal stem cells in a collagen matrix for Achilles tendon repair. *Journal of Orthopaedic Research*, *16*(4), 406-413.

Yuan, S., Jiang, T., Sun, L., Zheng, R., Ahat, N., & Zhang, Y. (2013). The Role of Bone Marrow Mesenchymal Stem Cells in the Treatment of Acute Liver Failure. *BioMed research international*, *2013*.**